공학석사학위논문

Synthesis and application of a TEG-based leveler and its derivatives on Cu electrodeposition

TEG 기반 평탄제 및 이의 유도체들의 합성과 구리 전해도금에서의 적용

2016년 2월

서울대학교 대학원

화학생물공학부

이 윤 재

Synthesis and application of a TEG-based leveler and its derivatives on Cu electrodeposition

TEG 기반 평탄제 및 이의 유도체들의 합성과 구리 전해도금에서의 적용

지도 교수 김 영 규

이 논문을 공학석사학위논문으로 제출함

2016년 2월

서울대학교 대학원

화학생물공학부

이 윤 재

이윤재의 공학석사학위논문을 인준함

2015년 12월

위 원 장 오 승 모 (인)

부위원장 김 영 규 (인)

위 원 김 재 정 (인)

Synthesis and application of a TEG-based leveler and its derivatives on Cu electrodeposition

By

Yoonjae Lee

February 2016

Thesis Adviser : Young Gyu Kim

Abstract

Synthesis and application of a TEG-based leveler and its derivatives on Cu electrodeposition

Yoonjae Lee
School of Chemical and Biological Engineering
The Graduate School
Seoul National University

Through-Silicon Via (TSV) is a vertical electrical interconnection passing through a silicon wafer or IC chip, and it provides the shortest interconnects between multiple chips. Although the smallest pad size can be achieved with TSV technology, the defect-free filling of TSV remains as a challenge for successful chip performance. To afford the defect-free filling, the bottom-up filling is required, and some organic additives are essential elements during the electrodeposition of Cu. Among the additives, a leveler has been known as a convection dependent adsorbent, which means it selectively adsorbs on the opening of feature and inhibits Cu-electrodeposition.

In this thesis, the structure-activity relation of a leveler, a key element for defect-free filling, has been studied with newly synthesized levelers. The triethylene glycol based leveler (Lev (1)), having simple linear center chain with ammonium functional groups at the end of the backbone, has been designed to closely investigate the properties of the levelers. Starting from ethylene glycol, epoxide rings have been introduced at the both ends after allylation. To introduce ammonium groups, the epoxide rings have been opened with N,N-dimethyl amine,

and following methylation successfully produces Lev (1) in 46% of overall yields. To find out the effect of the center chain, the Lev (1) was modified to levelers (Lev (2), (3), (4)) having various center chain. The levelers have been synthesized in 25~50% of overall yields. The electrochemical analyses of the levelers with linear sweep volatammetry (LSV) confirmed that the all synthesized levelers showed the desired convection dependent adsorption behavior and the longer, and aliphatic center structure showed stronger adsorption on the Cu surface. The levelers also afforded successful gap filling performance in the presence of an accelerator and a suppressor.

Keywords : leveler, Cu electrodeposition, TSV, organic additives, convection-dependent adsorption, gap-filling

Student Number : 2014-20569

TABLE OF CONTENTS

LIST OF FIGURES

LIST OF TABLES

LIST OF SCHEMES

LIST OF ABBREVIATIONS

ALD	Atomic layer deposition
Cu	Copper
CVD	chemical vapor deposition
EtOAc	Ethyl acetate
FAB	Fast atom bombardment
Hex	Hexane
HRMS	High resolution mass spectrometer
MC	Methylene chloride
*m*CPBA	*meta*-Chloroperoxybenzoic acid
MeOH	Methanol
MeI	Methyl iodide
NMR	Nuclear magnetic resonance
PEG	Polyethylene glycol
PPG	Polypropylene glycol
PVD	Physical vapor deposition
RDE	Rotating-disk electrode
SEM	Scaning electron microscope
SPS	bis(3-Sulfopropyl) disulfide
TBAI	Tetrabutylammonium iodide
THF	Tetrahydrofuran
TMS	Tetramethylsilane
TSV	Through silicon via
UV	Ultraviolte

1. Introduction

1.1. Through Silicon Via (TSV) for 3D integrated circuit

Small, high-speed, and high performance electronic devices have been continuously achieved by the decreasing the size of chip component over more than four decades. This continuous scaling down has been able to be achieved by amazing development in miniature technology mainly consist of photolithography and high integration technologies. However, Moore's law, a proposal of doubling the number of transistors in one IC chip doubles approximately every two years, is about to hit a wall because the limitation on the improvement of chip performance by miniature technology has come into sight in two regards.[2,3] The first is the difficulty of lithographic scaling for fine patterns down to sub-28 nm, and the cost issues related to extreme ultraviolet lithography. The second is RC delay time. The RC delay for on-chip wiring increases with scaling and becomes greater than the transistor delay. (Fig. 1)[4, 5] In order to overcome these problems, three-dimensional integration by Through-Silicon Via (TSV) technology is essential.

TSV is a vertical electrical interconnection passing through a silicon wafer or IC chip (Fig. 2). The TSV was first invented by William Shockley in 1958 with a patent describing "deep pits" to connect top and bottom side of wafer together.[6] Even though William Shockley is the one who first proposed the new concept of TSV, most people in industry think Merlin Smith and Emanuel Stern as the inventors of TSV owing to their patent "Methods of making thru-connections in semiconductor wafers" filled on December 28, 1964.[7] The term "Through-Silicon Via" was first mentioned as part of his original business plan in late 1990s by Dr. Sergey Savastiouk, the co-founder and current CEO of ALLVIA, Inc.. The intent of the business plan was making vertical interconnection pathway through silicon to

offer better performance over wire-bonds.

There are some other interconnection technologies including wire-bonding. Among them, the TSV technology is considered as the best technology for three-dimensional integration because it provides the shortest interconnections between multiple chips, as well as affords the smallest pad size. Besides to these mentioned advantages, the followings prove that the TSV technology is the best technology for three-dimensional integration.[8]

(a) Better electrical performance

(b) Lower power consumption

(c) Wider bandwidth

(d) Higher density

(e) Smaller form factor

(f) Lighter weight.

Even compared to wire-bonding, which is considered to be a mature, high density, and low-cost technology, the TSV is a better technology that is able to realize multi-function, higher performance, and higher integrity (Fig. 2).[9]

The fabrication process of TSV can be divided into 4 steps : (a) Via formation, (b) Via filling, (c) Thinning, (d) Bonding (Fig. 3).[10] Recently, many research groups have made their efforts to advance TSV process : etching,[11-13] barrier and seed layers deposition,[14-19] copper (Cu) electrodeposition,[20-26] CMP (chemical mechanical planarization) process,[27] wafer thinning,[28] and so on.

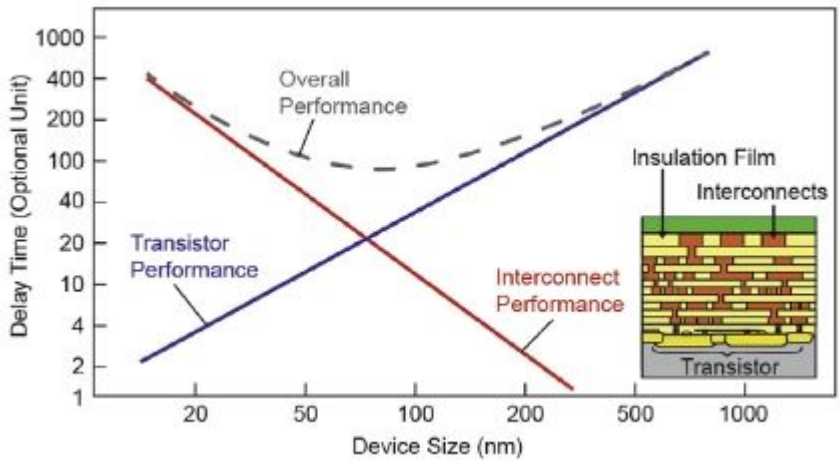

Fig. 1. Delay as a function of device size. Transistor delay decreases with scaling, whereas interconnect delay increases with scaling.

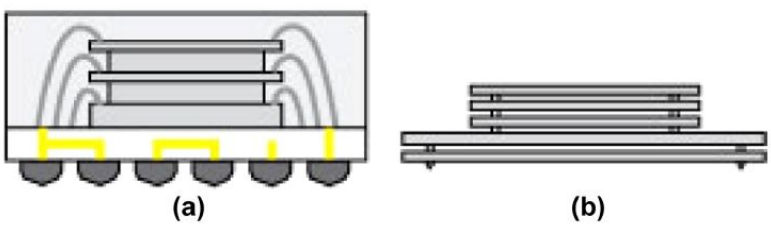

Fig. 2. Three-dimension IC stacking; (a) stacked-die with wire-bond; (b) stacked-die with TSV.

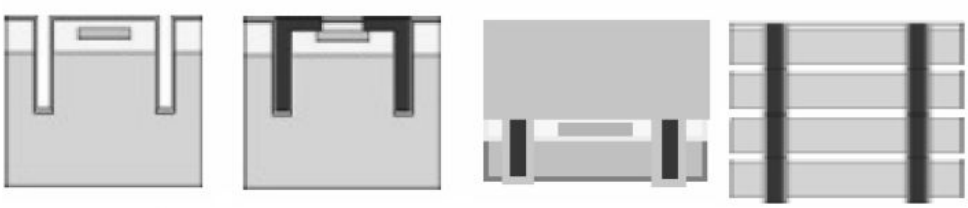

Fig. 3. Fabrication process of TSV; (a) Via formation; (b) Via filling; (c) Thinning ; (d) Bonding.

1.2. Cu electrodeposition

For TSV filling process, which is the second step of its fabrication process, choosing a suitable material is very important. There are three requirements for the conductor filling the TSV; (a) low resistivity, (b) capability of void-free filling, (c) high reliability. Doped polysilicon (180 μohm-cm),[29] tungsten (5.6 μohm-cm), and copper (1.7 μohm-cm) are the conductors that meet these requirements mentioned above and most commonly used. Among them, copper is preferred because it has the lowest resistivity.

There are several methods for deposition of Cu, such as physical vapor deposition (PVD), chemical vapor deposition (CVD), atomic layer deposition (ALD), electroless deposition, and electrodeposition. For Cu deposition, among these, electrodeposition method has been mostly used by reasons of its high rate of Cu deposition, good film properties, and good filling profile.

Cu electrodeposition uses the external electron source to reduce dissolved Cu ion in order to form a Cu film on an electrode. (Fig. 4)[30] There are three necessary components of Cu electrodeposition which are electrodes, power source and an electrolyte containing the Cu ion. The electrodes consist of a cathode where the reduction of Cu ions occurs to be plated and an anode where the oxidation of Cu ions occurs to complete the circuit. There have been various electrolytes such as cyanide, pyrophosphate, acid sulfate, and acid fluoborate-based system. However, Cu sulfate ($CuSO_4$) system is mostly used at present because cyanide, pyrophosphate, and fluoborated-base systems are toxic, pollutant, and relatively high cost compared to sulfate-system, respectively. Besides $CuSO_4$ electrolyte, supporting electrolyte is also added to the system because it reduces ohmic drop resulted by the electrolyte resistance in solution. Therefore, supporting electrolyte has to have high ionic mobility to reduce ohmic drop. In Cu sulfate-based

electrolyte, sulfuric acid (H_2SO_4) is used as a supporting electrolyte since the ionic species having the highest mobility is the proton (H^+). Occasionally, the reference electrode is used in addition to two electrodes (cathode and anode). Since there is physical distance between the cathode and the anode, ohmic drop is inevitable. Therefore, a reference electrode is placed close to the cathode to reduce the ohmic drop caused by electrolyte resistance between two electrodes so that one can monitor the actually applied potential on the cathode.

While electrodeposition is progressing, the filling profile can be classified into three profiles : (a) subconformal, (b) conformal, and (c) superconformal (Fig. 5).[30] The subconformal profile is caused by concentrated Cu reduction at the top surface of the via or trench, resulting void formation inside the trench. The conformal profile is caused by conformal reduction rate of Cu at the all positions of trench, resulting seam formation inside the trench. Both the void and the seam represent disconnection of Cu, so they increase in the electrical resistivity and are considered as defects. For a defect-free filling of Cu, the superconformal is necessary. The superconformal deposition is also called bottom-up filling because Cu deposition do not occurs at the top and the side wall but the bottom of the trench. With the bottom-up filling, no voids or seams inside the trench are formed, which requires for high speed and reliable interconnection of electronic devices.

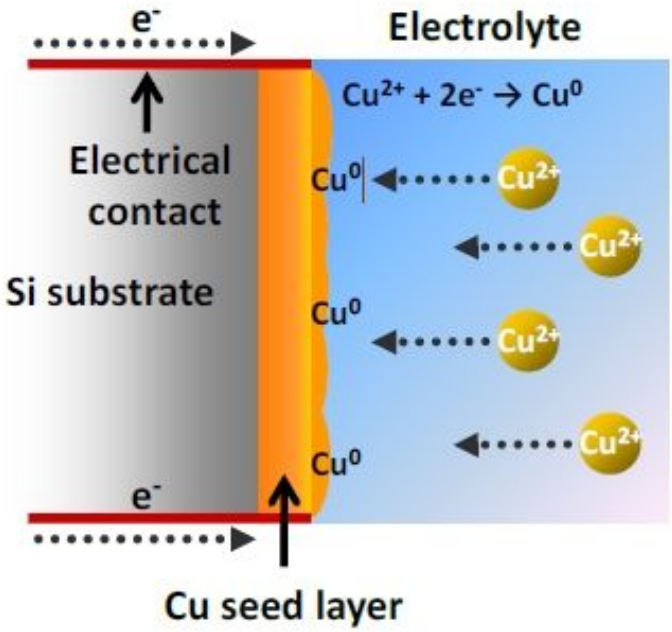

Fig. 4. A simple diagram of Cu electrodeposition.

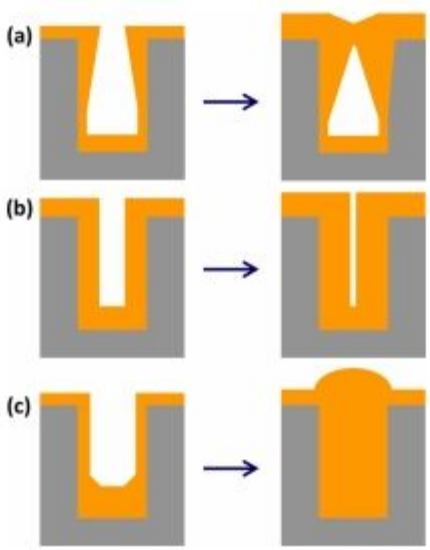

Fig. 5. The class of the filling profiles; (a) subconformal; (b) conformal; (c) superconformal profiles.

1.3. Organic additives

Bottom-up filling of Cu is not easily accomplished. To achieve bottom-up filling of trench, control of the deposition rate is required at the different regions of trenchs. That is selective reduction or enhancement of the deposition rate at the top or at the bottom surface of the trench, respectively. Organic additives can do this work. The organic additives affect the deposition rate according to the region of trench by adsorbing on the Cu surface.[31,32] They can be classified into three groups : accelerator, suppressor and leveler.

The accelerator usually has disulfide bonds (-S-S-) or mercapto functional group (-SH) and enhances the deposition rate at the bottom of the feature. [30,33,34,] The typical accelerators are listed in Table 1. Among them, bis(3-sulfopropyl) disulfide (SPS) is the most famous accelerator. The accelerators enhance the deposition rate by adsorbing on the Cu surface. They make a complex with Cu^{2+} to form Cu^{+}. Since the rate determining step is reduction of Cu^{2+} to Cu^{+}, the deposition rate increase by assist of accelerators.

The suppressors, which reduce the electrodeposition rate, usually have polyether group.[35,36,37] Polyethylene glycol (PEG), polypropylene glycol (PPG), and PEG-PPG block copolymer are the representative suppressors. In addition to PEG, chloride ion (Cl^{-}) is also added as an additive. Cl^{-} has ability to adsorb on the Cu surface without the solvation, like the other halogen ions. The solely adsorbed Cl^{-} is known to have acceleration effect of Cu electrodeposition.[38] When PEG is added with Cl^{-}, however, suppression of Cu electrodeposition occurs. PEG makes complex of PEG-Cu^{+}-Cl-Cu surface with lone-pair of oxygen atom of PEG. This complex blocks the electron transfer from Cu surface by approaching Cu ions through an inner sphere Cl bridge, which results in the suppression of Cu deposition.[35,37,39]

The proper combination of suppressing and accelerating effects at the different position of trench results in successful bottom-up filling. The common additive system consists of PEG, Cl^-, and SPS as suppressors and an accelerator, respectively. With this additive system, the complex of PEG-Cl first adsorbs on the Cu surface. As time passes, SPS starts to displace the PEG-Cl^- layer because of the stronger adsorption strength of SPS than that of PEG. Gradual increase of Cu electrodeposition rate is due to this replacement of the PEG-Cl layer by SPS.

Levelers are the third type of additives. They are also called as secondary suppressors because levelers show suppression effect. To adjust the level of Cu surface having topologic variations and to form a flat surface, levelers are added. The flat surface of Cu can be realized by adding levelers which produce relatively thick deposit of Cu in the recessed area and thin deposit on the protruded area. Unlike suppressors and accelerators, levelers have distinctive property which is called convection-dependent adsorption.

Table 1. The representative accelerators for Cu electrodeposition

Representative accelerators	*Molecular structure*
Bis(3-sulfopropyl) disulfide (SPS)	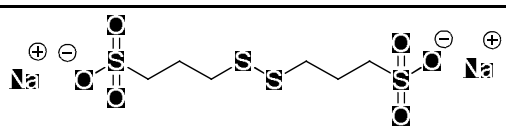
3-Mercapto-1-propanesulfonic acid (MPSA)	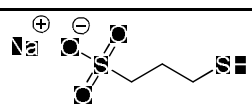
3-*N,N*-Dimethylamonodithiocarbamoy-1-propanesulfonic acid (DPS)	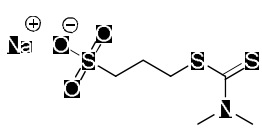

1.4. Distinctive property of levelers and design of new levelers

As mentioned above, the convection-dependent adsorption behavior is the distinctive property of levelers that no other additives have. Since the convection environment is different according to the position of trench, the convection-dependent adsorption is the key factor for bottom-up filling process. The flow of solution is certainly the highest at the outside of features, and it gradually diminishes along to the bottom of the trench. The degree of difference of flow rate between the top and bottom surface of trench is larger in the case of TSV like trench having high aspect ratio. It is predicted that the strong vortex of fluid motion at the opening and almost negligible fluid motion at the bottom of TSV-like trench. In this paper, the rotating speed of Cu RDE (rotating-disk electrode) was adjusted to 0 rpm and 1000 rpm to replicate this situation.[40] Strong fluidic motion, which is the situation of opening of TSV-like trench, corresponded to 1000 rpm, and negligible fluidic motion, which is the situation of the bottom of TSV-like trench, corresponded to 0 rpm.

Unlike the other additives, few researchers have been studied on the levelers. Therefore, many unsolved questions are left about the leveler: Which functional groups of the leveler is the adsorption site and how they adsorb on the Cu surface? What causes the convection-dependent adsorption behavior of levelers? The bottom-up filling is the result of the interaction between additives. Since the filling performance of Cu electrodeposition solution is not reflected the individual additives, investigate of the leveler remains a challenge.[40]

I particularly was interested in the structure of levelers and how they function as levelers. To investigate the properties of leveler closely, I thought it is necessary

to conduct the structure-activity relationship (SAR) study and have decided to synthesize new levelers having simple structure to conduct SAR study. Although many questions about the levelers left unclear, there have been many structures of levelers reported. The reported levelers are listed in table 2.[41-45] Note that the reported levelers generally contain amine or ammonium functional groups and halide counter ions. It was considered that Cu filling performance in the TSV was affected by the adsorption behavior of levelers, which was strongly influenced by their structures. Therefore, I have concluded the ammonium functional group, and halide counter ions are the key factors of effective levelers. In addition to these two functional groups, I focused on the structure of suppressor due to the fact that the levelers act as suppressors when the atmosphere is under strong convection. PEG and PPG, which are the most commonly used suppressors, have a polyether group. Therefore, I have chosen ethylene glycol group, which is a repeating unit of polyether, as a center chain of a new leveler.

In this study, I have synthesized four levelers having different center chains, which are shown in Fig. 6. These levelers have trimethyl ammonium groups at both ends of the center chains and iodide ions as counter anion in common. To find out the effect of center chains, the adsorption behavior of the synthesized levelers was examined by linear sweep voltammetry (LSV) which is a method of electrochemical analysis. Finally, the levelers were applied to Cu gap-filling with accelerator and suppressor.

Table 2. The reported levelers

Name of the levelers	*Molecular structure*
Janus green B (JGB)	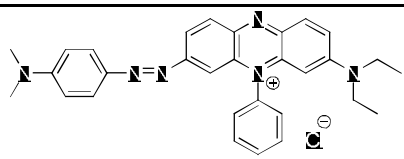
Nitrotetrazolium blue chloride monohydrate (NTBC)	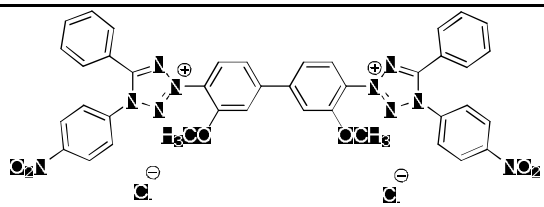
Methylene violet 3RAX (MV)	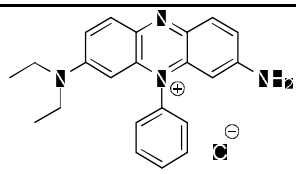
Polyethyleneimine (PEI)	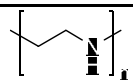
Diallylamine copolymers	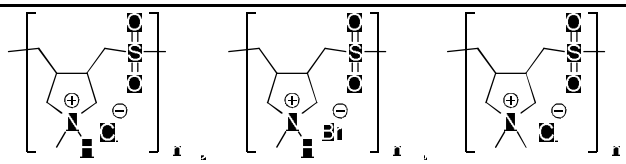

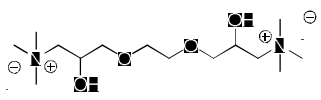

(a) Lev (1)

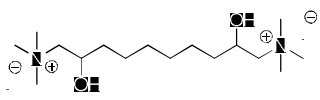

(b) Lev (2)

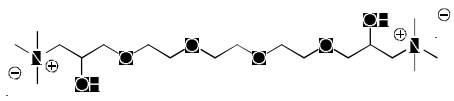

(c) Lev (3)

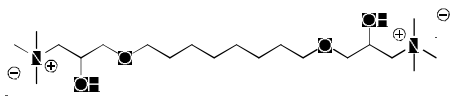

(d) Lev (4)

Fig 6. The structure of synthesized levelers.

2. General Procedure for Electrochemical Analyses

2.1. Electrochemical analyses of synthesized levelers

The adsorption of synthesized levelers was examined by linear sweep voltammetry by a potentiostat (273A, EG&G Princeton Applied Research Corporation). The basic electrolyte was composed of 1.0 M $CuSO_4 \cdot 5H_2O$ (Samchun Chemical), 0.5 M H_2SO_4 (Daejung Chemicals & Metals), and 1.37 mM Cl^- (from NaCl form, Samchun Chemical). To clarify the effect of levelers, the levelers were additionally added into the electrolyte. The levelers were denoted as 'Lev (1)', 'Lev (2)', 'Lev (3)' and 'Lev (4)', and their structures are shown in Fig. 1.6. The concentrations of levelers were fixed to 50 μM in all experiments. Also, poly(ethylene glycol)-block-poly(propylene glycol)-block-poly(ethylene glycol) (average Mn ~ 1,100, denoted as 'PEG-PPG', Sigma-aldrich) and bis(3-sulfopropyl) disulfide (denoted as 'SPS', RASCHIG GmbH) were adopted as the suppressor and accelerator for analyses of interactions of additives (leveler, accelerator, and suppressor). The concentrations of the suppressor and the accelerator were 50 μM and 10 μM, respectively. The temperature of electrolyte was fixed at 25 ˚C by a thermostat. LSV was performed in a three-electrode system, consisting of Cu rotating disk electrode (RDE, 0.196 cm^2 of geometric area, polished with 2000 grit sandpaper prior to every single analysis) as a working electrode, a 99.9% Cu wire as a counter electrode, and Ag/AgCl (KCl saturated) electrode as a reference electrode. LSV was carried out with sweeping the potential from 150 mV (vs. Ag/AgCl) to -350 mV at 10 mV/s of scan rate.

2.2. Cu gap-filling test by electrodeposition

Trenches with 40 μm of depth and 9 μm of width have been used for gap-filling test. The filling test was conducted by Cu electrodeposition. The diffusion barrier layer and Cu seed layers of trenches were deposited on SiO_2 as follows; Cu seed layer (1.2 μm at the top and 300 nm at the bottom of trench, physical vapor deposition, PVD) / Ta (25 nm, PVD) / TaN (50 nm, PVD) / SiO_2. The fragmented wafer was loaded in a Teflon holder, and immersed in ethanol for 30 s. The exposed area to the electrolyte of fragmented wafer was 1 cm^2. The electrolytes contained 10 μM SPS, 50 μM PEG-PPG, and 50 μM synthesized levelers. In addition, the same basic electrolyte was composed as the same components as used in LSV analysis. The rotating speed of fragmented wafer was 1000 rpm during Cu electrodeposition. The current density for Cu electrodeposition was fixed to -15 mA/cm^2, and the deposition time was 750 s regardless of the electrolytes. The potential response was measured by a potentiostat in the same manner as the electrochemical analyses. The cross-sectional profiles were observed by means of a field emission scanning electron microscope (FESEM, S-4800, Hitachi).

3. Results and Discussion

3.1. Lev (1)

3.1.1. Synthesis of Lev (1)

The two functional groups have been chosen to be introduced into Lev (1). Ammonium was a first functional group, and it has been chosen because of the fact that majority of the reported levelers contain ammoniums.[41-46] This ammonium functional group was expected to be highly related to the convection-dependent adsorption behavior. Another functional group I had concerned is ethylene glycol unit. Polyethylene glycol (PEG), which is a typical suppressor, is composed of ethylene glycol. The oxygen of the ethylene glycol unit is known to form a complex with Cu^{+} and Cl^{-} ions on the Cu surface of electrode, which blocks the approaching Cu ions on the electrode. For these reasons, ethylene glycol unit has been selected as a center chain, and two ammoniums have been introduced to the both ends of a new leveler.

A synthetic scheme of Lev (1) is shown in Scheme 1. Ethylene glycol was selected as a starting material, and allyaltion of the ethylene glycol successfully produced corresponding diallyl 1. In order to introduce the amino group, the epoxidation with *meta*-chloroperoxybenzoic acid (*m*CPBA) was conducted to form corresponding diepoxide 2, and the following epoxide opening by *N,N*-dimethylamine produced the corresponding diamine compound (3). Final methylation at the terminal tertiary amino groups at the both ends resulted in the formation of Lev (1) in overall 46% yields.

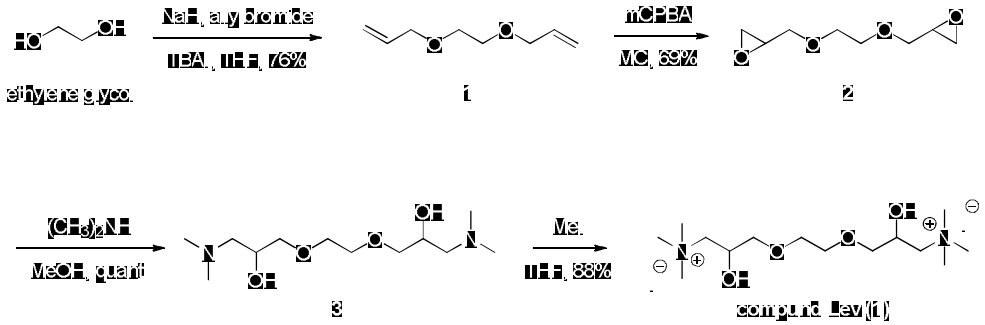

Scheme 1. Synthesis of Lev (1) from ethylene glycol.

3.1.2. Electrochemical analysis of Lev (1)

To investigate the adsorption characteristics of Lev (1), linear sweep voltammetry was conducted in the absence of other additives. As I mentioned above, convection-dependent adsorption of a leveler is a key characteristic for successful bottom-up filling. Generally, the different convection atmosphere is formed according to the position of TSV in the electrodeposition solution. In other words, the flow of solution is certainly higher at the opening of features, and it gradually diminishes along to the bottom of the trench. The degree of difference of flow rate between the top and the bottom surface of trench is larger in the case of TSV due to its high aspect ratio. It is predicted that the strong vortex of fluid motion at the opening and almost negligible fluid motion at the bottom of TSV. To replicate this atmosphere, LSV was conducted with the adjusted rotating speed of Cu RED to 0 rpm or 1000 rpm. The opening of TSV, which is under strong convection atmosphere, corresponded to 1000 rpm, and the bottom of TSV, which is under negligible fluidic motion, corresponded to 0 rpm. Linear sweep voltammograms of electrolytes with Lev (1), and without Lev (1) is shown in Fig. 7. In the absence of Lev (1), there was no considerable difference in voltammograms between 0 rpm

and 1000 rpm (Fig. 7 (a)). Although there was difference in the region of over -100 mV range, this is due to the concentration of Cu ions at the surface of electrode. As the potential continuously increase in negative direction, the concentration of Cu ions near working electrode decreased by reduction. Under 0 rpm, diffusion is only component for transferring Cu ions, so the concentration of Cu ions near the working electrode was relatively low, resulting in the reduction of current. Under 1000 rpm, however, strong convection helps the transport of Cu ions to the working electrode, so that there is a large amount of Cu ions near electrode. In contrast to Fig. 7 (a), the difference of voltammograms according to the rotating speed could be observed in the presence of Lev (1)(Fig. 7 (b)). There was obvious strong suppression effect under 1000 rpm condition while little suppression under 0 rpm. This change in suppression effect under different rotating speeds of Cu RDE can be referred as ‘convection-dependent adsorption.

The adsorption of Lev (1) in the presence of other additives and the interactions between Lev (1) and other additives have also been investigated. At first, the Lev (1) in the presence of PEG-PPG (suppressor, PEG-PPG-PPG block copolymer, average Mn ~ 1,100) was examined. (Fig. 8) Linear sweep voltammogram was obtained in the same way described above. When only PEG-PPG was added as an additive, there was strong suppression in both 0 rpm and1000 rpm condition, and no differences in voltammograms according to the rotating speed observed (Fig. 8 (a)). This suppression arose only from PEG-PPG, and it was stronger than that of Lev (1) (Fig. 7. (b) vs Fig. 8. (a)). In the presence of Lev (1) with PEG-PPG, no differences in voltammograms according to the rotating speed observed (Fig. 8 (b)). Note that the stronger suppression effect occurred in the presence of Lev (1) (Fig. 8 (a) vs Fig. 8 (b)). This observation implied that the suppression effect of PEG-PPG is enhanced by co-adsorption with Lev (1) regardless of the rotating speed of Cu

RDE. The convection-dependent adsorption of Lev (1) was not detected in presence of PEG-PPG.

Second, the Lev (1) in the presence of PEG-PPG (suppressor, PEG-PPG-PPG block copolymer, average Mn ~ 1,100), and SPS (accelerator, bis(3-sulfopopyl) disulfide) was examined (Fig. 9). In case of voltammogram without Lev (1), by adding SPS to PEG-PPG (Fig. 9 (a)), reduced suppression was observed regardless of convection conditions, while suppression in 1000 rpm condition was stronger than that in 0 rpm (Fig. 8 (a) vs Fig. 9 (a)). This observation implied that competitive adsorption between SPS and PEG-PPG occured, and the effect of SPS was stronger under 0 rpm than 1000 rpm condition. However, when the Lev (1) was added to PEG-PPG and SPS combination, the reduction of suppression effect was observed only in 0 rpm condition (Fig. 9. (b)). This observation implied that the competitive adsorption between SPS and PEG-PPG, Lev (1) occured only under 0 rpm condition, which meat the effect of SPS under 1000 rpm was almost completely eliminated by adding the Lev (1) The SPS only adsorbed on the Cu surface under 0 rpm resulting in the reduction of suppression effect. Therefore, the considerable convection-dependent adsorption was achieved with enhancement of Cu reduction selectively under 1000 rpm condition by adding the Lev (1) into the combination of PEG-PPG and SPS.

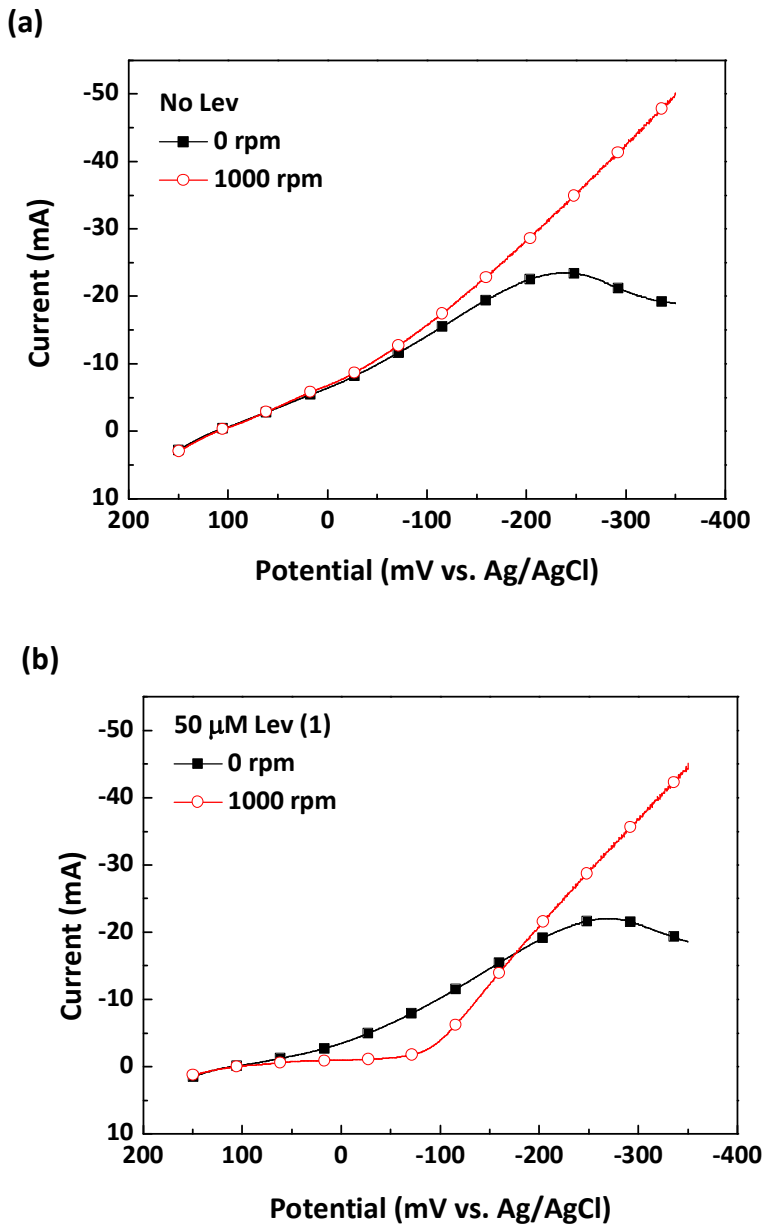

Fig. 7. Linear sweep voltammograms according to the rotating speed of Cu RDE (a) without and (b) with Lev (1). The basic electrolyte consisted of 1.0 M $CuSO_4$, 0.5 M H_2SO_4, 1.37 mM Cl^-.

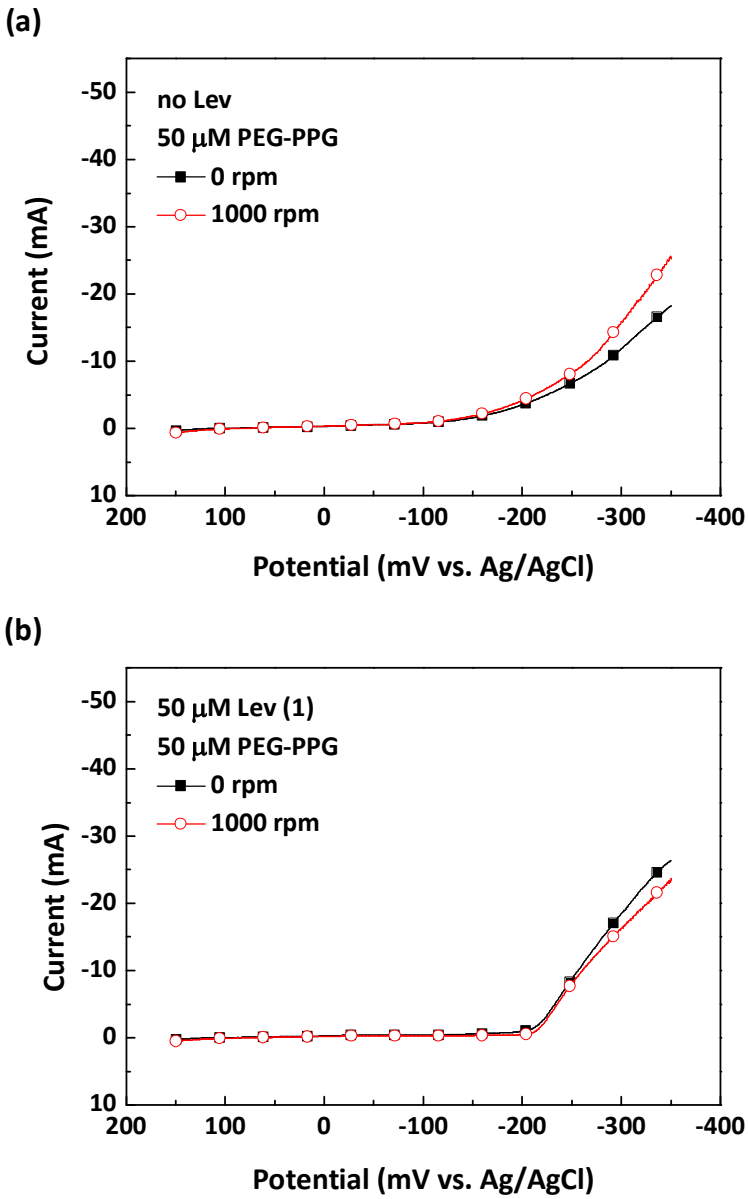

Fig. 8. Linear sweep voltammograms according to the rotating speed of Cu RDE (a) without Lev (1), (b) with Lev (1) in the presence of 50 μM of PEG-PPG. The basic electrolyte consisted of 1.0 M $CuSO_4$, 0.5 M H_2SO_4, 1.37 mM Cl^-.

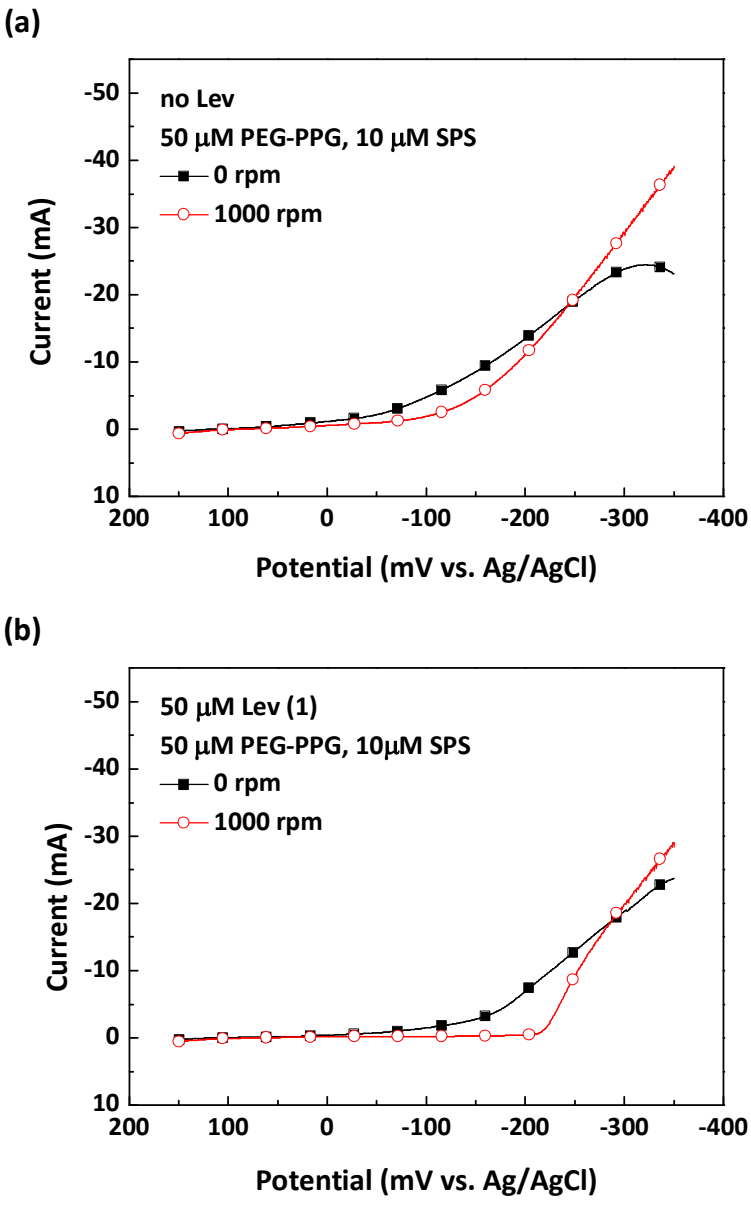

Fig. 9. Linear sweep voltammograms according to the rotating speed of Cu RDE (a) without Lev (1), (b) with Lev (1) in the presence of 50 μM of PEG-PPG and 10 μM of SPS. The basic electrolyte consisted of 1.0 M $CuSO_4$, 0.5 M H_2SO_4, 1.37 mM Cl^-.

3.2. Lev (2), Lev (3), and Lev (4)

Encouraged by the LSV analyses of Lev (1), I decided to modify the structure of Lev (1). The center chain of Lev (1) has been modified.

3.2.1. Synthesis of Lev (2)

The ethylene glycol unit was introduced to Lev (1) as the center chain since it is a repeating unit of PEG, which is a typical suppressor. As I mentioned above, the oxygen of the ethylene glycol unit forms a complex with Cu^{+} and Cl^{-} ions on the Cu surface on the electrode, which blocks the approaching Cu ions on the electrode. To confirm whether the ethylene glycol unit is related with convection-dependent adsorption, I have designed the Lev (2) (Fig. 6 (b)). The Lev (2) has the same structure with the Lev (1) except that it has no ether bond at the center chain.

A synthetic scheme of Lev (2) is shown in Scheme 2. 1,9-Decadiene was selected as a starting material, and the epoxidation with *m*CPBA of the starting material successfully produced corresponding diepoxide 4. In order to introduce the amino group, opening of epoxide ring by *N,N*-dimethylamine produced the corresponding diamine 5. The diepoxide 4 was purified by column chromatography. The diamine 5 was hydrophobic enough to be extracted by ethyl acetate while diamine 3 of Lev (1) could not be extracted by organic solvent due to its high polarity. The extracted compound 5 was highly pure based on ^{1}H-NMR analysis, further purification was left out. The final methylation at the terminal tertiary amino groups at the both ends results in formation of Lev (2) in overall 50% yields.

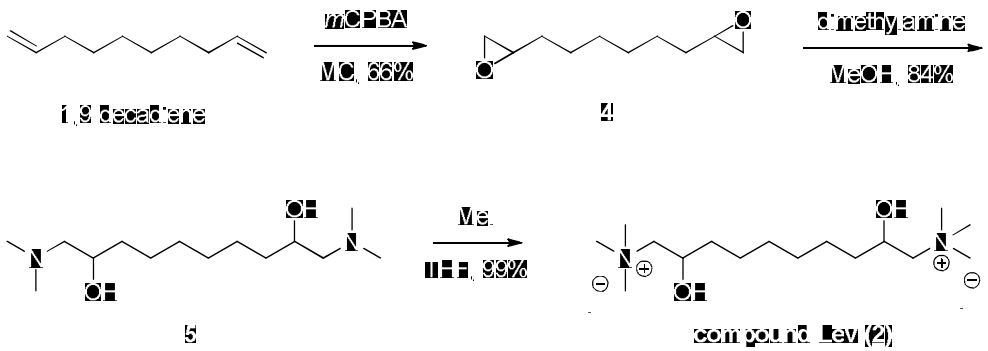

Scheme 2. Synthesis of Lev (2) from 1,9-decadiene.

3.2.2. Synthesis of Lev (3)

The leveler having triethylene glycol center chain (Lev (3), Scheme 3) has also been synthesized for confirming the effect of longer ethylene glycol unit. Stronger convection-dependent adsorption would be observed if the convection-dependent adsorption behavior was come from ethylene glycol unit.

A synthetic scheme of Lev (3) is shown in Scheme 3. Triethylene glycol was selected as a starting material, and allyaltion of the triethylene glycol successfully produced corresponding diallyl 6. In order to introduce the amino group, the epoxidation with *meta*-chloroperoxybenzoic acid (*m*CPBA) was conducted to form corresponding diepoxide 7, and following epoxide opening by *N,N*-dimethylamine produced the corresponding diamine 8. The diallyl 6 and diepoxide 7 were purified by column chromatography, while the diamine 8 was not, because of its high polarity. The diamine 8 was extracted by distilled water. The final methylation at the terminal tertiary amino groups at the both ends results in formation of Lev (3) in overall 45% yields.

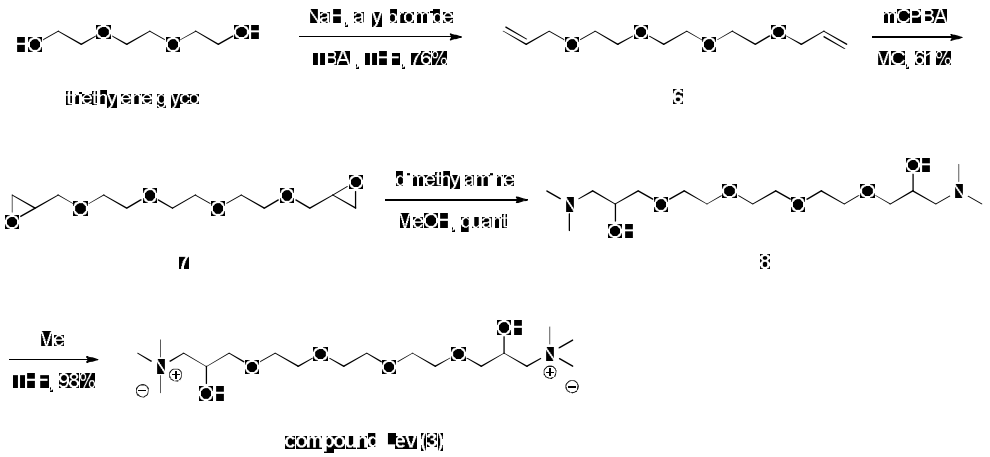

Scheme 3. Synthesis of Lev (3) from triethylene glycol.

3.2.3. Synthesis of Lev (4)

The leveler having 1,8-octanediol ether center chain (Lev (4), Scheme 4) has also been synthesized to compare with Lev (3). The Lev (3) has highly polar center chain which is the triethylene glycol unit. The 1,8-octanediol ether center chain is much less polar than triethylene glycol. Since the number of atoms in the Lev (3) and Lev (4) are the same, it was expected that the influence of center chain polarity on convection-dependent adsorption would be examined by comparing Lev (3) with Lev (4).

A synthetic scheme of Lev (4) is shown in Scheme 4. 1,8-Octanediol was selected as a starting material, and allyaltion of the 1,8-octanediol at 50 ^{o}C successfully produced corresponding diallyl 9. In order to introduce the amino group, the epoxidation with *meta*-chloroperoxybenzoic acid (*m*CPBA) was conducted to form corresponding diepoxide 10, and following epoxide opening by *N,N*-dimethylamine produced the corresponding diamine 11. The diallyl 9 and

diepoxide 10 were purified by column chromatography, while the diamine 11 was not, because of its high polarity. The diamine 11 was extracted by distilled water. The final methylation at the terminal tertiary amino groups at the both ends results in formation of Lev (4) in overall 25% yields.

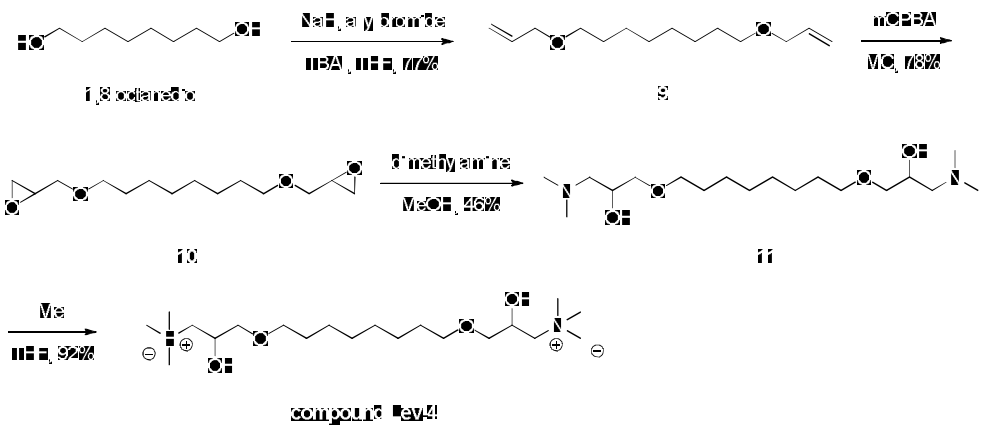

Scheme 4. Synthesis of Lev (4) from 1,8-decanediol.

3.2.4. Electrochemical analyses of Lev (2), Lev (3), and Lev (4)

Linear sweep voltammetry of synthesized levelers in the absence of other additives were also conducted, and the results are shown in Fig. 10 (a), (b), (c) which are the voltammograms of Lev (2), Lev (3), and Lev (4), respectively. Comparing with Fig. 7 (a), it was obvious that all of the synthesized levelers have convection-dependent adsorption nature. Note that 0 rpm and 1000 rpm represent the fluidic situation of the bottom and top surface of the TSV, respectively.

Voltammograms of all synthesized levelers including Lev (1) in the absence of other additives according to the convection rate are shown in Fig. 11. Under the 0 rpm condition, all the levelers showed little suppression effect comparing to the voltammogram of without leveler. In other words, little amounts of the levelers

adsorb on the Cu surface of electrode under negligible convection. The difference of suppression effect between them was not considerable. Under the 1000 rpm condition, however, strong suppression effects of all levelers were observed, which meant large amounts of the levelers strongly adsorbed on the Cu surface of electrode. Besides, considerable difference of suppression effect between the levelers was observed unlike the results under 0 rpm condition. The suppression effects of the levelers are increased in order of Lev (1) ≒ Lev (2) < Lev (3) < Lev (4). From these results, two kinds of information about structure activity relation of levelers can be inferred.

First, the longer center chain a leveler possessed, the stronger adsorption behavior observed. Comparing the voltammograms of the levelers having short center chains (Lev (1), Lev (2)) to the levelers having long center chains, (Lev (3), Lev (4)) a definite stronger suppression effects of the latter observed under 1000 rpm condition (Fig. 11 (b)).

Second, the levelers having aliphatic center chains showed better suppression effects than those having ethylene glycol center chains (Fig. 11 (b)). Comparing the voltammograms of all synthesized levelers, the levelers having aliphatic center chains (Lev (2), Lev (4)) showed better suppression effects even if the differences were bigger in comparison between Lev (3) and Lev (4). The same trend of suppression strength was observed under both 0 and 1000 rpm according to the levelers. However, the differences under 0 rpm were not considerable, which meant the adsorption characteristics of the levelers enhanced under strong convection condition.

The synthesized levelers in the presence of PEG-PPG (suppressor) were also examined by LSV (Fig. 12). Similar to the results of Lev (1) (Fig. 8), stronger suppression effect showed in the presence of the synthesized levelers. It was implied that the suppression effect of PEG-PPG was enhanced by co-adsorption

with the levelers. The convection-dependent adsorption of levelers was not detected in the presence of PEG-PPG. Voltammograms of all synthesized levelers including Lev (1) in the presence of PEG-PPG according to the convection rate are shown in Fig. 13. Unlike the results of the levelers in the absence of other additives, there were almost no differences between the levelers in the presence of PEG-PPG. Even though there were some differences in the region of over -200 mV range under 1000 rpm condition (Fig 13 (a)), these deserve little consideration since the co-adsorption layer of the levelers and PEG-PPG was already broken in these region. Therefore, the co-adsorption of the synthesized levelers and PEG-PPG was consistent regardless of the center chain structures of levelers

Finally, the synthesized levelers in the presence of all other additives which are PEG-PPG and SPS were examined by LSV (Fig. 14). All the synthesized levelers showed convection-dependent adsorption behaviors in the presence of PEG-PPG and SPS. The levelers strongly co-adsorbed on the Cu surface under 1000 rpm condition, and the competitive adsorption of SPS, PEG-PPG and the levelers occurred under 0 rpm condition. Taking a look at Fig. 15, there were almost no differences between the synthesized levelers like the results of the levelers with PEG-PPG. These results implied that center chain structures of the levelers have negligible effect on the interaction with other additives.

To summarize the above analyses, it was confirmed that the all synthesized levelers showed convection-dependent adsorption behaviors in the absence of other additives. In addition, the strength of the convection-dependent behavior was different according to the center chains of levelers. The longer, and aliphatic center chains showed stronger adsorption on the Cu surface, and the differences in adsorption between the levelers were greater under 1000 rpm that at 0 rpm. In the presence of PEG-PPG and SPS, the synthesized levelers co-adsorbed on the Cu surface with PEG-PPG under strong convection, resulting enhancement of

suppression whereas these co-adsorbed layers underwent competitive adsorption with SPS were not observed under negligible convection, resulting decrease in suppression of Cu reduction. The differences in suppression effect according to the synthesized levelers were not detected in the presence of PEG-PPG and SPS. These results implied that the interactions of the levelers were consistent regardless of the center chain structures of the levelers.

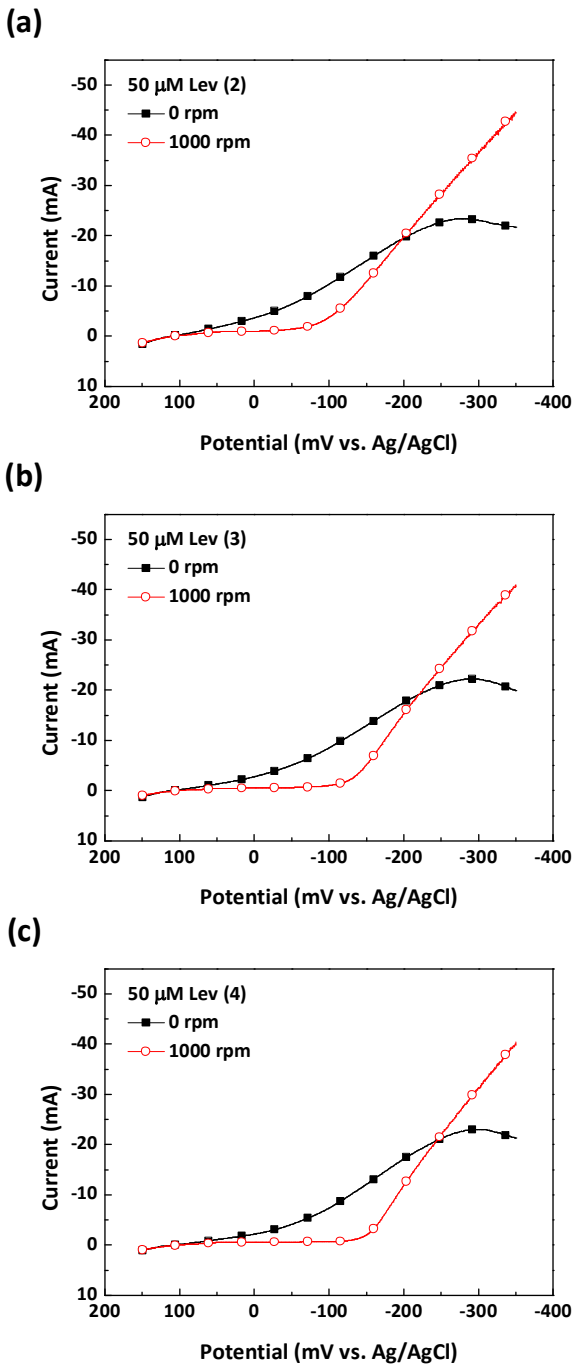

Fig. 10. Linear sweep voltammograms of (a) Lev (2) (b) Lev (3) (c) Lev (4) according to the rotating speed of Cu RDE. The basic electrolyte consisted of 1.0 M $CuSO_4$, 0.5 M H_2SO_4, 1.37 mM Cl^-.

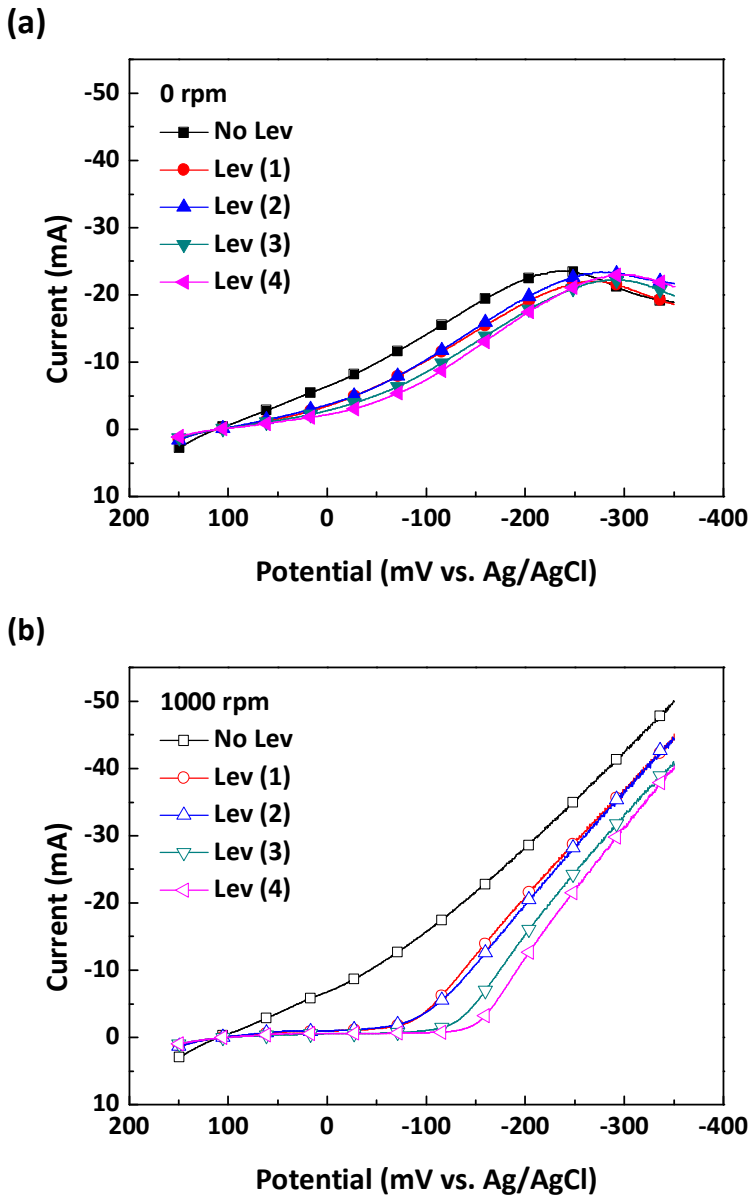

Fig. 11. Linear sweep voltammograms of all synthesized levelers in the absence of other additives under (a) 0 rpm, (b) 1000 rpm. The basic electrolyte consisted of 1.0 M $CuSO_4$, 0.5 M H_2SO_4, 1.37 mM Cl^-

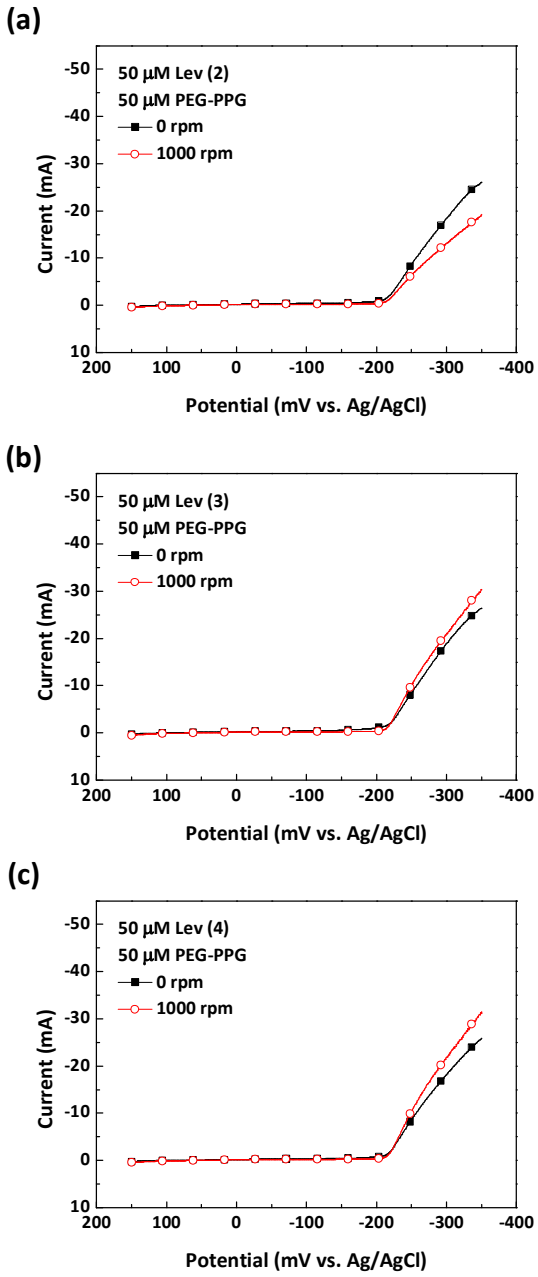

Fig. 12. Linear sweep voltammograms of (a) Lev (2), (b) Lev (3), and (c) Lev (4) in the presence of 50 μM of PEG-PPG according to the rotating speed of Cu RDE. The basic electrolyte consisted of 1.0 M $CuSO_4$, 0.5 M H_2SO_4, 1.37 mM Cl^-.

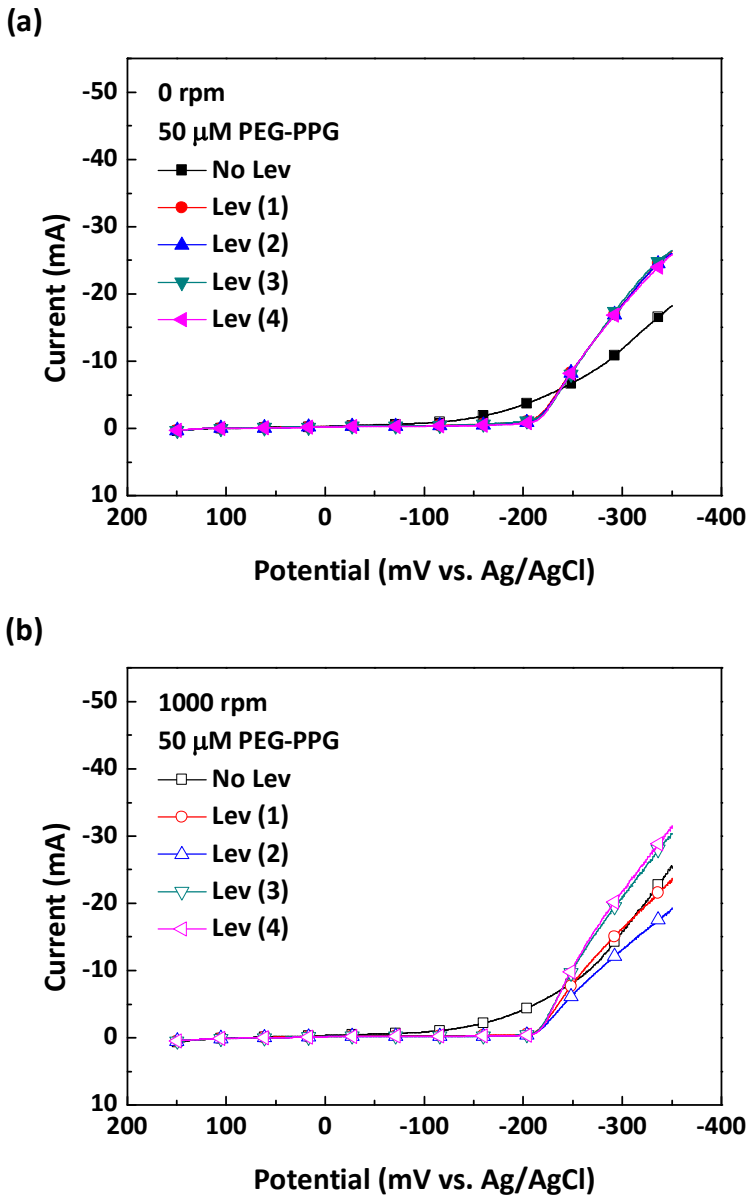

Fig. 13. Linear sweep voltammograms of all synthesized levelers in the presence of PEG-PPG under (a) 0 rpm, (b) 1000 rpm. The basic electrolyte consisted of 1.0 M $CuSO_4$, 0.5 M H_2SO_4, 1.37 mM Cl^-.

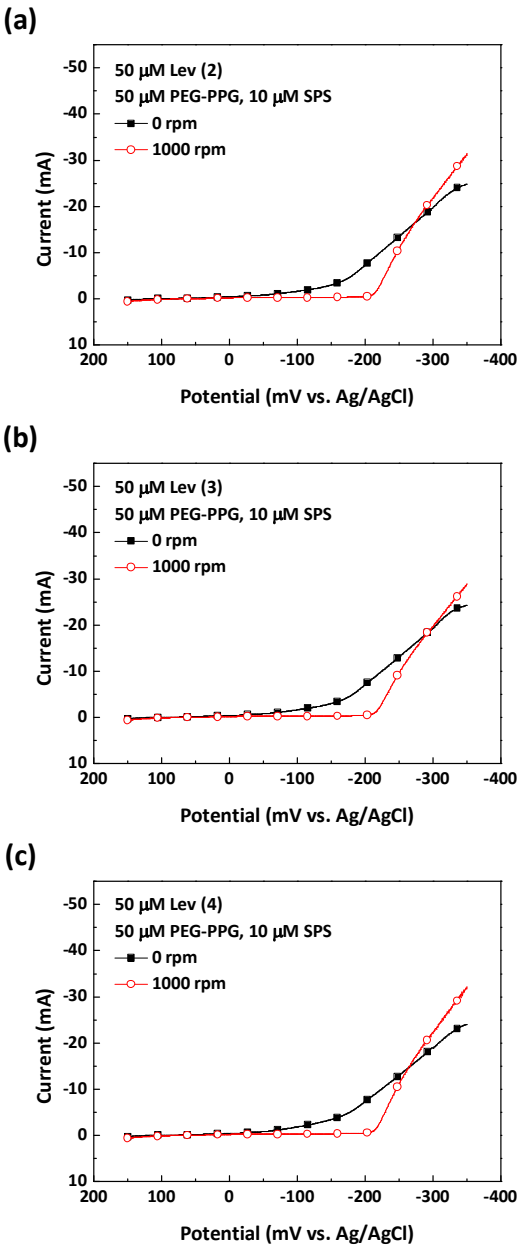

Fig. 14. Linear sweep voltammograms of (a) Lev (2), (b) Lev (3), and (c) Lev (4) in the presence of 50 μM of PEG-PPG and 10 μM of SPS according to the rotating speed of Cu RDE. The basic electrolyte consisted of 1.0 M $CuSO_4$, 0.5 M H_2SO_4, 1.37 mM Cl^-.

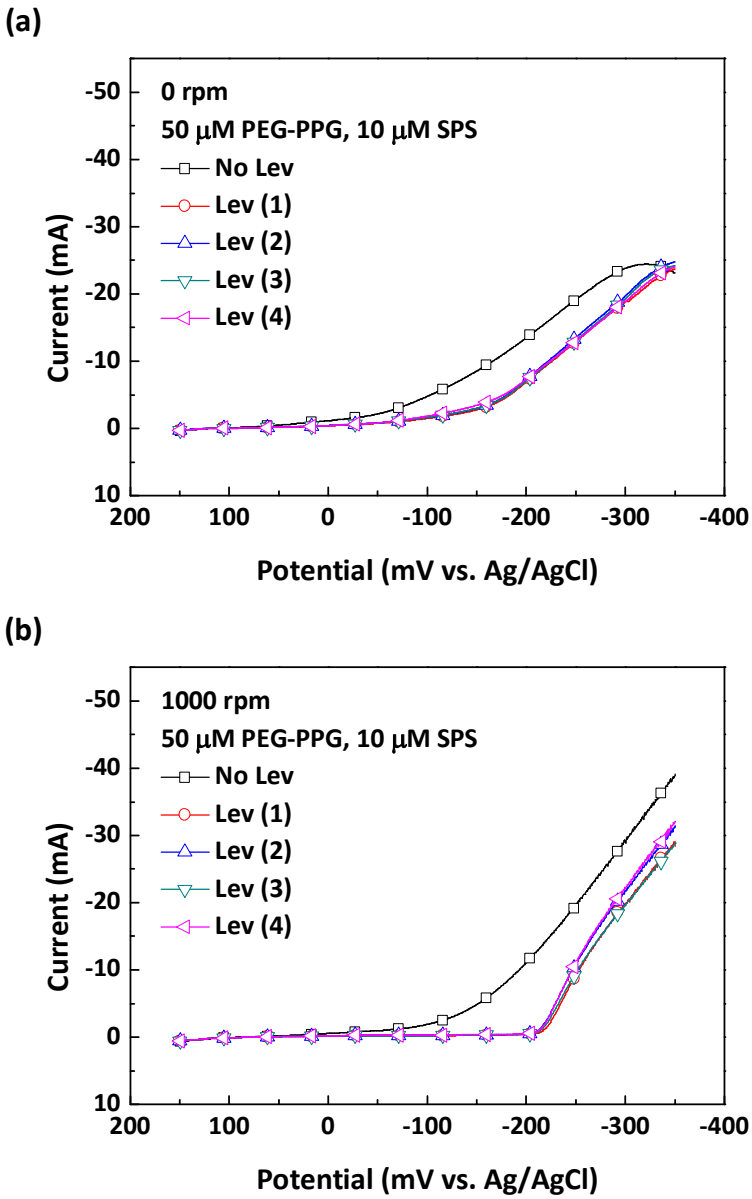

Fig. 15. Linear sweep voltammograms of all synthesized levelers in the presence of PEG-PPG and 10 μM of SPS under (a) 0 rpm, (b) 1000 rpm. The basic electrolyte consisted of 1.0 M $CuSO_4$, 0.5 M H_2SO_4, 1.37 mM Cl^-.

3.3 Gap-filling test

Based on the electrochemical analyses of the levelers above, the defect-free filling of trenches was anticipated. To confirm this anticipation, four synthesized levelers have been applied on the gap-filling tests in the presence of PEG-PPG and SPS, and gap-filling was also applied without levelers. To apply the strong convection environment around trenches, the test was conducted under 1000 rpm rotating speed. Trenches with 40 μm of depth and 9 μm of width have been used for gap-filling test. As I mentioned above, since trenches are narrow and deep, the bottom of trench was expected to experience negligible convection, while the top was expected to experience strong convection. The resulted gap-filling profiles are shown in Fig. 16.

In the absence of the levelers, conformal deposition profile was obtained (Fig. 16 (a)). However, the trench was not filled completely, and it was expected to form seam under extended deposition time. Note that considerable amounts of Cu deposition layer were formed on the top of trenches. It meant suppression effect was not enough to prevent approaching of Cu ions on this region. This almost conformal profile could be achieved by the interaction of PEG-PPG and SPS. This is results of little convection-dependent adsorption behavior of PEG-PPG and SPS (Fig. 9 (a)). To achieve the successful bottom-up filling, suppression effect on the top of trench should be enhanced. According to the results of voltammograms of the levelers with PEG-PPG and SPS, the bottom-up filling was able to achieve by adding the levelers to the prior electrolyte.

The gap-filling results of Lev (1), (2), (3), and (4) with the combination of PEG-PPG, and SPS are shown in Fig. 16 (b), (c), (d), and (d), respectively. As expected, complete filling of Cu in the trenches was obtained by adding the synthesized levelers. For all synthesized levelers, bottom-up filling was observed,

and these results correspond to the results of linear sweep voltammograms Fig. 15. There were no differences in suppression effect between the levelers in the presence of other additives while different suppression was observed when the levelers used as only additive (Fig. 11). In addition, suppression was significantly enhanced by assistance of the synthesized levelers. In comparison to the filling results without any levelers, almost complete inhibition of Cu deposition on the top surface was achieved with the levelers, and this is the results of the special convection dependent adsorption of the levelers.

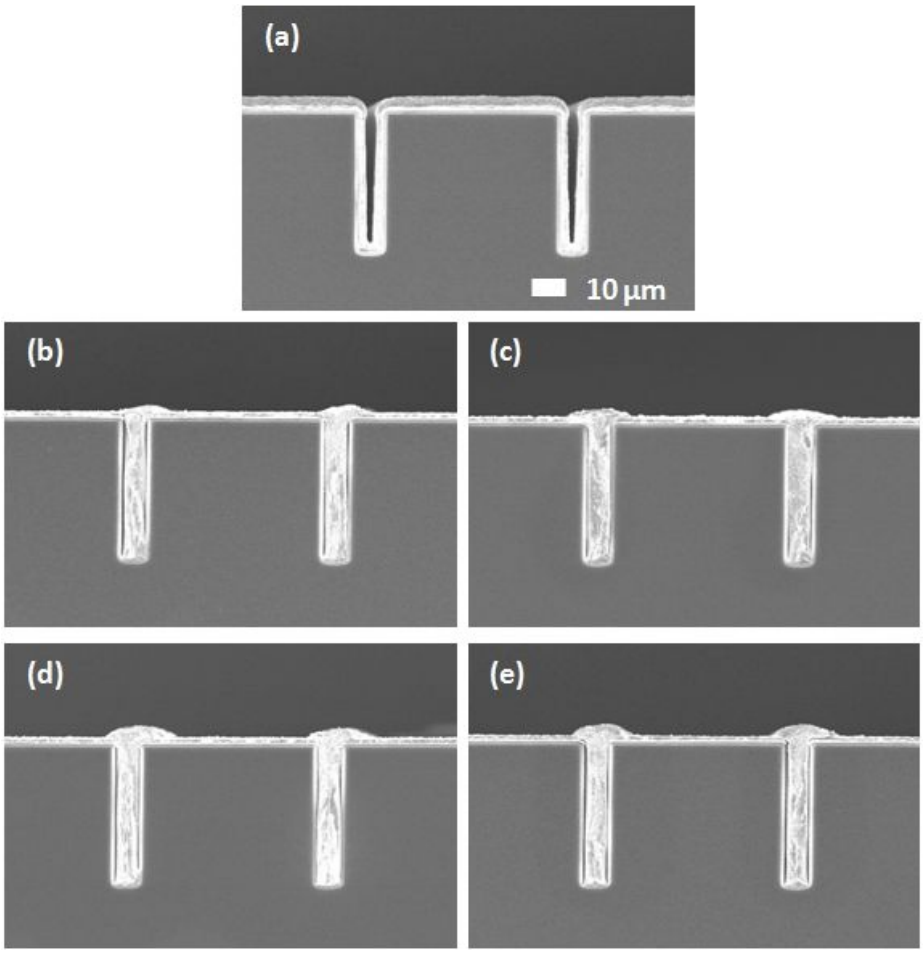

Fig. 16. The cross-section images of trenches filled (a) without leveler, with (b) Lev (1), (c) Lev (2), (d) Lev (3), and (e) Lev (4).

4. Conclusions.

Four new levelers having ammonium functional groups at the both ends and various center chains have been synthesized. It was confirmed that all synthesized levelers showed convection-dependent adsorption behavior when the leveler was applied as a sole additive. There were differences in adsorption strength between the synthesized levelers. The levelers having longer and aliphatic center chains structure showed stronger adsorption behaviors on the Cu surface. Interactions of the synthesized levelers with PEG-PPG and SPS have been also investigated. First, interactions of the synthesized levelers with PEG-PPG resulted in synergistic suppression of Cu reduction under both 0 and 1000 rpm condition. This synergistic suppression arose from co-adsorption of the levelers and PEG-PPG. Second, interactions of the levelers with PEG-PPG and SPS resulted in convection-dependent adsorption. Under 1000 rpm condition, co-adsorption of the levelers and PEG-PPG was dominant, and the effect of SPS was negligible, resulting significant suppression of Cu reduction. However, under 0 rpm condition, the competitive adsorption between SPS and PEG-PPG, levelers occurred, resulting decrease in Cu reduction. The differences in adsorption strength according to the synthesized levelers were not detected in the presence of PEG-PPG and SPS. These results implied that the co-adsorption caused by the interactions of the levelers and PEG-PPG was not affected by center chains of the levelers. The four synthesized levelers have also applied to the gap-filling of trenches. By assistance of the synthesized levelers complete bottom-up filling of trenches was achieved while failure of trench filling was observed in the absence of levelers, which corresponds to the results of electrochemical analyses. Although the different adsorption behaviors of the synthesized levelers were observed in the absence of other additives, no significant differences were observed in the presence of other

additives. This meant the interactions of the synthesized leveler with other additives were rarely affected by center chains of the levelers. Therefore, further investigation on the other functional groups, ammonium, and iodide counter anion, should be investigated the relation between structures and activities of levelers.

5. Experimental

5.1. General procedure

All materials were obtained from commercial sources and were used without further purification. Tetrahydrofuran (THF) was distilled immediately prior to use in the presence of sodium under N_2 atmosphere. Air or moisture sensitive reactions were conducted under nitrogen atmosphere using oven-dried glassware and standard syringe/septa techniques. The reactions were monitored with SiO_2 TLC plates under UV light (254 nm) followed by visualization with a phosphomolybdic acid or a ninhydrin stain solution. Column chromatography was performed on silica gel 60 (70-230 mesh). ^{1}H and ^{13}C nuclear magnetic resonance (NMR) spectra were measured at 400 MHz and 100 MHz, respectively, in deuterated chloroform ($CDCl_3$) or deuterated methanol (MeOH-d_4) with Bruker Avance-400. The ^{1}H NMR spectroscopic data were reported as follows in ppm (δ) from the internal standard (TMS, 0.0 ppm) in $CDCl_3$ or 3.31 resonance of MeOH-d_4 : chemical shift (integration, multiplicity, coupling constant in Hz). The ^{13}C NMR spectra data were referenced with the 77.16 resonance of $CDCl_3$, or 49.00 resonance of MeOH-d_4. High resolution mass spectra (HRMS) were measured by the fast atom bombardment (FAB) ionization method and analyzed with a magnetic sector mass analyzer.

5.1.1 Allylation.

[Synthesis of diallyl-ethylene glycol 1]

To a solution of ethylene glycol (1.1 mL, 20.00 mmol) in anhydrous tetrahydrofuran (THF, 40 mL), sodium hydride (NaH, 3 equiv.) was portionwisely added at 0 ˚C and stirred for 30 min under N_2 atmosphere. After 30 minutes, *n*Bu_4NI (0.2 equiv.) and allyl bromide (3 equiv.) were added, and the reaction mixture was stirred at room temperature for 5 hrs. The reaction mixture was quenched with H_2O, and the quenched reaction mixture was partitioned between ethyl acetate (EtOAc, 40 mL) and additional H_2O (20 mL). The separated organic layer was washed with H_2O (20 mL × 2), and the combined organic layers were dried over $MgSO_4$, filtered, concentrated under the reduced pressure. Purification by silica gel column chromatography (16:1 v/v, EtOAc:hexane) afforded diallyl-ethylene glycol 1 (2.14 g, 89%) as colorless liquid. ^{1}H NMR($CDCl_3$) δ 3.64(4H, s), 4.06(4H, m), 5.19-5.34(4H, m), 5.91-6.00(2H, m); ^{13}C NMR($CDCl_3$) δ 69.6, 72.4, 117.3, 134.9.

[Synthesis of diallyl-triethylene glycol 6]

To a solution of triethylene glycol (1.0 mL, 7.52 mmol) in anhydrous tetrahydrofuran (THF, 50 mL), sodium hydride (NaH, 3 equiv.) was portionwisely added at 0 ˚C and stirred for 1 hr under N_2 atmosphere. After 1 hr, *n*Bu_4NI (0.2 equiv.) and allyl bromide (3 equiv.) were added and the reaction mixture was stirred at room temperature for 6 hrs. The reaction mixture was quenched with H2O, and the quenched reaction mixture was partitioned between ethyl acetate (EtOAc, 60 mL) and additional H_2O (30 mL). The separated organic layer was washed with H_2O (30 mL × 2), and the combined organic layers were dried over $MgSO_4$, filtered, concentrated under the reduced pressure. Purification by silica gel

column chromatography (8:1 v/v, EtOAc:hexane) afforded diallyl-triethylene glycol 6 (1.86 g, quant.) as colorless liquid. 1H NMR($CDCl_3$) δ 3.59-3.61(4H, m), 3.62-3.67(4H, m) 3.67(4H, s), 4.02-4.04(4H. m), 5.16-5.30(4H, m), 5.87-5.97(2H, m); 13C NMR($CDCl_3$) δ 69.4, 70.6, 72.1, 116.9, 134.7.

[Synthesis of diallyl-octanediol 9]

To a solution of (1.462 g, 10.00 mmol) in anhydrous tetrahydrofuran (THF, 30 mL), sodium hydride (NaH, 3 equiv.) was portionwisely added at 0 ˚C and stirred for 1 hr under N_2 atmosphere. After 1 hr, *n*Bu_4NI (0.2 equiv.) and allyl bromide (3 equiv.) were added and the reaction mixture was stirred at 50 ˚C for 4 hrs. The reaction mixture was quenched with H_2O, and the quenched reaction mixture was partitioned between ethyl acetate (EtOAc, 40 mL) and additional H_2O (20 mL). The separated organic layer was washed with H_2O (20 mL × 2), and the combined organic layers were dried over $MgSO_4$, filtered, concentrated under the reduced pressure. Purification by silica gel column chromatography (16:1 v/v, EtOAc:hexane) afforded diallyl-octanediol 9 (1.73 g, 77%) as colorless liquid. 1H NMR($CDCl_3$) δ 1.26-1.36(8H, m) 1.54-1.62(4H, m), 3.40-3.43(4H, t), 3.95-3.97(4H, m), 5.15-5.30(4H, m), 5.87-5.97(2H, m); 13C NMR($CDCl_3$) δ 20.6, 21.0, 70.4, 71.9, 116.6, 135.7.

5.1.2. Epoxidation

[Synthesis of bis(oxiran-2-methoxy)ethylene glycol 2]

To the dichloromethane (CH_2Cl_2, 30 mL) solution of diallylethylene glycol 1 (1.64 g, 11.67 mmol), *meta*-chloroperoxybenzoic acid (*m*CPBA, 3 equiv.) was added and stirred at room temperature for 10 min. After then, the reaction mixture was refluxed for 5 hrs. The resulting solution was diluted with CH_2Cl_2 (20 mL) and

washed with an aqueous saturated solution of $NaHCO_3$ (60 mL × 3). The organic layer was dried over $MgSO_4$, filtered and concentrated under the reduced pressure. Through the silica gel chromatography with the gradient elution (Hex : EtOAc = from 4:1 to 1:2 v/v), the desired bis(oxiran-2-methoxy)ethylene glycol 2 (1.41 g, 69%) was obtained as colorless liquid. ^{1}H NMR($CDCl_3$) δ 2.64(2H, m), 2.83(2H, dd, *J*=4.0, 4.8), 3.20(2H, m), 3.03(2H, m), 3.66-3.78(4H, m), 3.82-3.86(2H, m); ^{13}C NMR($CDCl_3$) δ 44.4, 51.0, 70.9, 72.2.

[Synthesis of bis(oxiran-2-methoxy)triethylene glycol 7]

To the dichloromethane (CH_2Cl_2, 30 mL) solution of diallyltriethylene glycol 6 (1.18 g, 5.12 mmol), *meta*-chloroperoxybenzoic acid (*m*CPBA, 3 equiv.) was added and stirred at room temperature for 10 min. After then, the reaction mixture was refluxed for 20 hrs. The resulting solution was diluted with CH_2Cl_2 (20 mL) and washed with an aqueous saturated solution of $NaHCO_3$ (60 mL × 3). The organic layer was dried over $MgSO_4$, filtered and concentrated under the reduced pressure. Through the silica gel chromatography with the gradient elution (Hex : EtOAc = from 2:1 to 1:2 v/v), the desired bis(oxiran-2-methoxy)triethylene glycol 7 (0.82 g, 61%) was obtained as colorless liquid. ^{1}H NMR($CDCl_3$) δ 2.60-2.62(2H, q, *J*=2.8), 2.78-2.80(2H, dd, *J*=4.0, 4.8), 3.14-3.18(2H, m), 3.42-3.46(2H, m), 3.64-3.72(12H, m), 3.77-3.81(2H, m); ^{13}C NMR($CDCl_3$) δ 44.1, 51.7, 70.49, 70.52, 70.64, 71.9

[Synthesis of bis(oxiran-2-methoxy)octanediol 10]

To the dichloromethane (CH_2Cl_2, 30 mL) solution of diallyloctanediol 9 (1.68 g, 7.41 mmol), *meta*-chloroperoxybenzoic acid (*m*CPBA, 3 equiv.) was added and stirred at room temperature for 10 min. After then, the reaction mixture was refluxed for 17 hrs. The resulting solution was diluted with CH_2Cl_2 (20 mL) and washed with an aqueous saturated solution of $NaHCO_3$ (60 mL × 3). The organic

layer was dried over $MgSO_4$, filtered and concentrated under the reduced pressure. Through the silica gel chromatography with the gradient elution (Hex : EtOAc = from 4:1 to 1:2 v/v), the desired bis(oxiran-2-methoxy)octanediol 10 (1.49 g, 78%) was obtained as colorless liquid. ^{1}H NMR($CDCl_3$) δ 1.32-1.36(8H, m), 1.54-1.60(4H, m), 2.60-2.62(2H, q, *J*=2.4), 2.79-2.812(2H, dd, *J*=4.0, 4.8), 3.13-3.17(2H, m), 3.36-3.40(2H, q, *J*=2.4), 3.43-3.54(4H, m), 3.69-3.72(2H, dd, *J*=3.2, 5.6); ^{13}C NMR δ 26.0, 29.3, 29.6, 44.3, 50.8, 71.4, 71.6.

[Synthesis of 1,6-di(oxiran-2-yl)hexane 4]

To the dichloromethane (CH_2Cl_2, 30 mL) solution of 1,9-decadiene (1.84 mL, 10.00 mmol), *meta*-chloroperoxybenzoic acid (*m*CPBA, 3 equiv.) was added and stirred at room temperature for 10 min. After then, the reaction mixture was refluxed for 17 hrs. The resulting solution was diluted with CH_2Cl_2 (20 mL) and washed with an aqueous saturated solution of $NaHCO_3$ (60 mL × 3). The organic layer was dried over $MgSO_4$, filtered and concentrated under the reduced pressure. Through the silica gel chromatography with the gradient elution (Hex : EtOAc = from 4:1 to 1:2 v/v), the desired 1,6-di(oxiran-2-yl)hexane 4 (1.21 g, 66%) was obtained as colorless liquid. ^{1}H NMR($CDCl_3$) δ 1.35-1.38(4H, m), 1.40-1.55(8H, m), 2.46-2.48(2H, q, *J*=2.8), 2.74-2.76(2H, dd, *J*=4.0, 4.8), 2.89-2.93(2H, m); ^{13}C NMR δ 25.8, 29.2, 32.4, 46.9, 52.2.

5.1.3. Amination

[Synthesis of bis(3-(dimethylamino)-2-propanol-oxy)ethylene glycol 3]

To a solution of bis(oxiran-2-methoxy)ethylene glycol 2 (1.57 g, 8.94 mmol), 50% methanol solution of dimethyl amine (30 equiv.) was added at room temperature. After 10 hrs, the reaction mixture was concentrated under the reduced

pressure. The obtained crude mixture was diluted with H_2O (40 mL) and washed with ethyl acetate (EtOAc, 20 mL) and the combined aqueous layer was concentrated under the reduced pressure to give a bis(3-(dimethylamino)-2-propanol-oxy)ethylene glycol 3 as viscous yellowish liquid (2.35 g, quant.). ^{1}H NMR(MeOH-d_4) δ 2.31(2H, m), 2.33(12H, s), 2.48(2H, m), 3.49(2H, m), 3.57(2H, m), 3.70(4H, s), 3.90(2H, m); ^{13}C NMR(MeOH-d_4) δ 45.8, 61.9, 67.0, 70.9, 74.1.

[Synthesis of bis(3-(dimethylamino)-2-propanol-oxy)triethylene glycol 8]

To a solution of bis(oxiran-2-methoxy)triethylene glycol 7 (1.15 g, 4.37 mmol), 50% methanol solution of dimethyl amine (30 equiv.) was added at room temperature. After 10 hrs, the reaction mixture was concentrated under the reduced pressure. The obtained crude mixture was diluted with H_2O (40 mL) and washed with ethyl acetate (EtOAc, 20 mL) and the combined aqueous layer was concentrated under the reduced pressure to give a bis(3-(dimethylamino)-2-propanol-oxy)triethylene glycol 8 as viscous yellowish liquid (1.52 g, quant.). ^{1}H NMR(MeOH-d_4) δ 2.30(12H, s), 2.35-2.45(4H, m), 3.41-3.45(4H, m), 3.64-3.87(12H, m), 3.87-3.93(2H, m); ^{13}C NMR(MeOH-d_4) δ 44.8, 62.0, 67.8, 67.8, 70.2, 70.3, 74.0.

[Synthesis of 1,8-bis(3-(dimethylamino)-2-propanol-oxy)octane 11]

To a solution of bis(oxiran-2-methoxy)octanediol 10 (1.42 g, 5.51 mmol), 50% methanol solution of dimethyl amine (30 equiv.) was added at room temperature. After 10 hrs, the reaction mixture was concentrated under the reduced pressure. The obtained crude mixture was diluted with ethyl acetate (EtOAc, 40 mL × 5) and washed with brine (20 mL) and the combined aqueous layers were concentrated under the reduced pressure to give a 1,8-bis(3-(dimethylamino)-2-propanol-oxy)octane 11 as yellowish solid (0.88 g, 46%). ^{1}H NMR(MeOH-d_4) δ 1.36-

1.41(8H, br m), 1.56-1.61(4H, q, *J*=6.4), 2.35-2.46(4H, m), 3.35-3.43(4H, m), 3.46-3.50(4H, t, *J*=6.4), 3.85-3.91(2H, m); ^{13}C NMR δ 25.8, 29.2, 29.3, 44,8, 62.3, 67.8, 71.2, 73.5.

[Synthesis of 1,10-bis(dimethylamino)decane-2,9-diol 5]

To a solution of 1,6-di(oxiran-2-yl)hexane 4 (0.92 g, 5.42 mmol), 50% methanol solution of dimethyl amine (30 equiv.) was added at room temperature. After 10 hrs, the reaction mixture was concentrated under the reduced pressure. The obtained crude mixture was diluted with ethyl acetate(EtOAc, 40 mL × 3) and washed with brine (20 mL) and the combined aqueous layers were concentrated under the reduced pressure to give a 1,10-bis(dimethylamino)decane-2,9-diol 5 as yellowish solid (1.19 g, 84%). ^{1}H NMR(MeOH-d_4) δ 1.36-1.41(8H,m, br m), 1.47-1.50(4H, m, br m), 2.26-2.38(4H, m), 2.29(12H, s), 3.70-3.71(2H, m); ^{13}C NMR δ 25.3, 29.4, 35.5, 65.7, 68.2.

5.1.4. Methylation

[Synthesis of bis(3-(trimethylammonio)-2-propanol-oxy)ethylene glycol diiodide Lev (1)]

To a solution of bis(3-dimethylamino)-2-propanol-oxy)triethylene glycol 3 (0.84 g, 2.38 mmol) in methanol (5 mL), iodomethane (2.2 equiv.) was added dropwise at room temperature and stirred for 12 hrs. The reaction mixture was concentrated under the reduced pressure. The obtained crude mixture was disluted with H_2O (40 mL) and washed with ethyl acetate (EtOAc, 20 mL) and the combined aqueous layer was concentrated under the reduced pressure to give a (3-(trimethylammonio)-2-propanol-oxy)ethylene glycol diiodide Lev (1) as viscous yellowish liquid (1.58 g, 88%). ^{1}H NMR(MeOH-d_4) δ 3.29(18H, s), 3.47-3.55(4H,

m), 3.57-3.62(4H, m), 3.71(4H, s), 4.36-4.38(2H, m); ^{13}C NMR(MeOH-d_4) 54.1, 54.2, 65.0, 68.6, 70.5, 73.0. HRMS (FAB) calcd for $C_{14}H_{34}IN_2O_4^+$ 421.1563.([M]$^+$), found 421.1558.

[Synthesis of bis(3-(trimethylammonio)-2-propanol-oxy)triethylene glycol diiodide Lev (3)]

To a solution of bis(3-dimethylamino)-2-propanol-oxy)ethylene glycol 8 (0.87 g, 3.27 mmol) in methanol (5 mL), iodomethane (2.2 equiv.) was added dropwise at room temperature for 12 hrs. The reaction mixture was concentrated under the reduced pressure. The obtained crude mixture was disluted with H_2O (40 mL) and washed with ethyl acetate (EtOAc, 20 mL) and the combined aqueous layer was concentrated under the reduced pressure to give a (3-(trimethylammonio)-2-propanol-oxy)ethylene glycol diiodide Lev (3) as yellowish liquid (1.58 g, 88%). ^{1}H NMR(MeOH-d_4) δ 3.27(18H, s), 3.43-3.51(4H, m), 3.53-3.58(4H, m), 3.66-3.72(12H, br m), 4.33-4.36(2H, m); ^{13}C NMR(MeOH-d_4) δ 53.8, 65.0, 68.7, 70.1, 70.4, 72.9, 74.5. HRMS (FAB) calcd for $C_{18}H_{42}IN_2O_6^+$ 509.2088 ([M]$^+$), found 509.2089.

[Synthesis of 1,8-bis(3-(trimethylammonio)-2-propanol-oxy)octane diiodide Lev (4)]

To a solution of 1,8-bis(3-(dimethylamino)-2-propanol-oxy)octane 11 (0.88 g, 2.52 mmol) in methanol (5 mL), iodomethane (2.2 equiv.) was added dropwise at room temperature for 12 hrs. The reaction mixture was concentrated under the reduced pressure. The obtained crude mixture was disluted with H_2O (40 mL) and washed with ethyl acetate (EtOAc, 20 mL) and the combined aqueous layer was concentrated under the reduced pressure to give a 1,8-bis(3-(trimethylammonio)-2-propanol-oxy)octane diiodide Lev (4) as yellowish solid (1.47 g, 92%). ^{1}H

NMR(MeOH-d_4) δ 1.36-1.41(8H, br s), 1.158-1.63(4H, m), 3.30(18H, s), 3.42-3.45(4H, m), 3.48-3.55(8H, m), 4.30-4.35(2H, m); ^{13}C NMR(MeOH-d_4) δ 25.9, 29.2, 29.3, 54.2, 65.0, 68.0, 71.5, 72.6. HRMS (FAB) calcd for $C_{20}H_{36}IN_2O_4^+$ 425.2502 ($[M]^+$), found 505.2505.

[Synthesis of 1,10-bis(trimethylammonio)decane-2,9-diol diiodide Lev(2)]

To a solution of 1,10-bis(dimethylamino)decane-2,9-diol 5 (1.16 g, 4.44 mmol) in methanol (5 mL), iodomethane (2.2 equiv.) was added dropwise at room temperature for 12 hrs. The reaction mixture was concentrated under the reduced pressure. The obtained crude mixture was disluted with H_2O (40 mL) and washed with ethyl acetate (EtOAc, 20 mL) and the combined aqueous layer was concentrated under the reduced pressure to give a 1,10-bis(trimethylammonio)decane-2,9-diol diiodide Lev (2) as yellowish solid (2.39 g, 99%). ^{1}H NMR(MeOH-d_4) δ 1.42-1.52(12H, br m), 3.26(18H, s), 3.44-3.49(4H, m), 4.16-4.18(2H, m); ^{13}C NMR(MeOH-d_4) δ 25.5, 29.0, 29.1, 35.2, 35.5, 53.9, 65.7, 70.7. HRMS (FAB) calcd for $C_{16}H_{38}IN_2O_2^+$ 417.1978 ($[M]^+$), found 417.1978.

References

1. Wang, C.; Zhang, J.; Yang, P.; An, M.; *Int. J. Electrochem. Sci*., 2012, 7, 10644

2. Moore, G.; Cramming More Components Onto Integrated Circuits, *Electronics*, 1965, 38(8), 114–117.

3. John H. L.; *Journal of Electronic Packaging*, 2014, Vol. 136, 040801-1.

4. Eloy. J.; Market Trends for 3D Stacking, *EMC 3D*, 2007.

5. Gambino, J.P.; Adderly, S.A.; Knickerbocker, J.U.; *Microelectronic Engineering*, 2015, 135, 73.

6. Shockley, W.; Semiconductive wafer and method of making the same, 1962, US Patent No. 3044909 A.

7. Smith, M.; Stern, E.; Methods of making thru-connections in semiconductor wafers, 1967, US Patent No. 3343256.

8. Yan, L. L.; Lee, C.K.; Yu, D. Q.; Yu, A.-B.; Choi, W.-K.; Lau, J.-H.; and Yoon, S.-U.; *J. Electron. Mater*., 2009, 38, 200.

9. Wolter, K. System integration by advanced electronics packaging; Bio and Nano Packaging Techniques for Electron Devices; Springer-Verlag, Berlin; 2012.

10. Yoon, M-S.; *Journal of the Microelectronics & Packaging Society*, 2009, 16, 1.

11. Nagarajan, R.; Prasad, K.; Ebin, L.; and Narayanan, B.; *Sens. Actuator A-Phys.*, 2007, 139, 323.

12. Wu, B.; Kumar, A.; Pamarthy, S.; *J. Appl. Phys.* 2010, 108, 051101.

13. Ham, Y.-H.; Kim, D.-P.; Park, K.-S.; Jeong, Y.-S.; Yun, H.-J.; Baek, K.-H.; Kwon, K.-H.; Lee, K.; and Do, L.-M.; *Thin Solid Films* 2011, 519, 6727.

14. Park, K.J.; Kim, M.J.; Lim, T.; Koo, H.-C.; and Kim, J.J.; *Electrochem. Solid-State Lett.* 2012, 15, D26.

15. Inoue, F.; Philipsen, H.; Radisic, A.; Armini, S.; Civale, Y.; Leunissen, P.; Kondo, M.; Webb, E.; and Shingubara, S.; *Electrochim. Acta,* 2013, 100, 203.

16. Armini, S.; El-Mekki, Z.; Vandersmissen, K.; Philipsen, H.; Rodet, S.; Honore, M.; Radisic, A.; Civale, Y.; Beyne, E.; and Leunissen, L.; *J. Electrochem. Soc*. 2011, 158, H160.

17. Au, Y.; Wang, Q.M.; Li, H.; Lehn, J.-S.M.; Shenai, D.V.; and Gordon, R.G.; *J. Electrochem. Soc.* 2012, 159, D382.

18. Lühn, O.; Van Hoof, C.; Ruythooren, W.; and Celis, J.-P.; *Microelectron. Eng.* 2008, 85, 1947.

19. Wojcik, H.; Junige, M.; Bartha, W.; Albert, M.; Neumann, V.; Merkel, U.; Peeva, A.; Gluch, J. ; Menzel, S.; Munnik, F.; Liske, R.; Utess, D.; Richter, I.; Klein, C.; Engelmann, H.J.; Ho, P.; Hossbach, C.; and Wenzel, C.; *J. Electrochem. Soc.* 2012,159, H166.

20. Moffat, T.P. ; and Josell, D.; *J. Electrochem. Soc*. 2012, 159, D208.

21. Josell, D. ; Wheeler, D.; and Moffat, T.P. ; *J. Electrochem. Soc.* 2012, 159, D570.

22. M.J. Kim, H.C. Kim, S. Choe, J.Y. Cho, D. Lee, I. Jung, W.-S. Cho, J.J. Kim, J. Electrochem. Soc. 160 (2013) D3221.

23. Kim, H.C.; Choe, S.H.; Cho, J.Y.; Lee, D.; Jung, I.; Cho, W.-S.; Kim, M.J. ; and Kim, J.J.; *J. Electrochem. Soc.* 2015, 162, D109.

24. Jin, S.; Wang, G.; and Yoo, B.; *J. Electrochem. Soc.* 2013, 160, D3300.

25. Zhu, Q.S.; Toda, A.; Zhang, Y.; Itoh, T.; and Maeda, R.; *J. Electrochem. Soc.* 2014, 161, D263.

26. Kondo, K.; Funahashi, C.; Miyake, Y.; Takeno, Y.; Hayashi, T.; Yokoi, M.; Okamoto, N.; and Saito, T.; *J. Electrochem. Soc*. 2014, 161, D791.

27. Tsai, T.C.; Tsao, W.C.; Lin, W.; Hsu, C.L.; Lin, C.L.; Hsu, C.M.; Lin, J.F.; Huang, C.C.; and Wu, J.Y.; *Microelectron. Eng.* 2012, 92, 29.

28. Che, F.X.; *IEEE Trans, Compon. Pack. Manuf. Technol*. 2014, 4, 1432.

29. D. Henry, Via first technology development based on high aspect ratio trenches

filled with doped polysilicon, *2007 Proceedings 57th Electronic Components and Technology Conference*, 2007, pp. 830–835.

30. Kim, M. J., "The Influences of Pulse and Pulse-reverse Electrodeposition on the Properties of Cu Thin Films and Superfilling for the Fabrication of Cu Interconnection," Ph.D. Dissertation, Seoul National University, Seoul(2013).

31. Gallaway, J. W.; Willey, M. J.; and West, A. C.; *J. Electrochem. Soc.*, 2009, 156, D287

32. Bonou, L.; Eyraud, M.; Denoyel, R.; and Massiani, Y.; *Electrochim. Acta*, 2002, 47, 4139

33. Frank A.; and Bard, A. J. ; *J. Electrochem. Soc*., 2003, 150, C244

34. Kang M. ; and Gewirth, A. A. ; *J. Electrochem. Soc*., 2003, 150, C426

35. Healy, J. P. ; Pletcher, D.; and Goodenough, M.; *J. Electronal. Chem*., 1992, 338, 155

36. Dow, W.-P.; Yen, M.-Y. ; Lin, W.-B.; and Ho, S.-W.; *J. Electrochem. Soc*., 2005, 152, C769

37. Wang, W.; and Li, Y.-B.; *J. Electrochem. Soc*., 2008, 155, D263

38. Nagy, Z.; Blaudeau, J. P.; Huang, N. C.; Curtiss, L. A.; and Zurawski, D. J.; *J. Electrochem. Soc*. 1995, 142, L87

39. Walker, M. L.; Richter, L. J.; and Moffat, T. P.; *J. Electrochem. Soc*., 2005, 152, C403

40. Huang, S.-M.; Liu, C. -W.; and Dow, W. -P.; *J. Electrochem. Soc.,* 2012, 159, D135

41. Dow, W. -P.; Li, C. -C.; Lin, M. -W.; Su, G. -W.; and Huang, C. -C.; *J. Electrochem. Soc.,* 2009, 156, D314

42. Lin, G. -Y.; Yan, J. -J.; M. -Y. Yen, M. -Y.; Dow, W. -P.; Huang, S.-M.; *J. Electrochem. Soc.,* 2013, 160, D3028

43. Hayashi, T.; Kondo, K.; Saito, T.; Takeuchi, M.; and Okamotoa, N.; *J.*

Electrochem. Soc., 2011, 158, D715

44. Takeuchi, M.; Kondo, K.; Kuri, H.; Bunya, M.; Okamoto, N.; and Saito, T. *J. Electrochem. Soc.,* 2012, 159, D230

45. Hayase, M.; and Nagao, M.; *J. Electrochem. Soc.,* 2013, 160, D3

APPENDICES

List of ^{1}H NMR Spectra of Selected Compounds

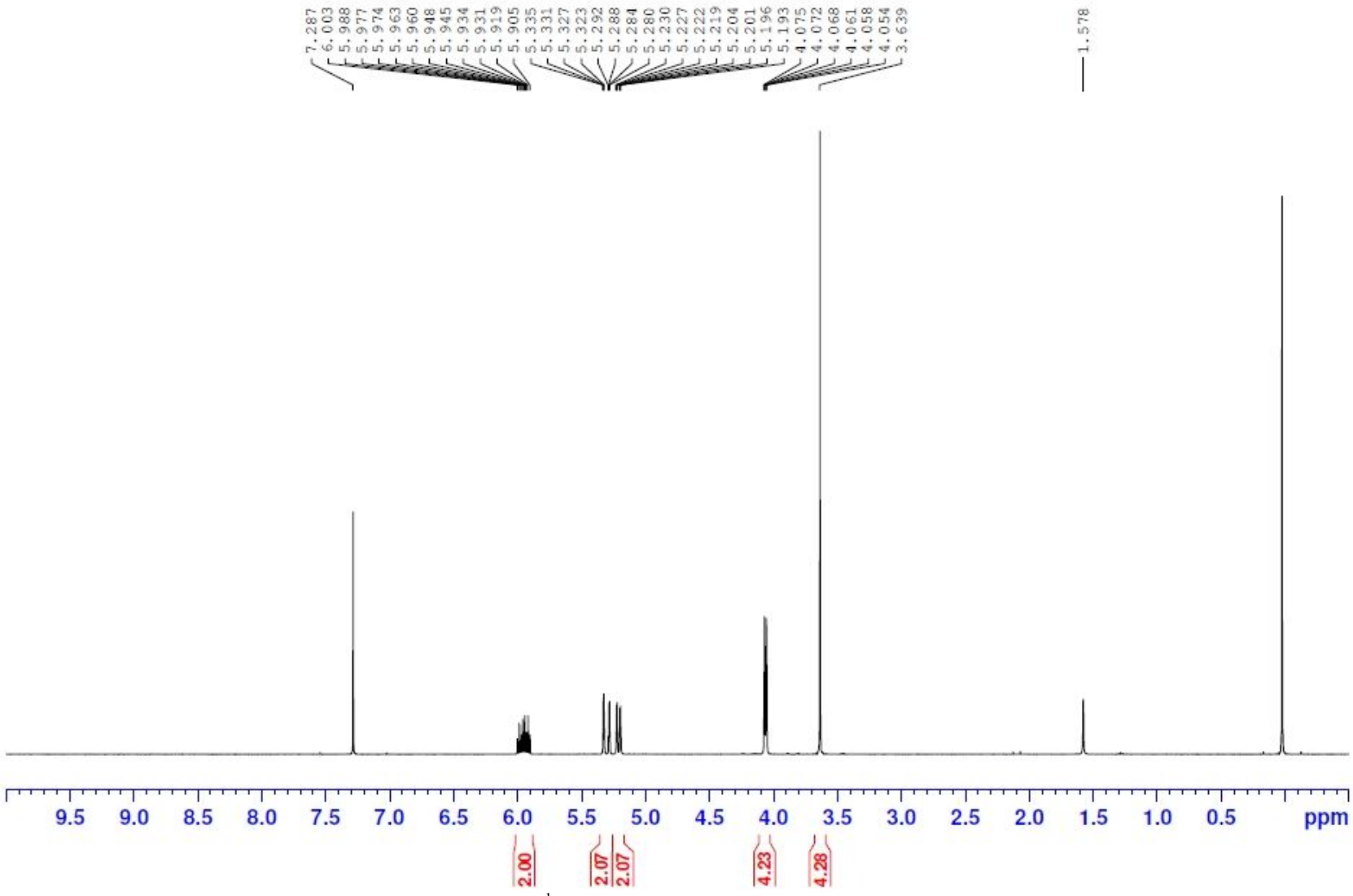

400 MHz ^{1}H NMR Spectrum ($CDCl_3$) of compound 1

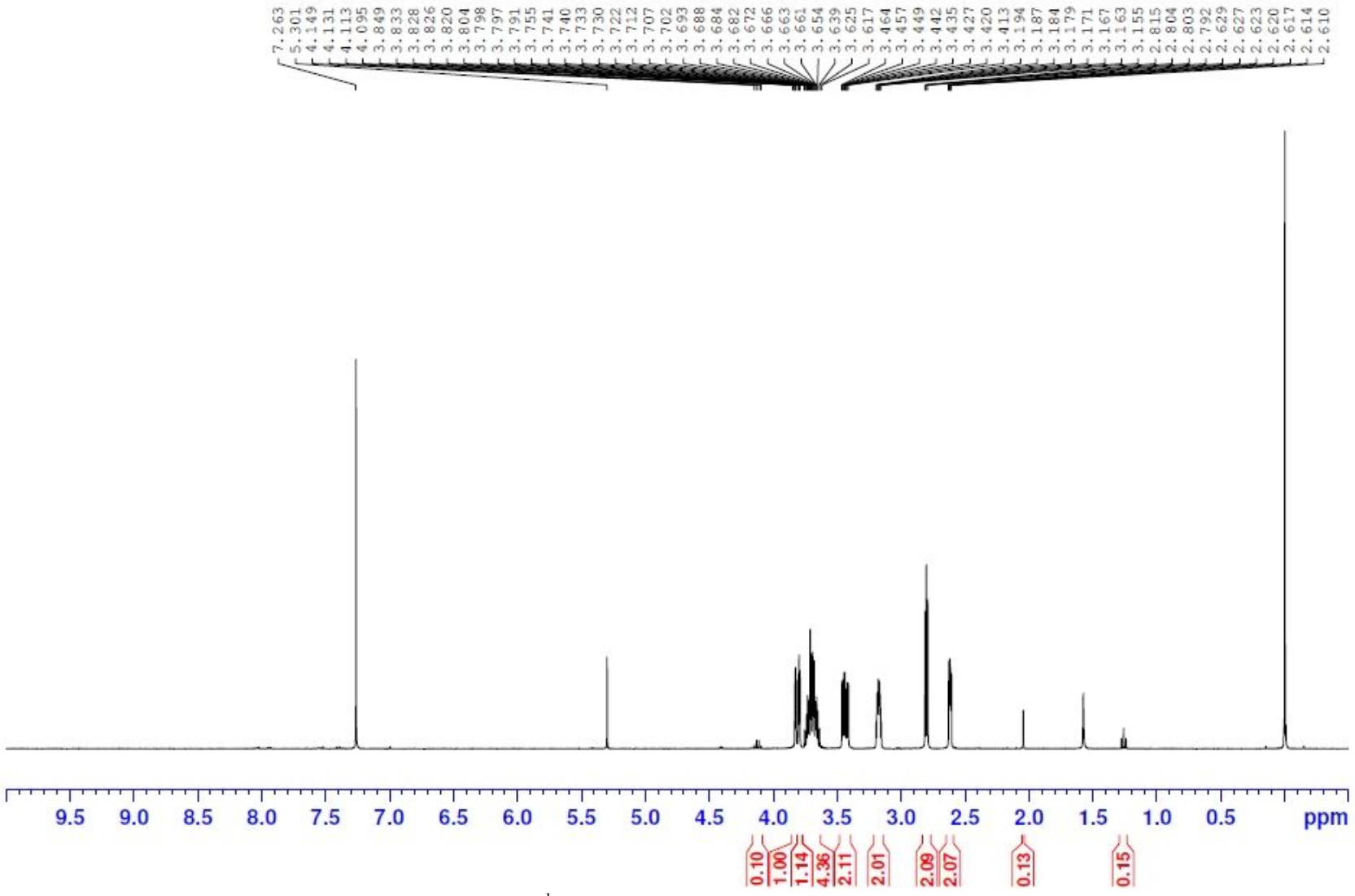

400 MHz ^{1}H NMR Spectrum ($CDCl_3$) of compound 2

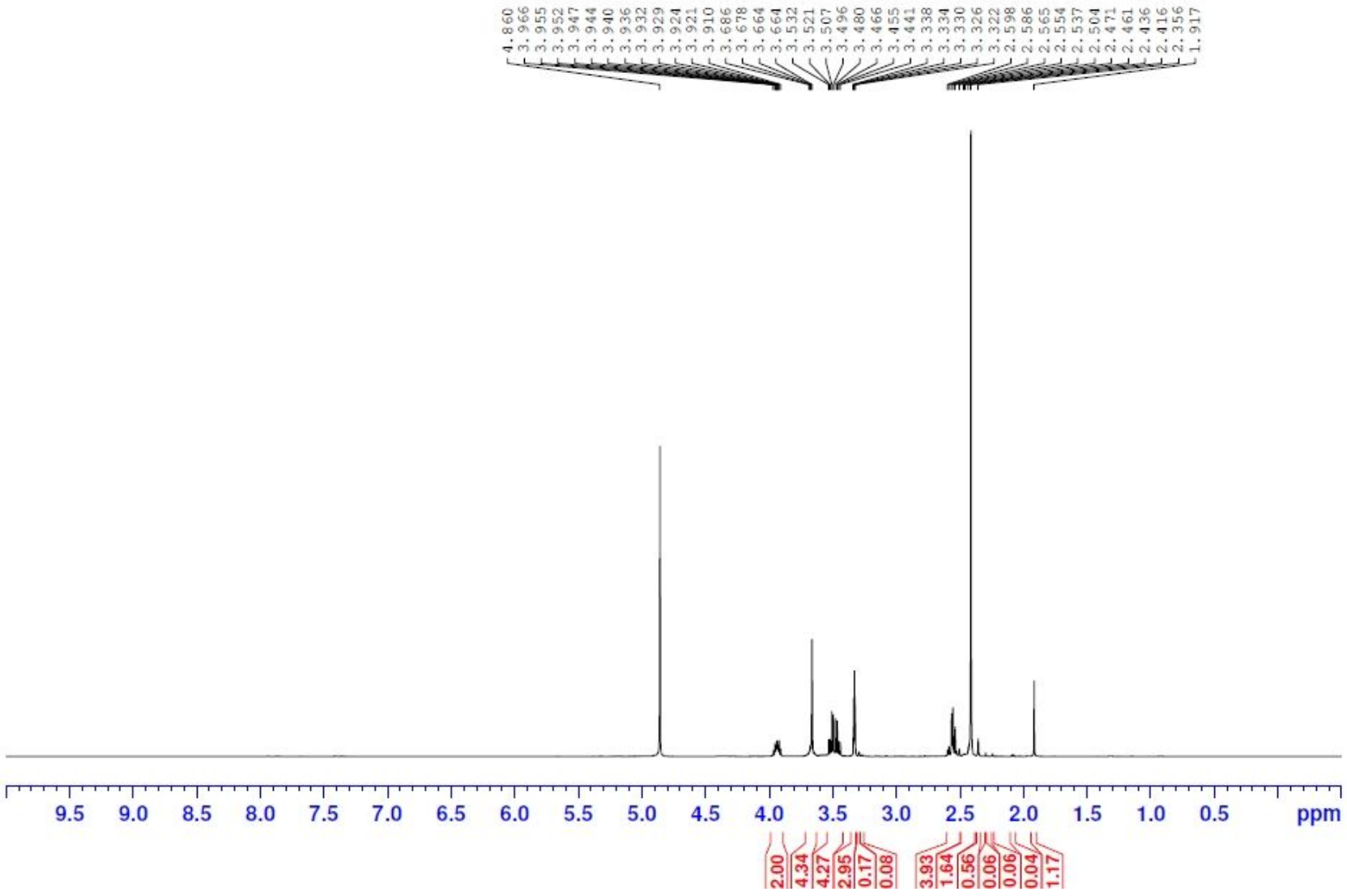

400 MHz ^{1}H NMR Spectrum ($CDCl_3$) of compound 3

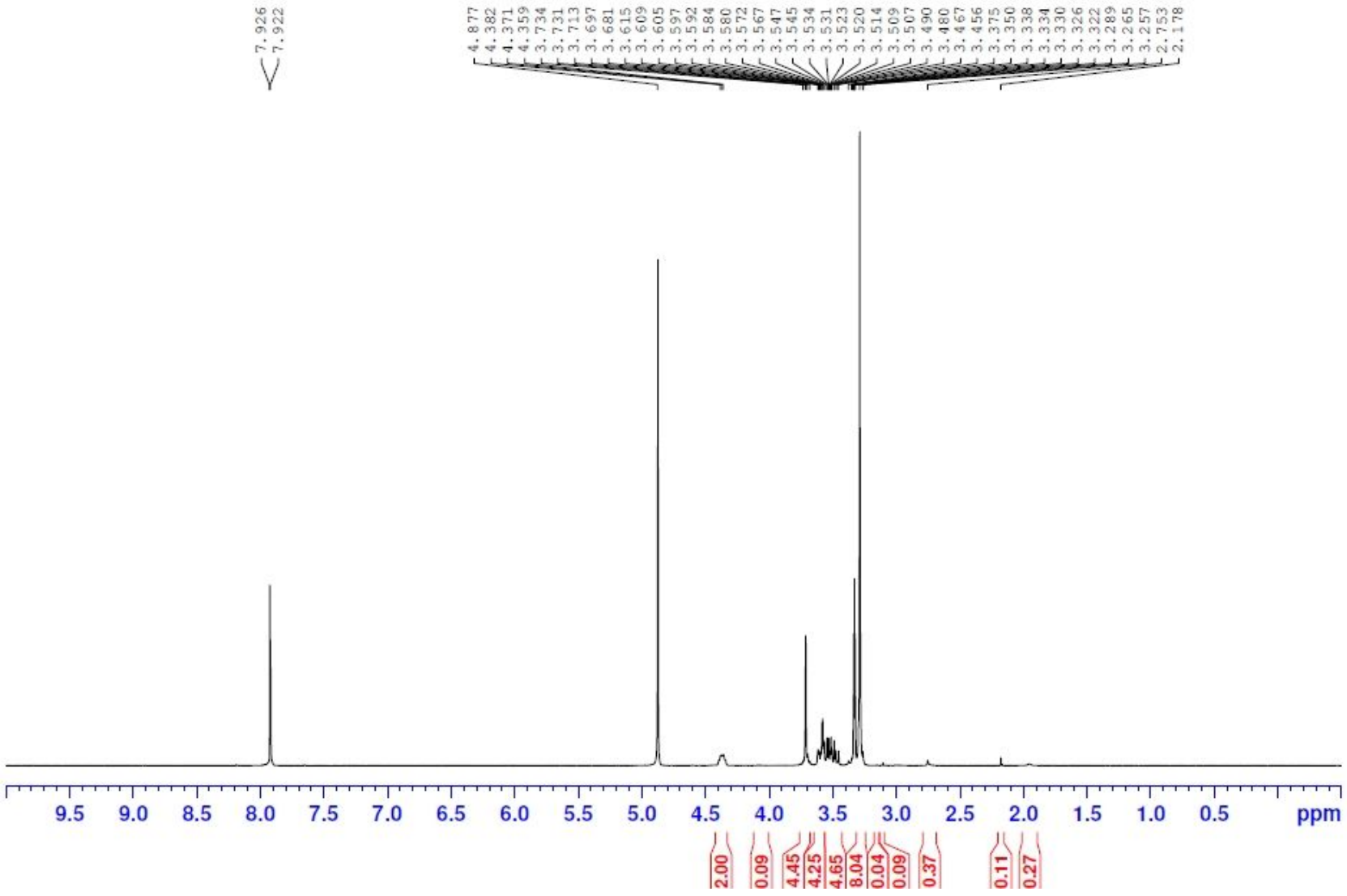

400 MHz ^{1}H NMR Spectrum ($CDCl_3$) of compound Lev (1)

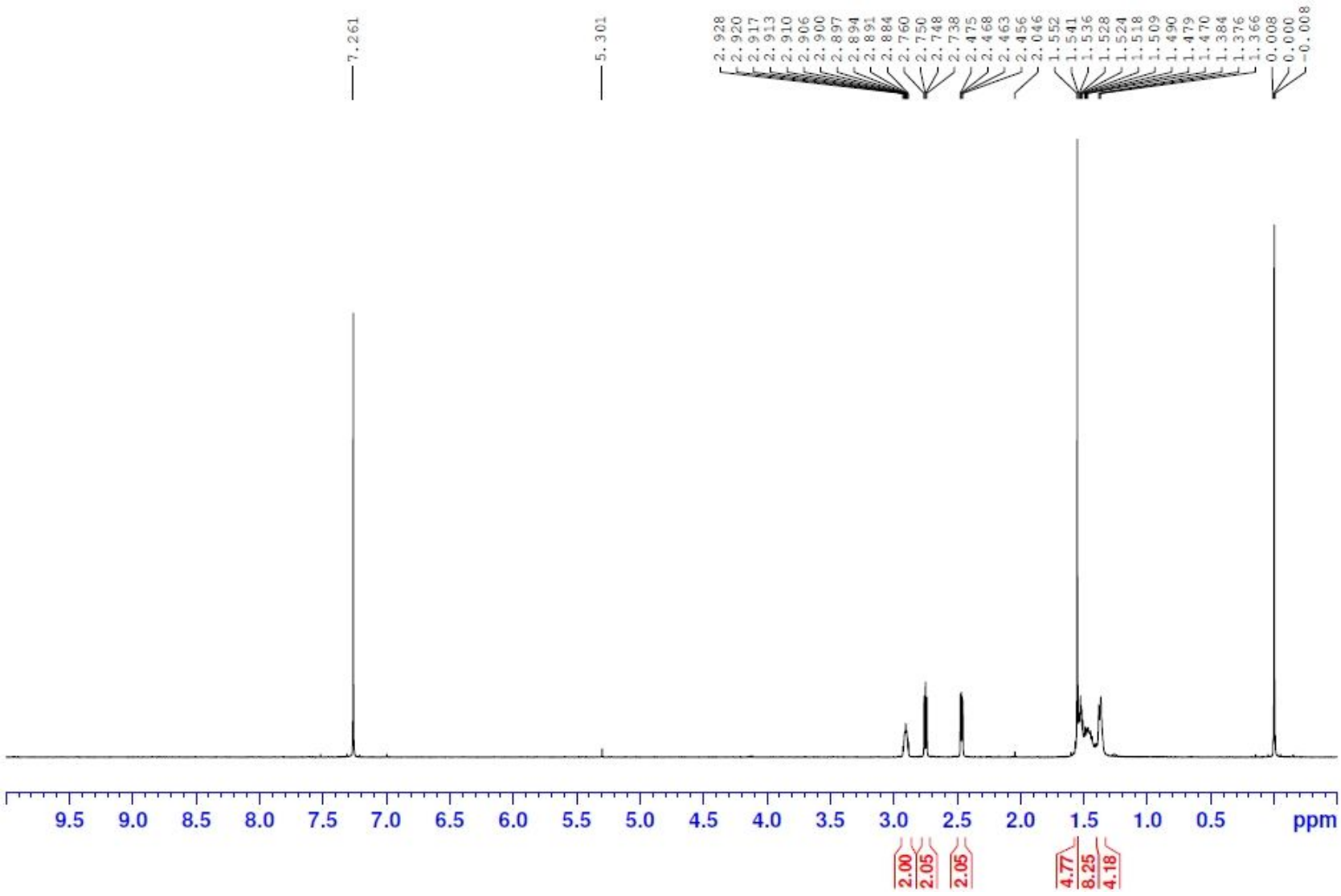

400 MHz ^{1}H NMR Spectrum ($CDCl_3$) of compound 4

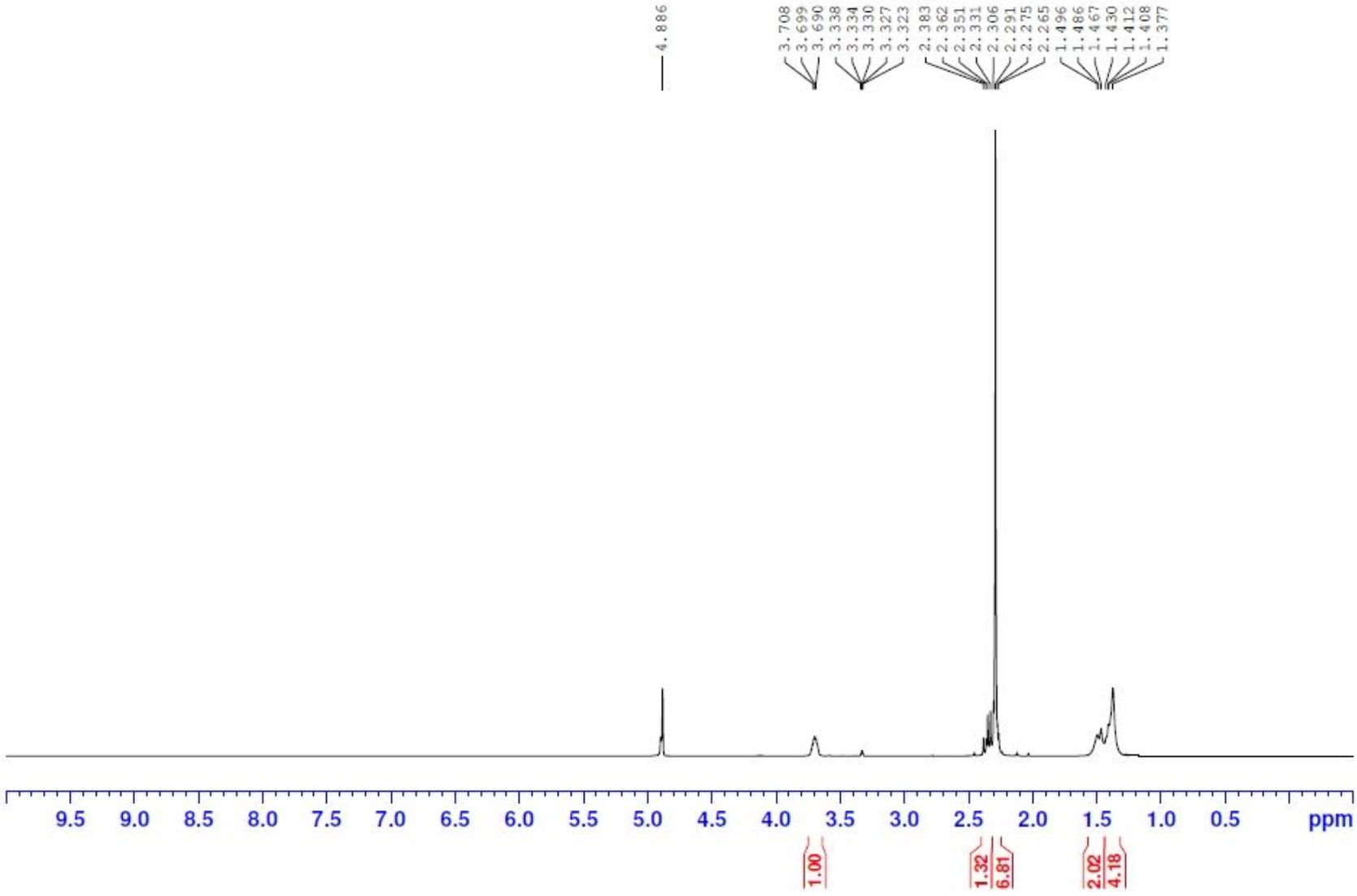

400 MHz ^{1}H NMR Spectrum ($CDCl_3$) of compound 5

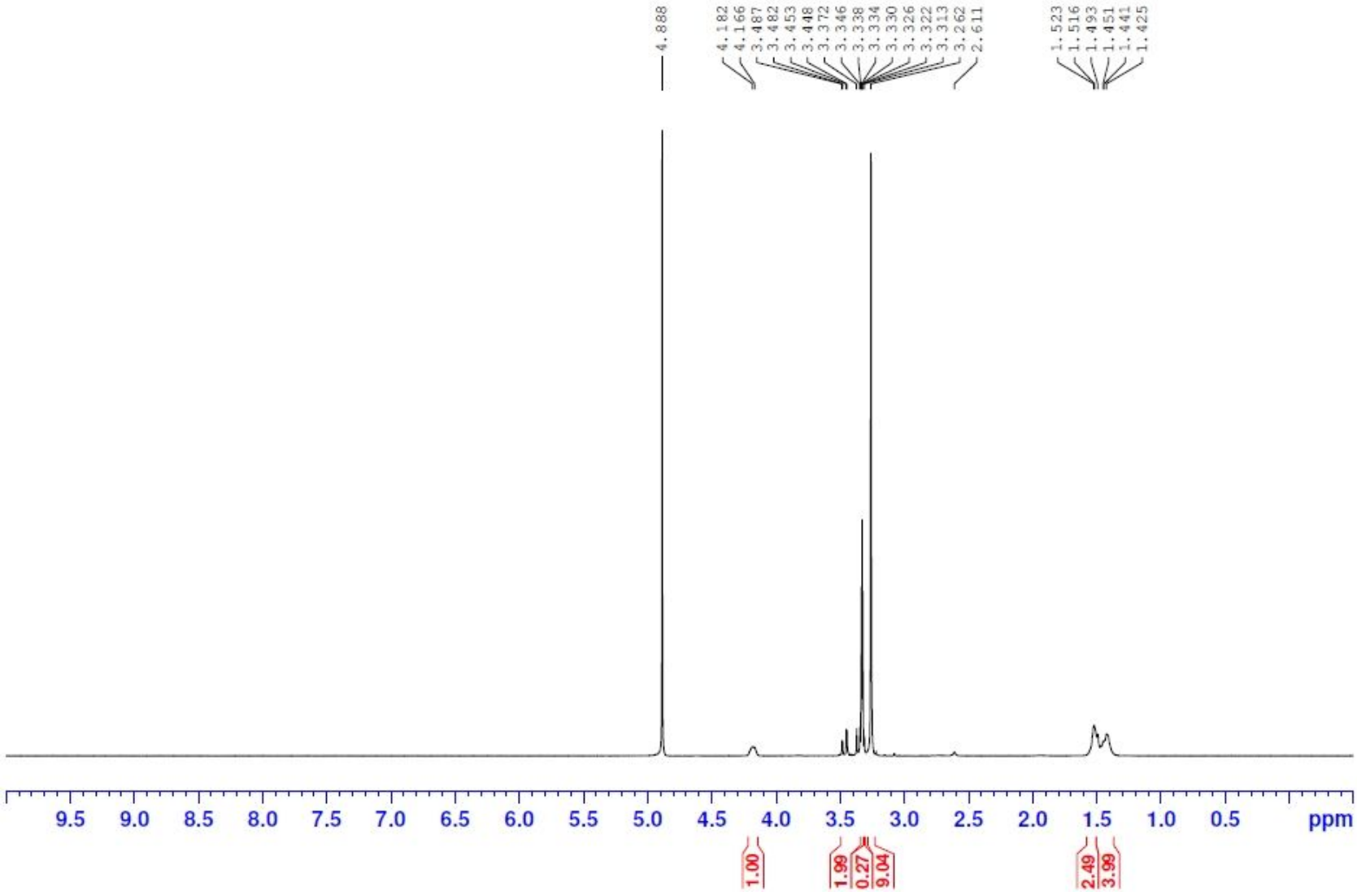

400 MHz ^{1}H NMR Spectrum ($CDCl_3$) of compound Lev (2)

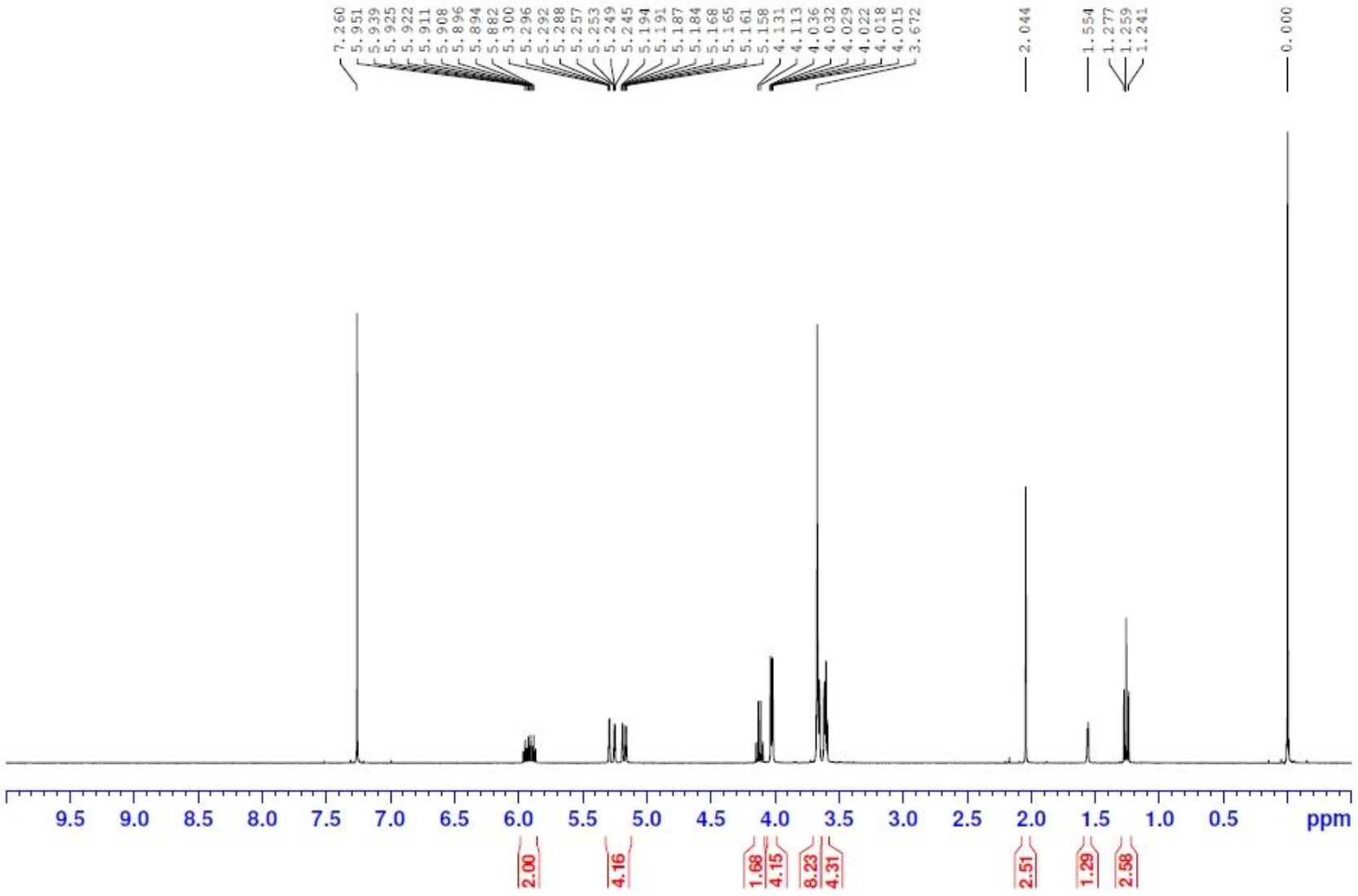

400 MHz ^{1}H NMR Spectrum ($CDCl_3$) of compound 6

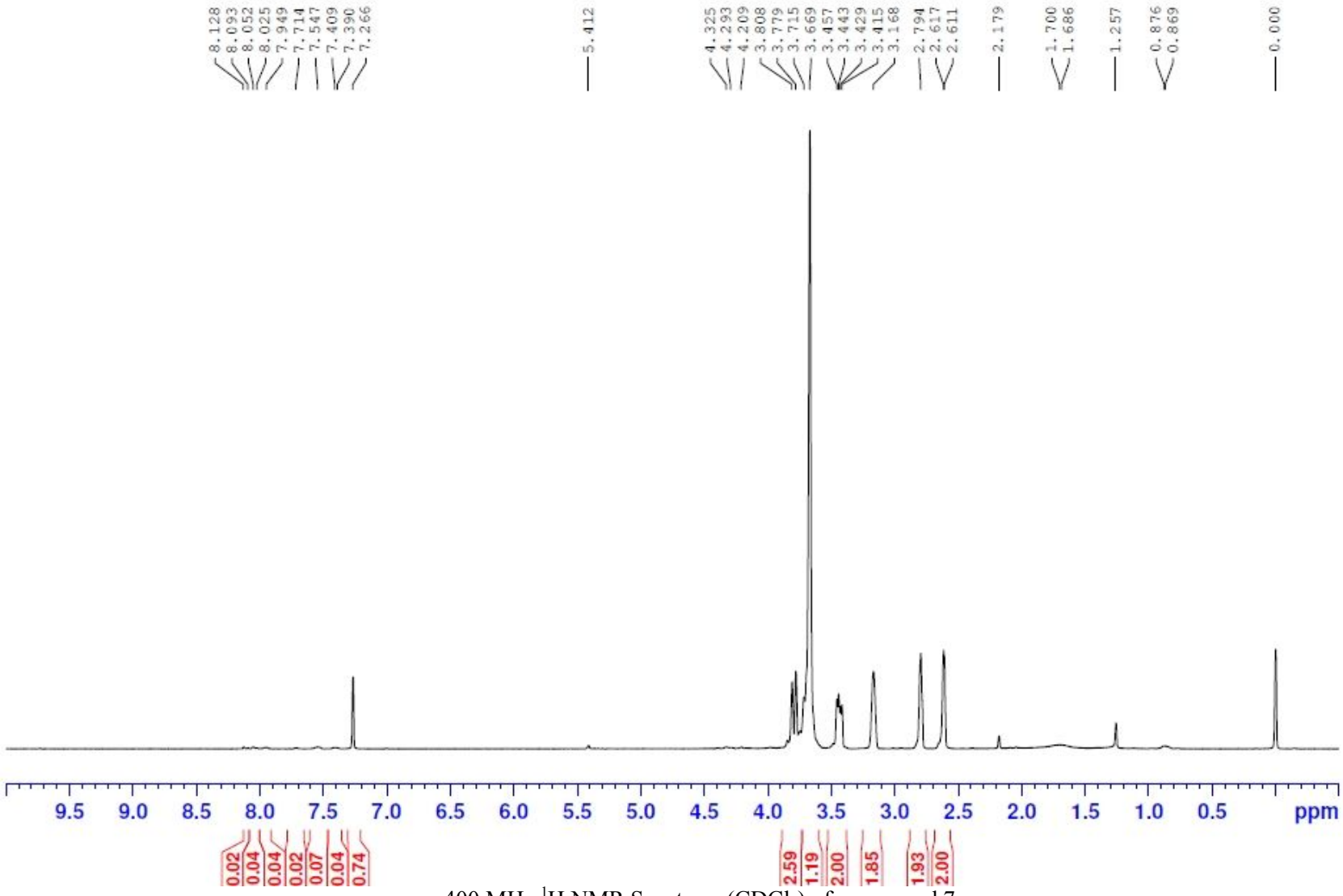

400 MHz ^{1}H NMR Spectrum ($CDCl_3$) of compound 7

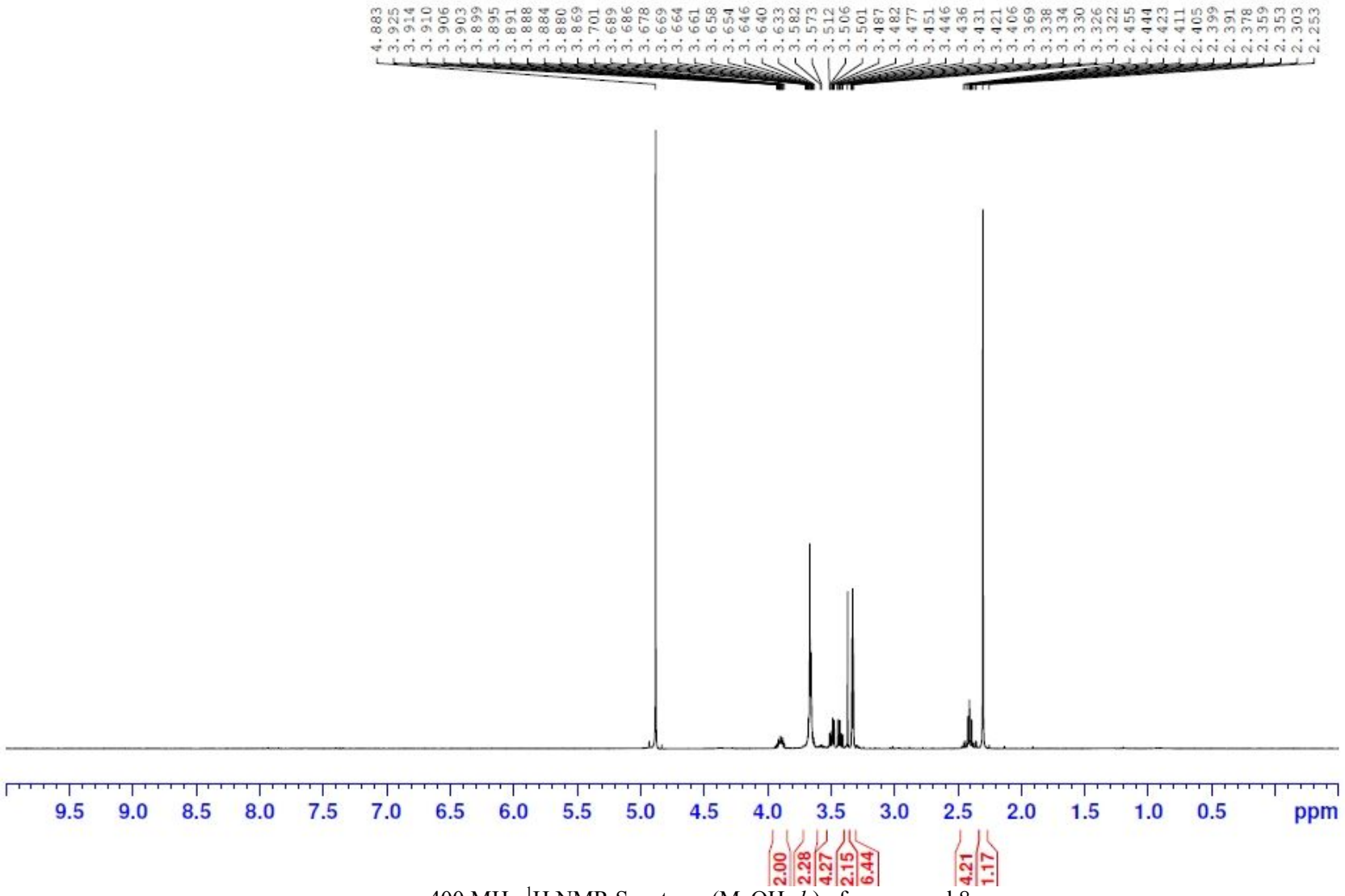

400 MHz ^{1}H NMR Spectrum (MeOH-d_4) of compound 8

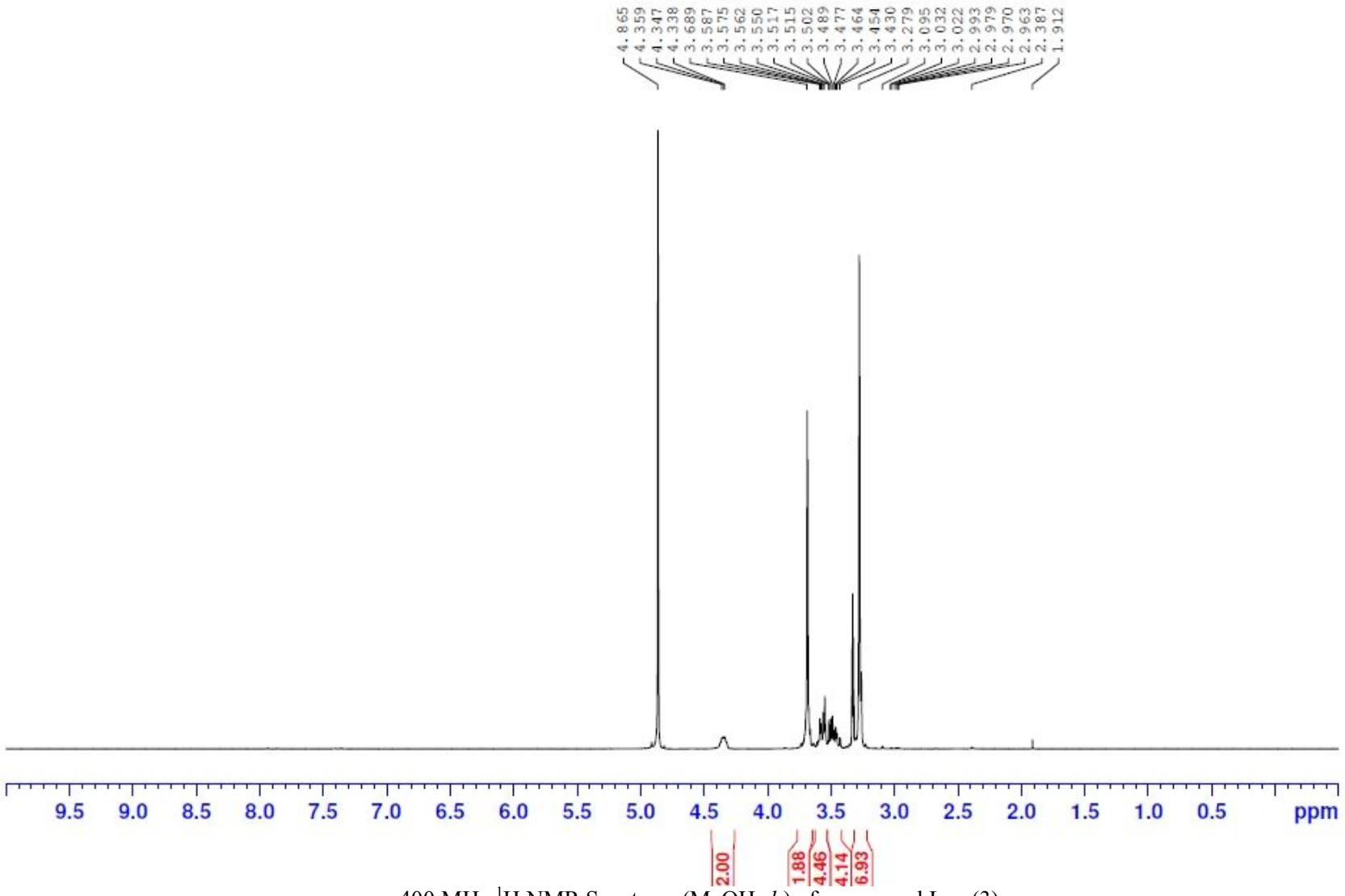

400 MHz ^{1}H NMR Spectrum (MeOH-d_4) of compound Lev (3)

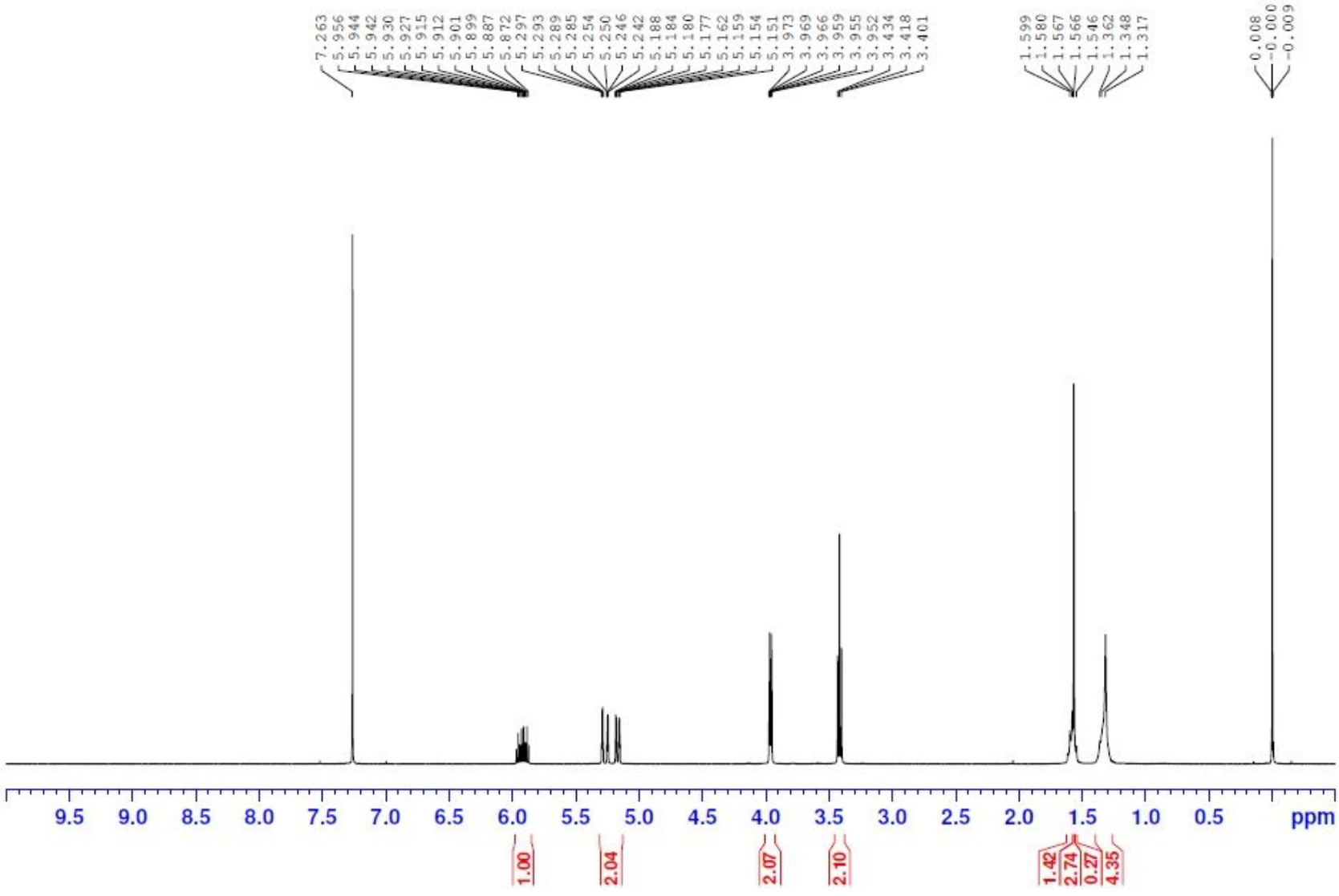

400 MHz ^{1}H NMR Spectrum ($CDCl_3$) of compound 9

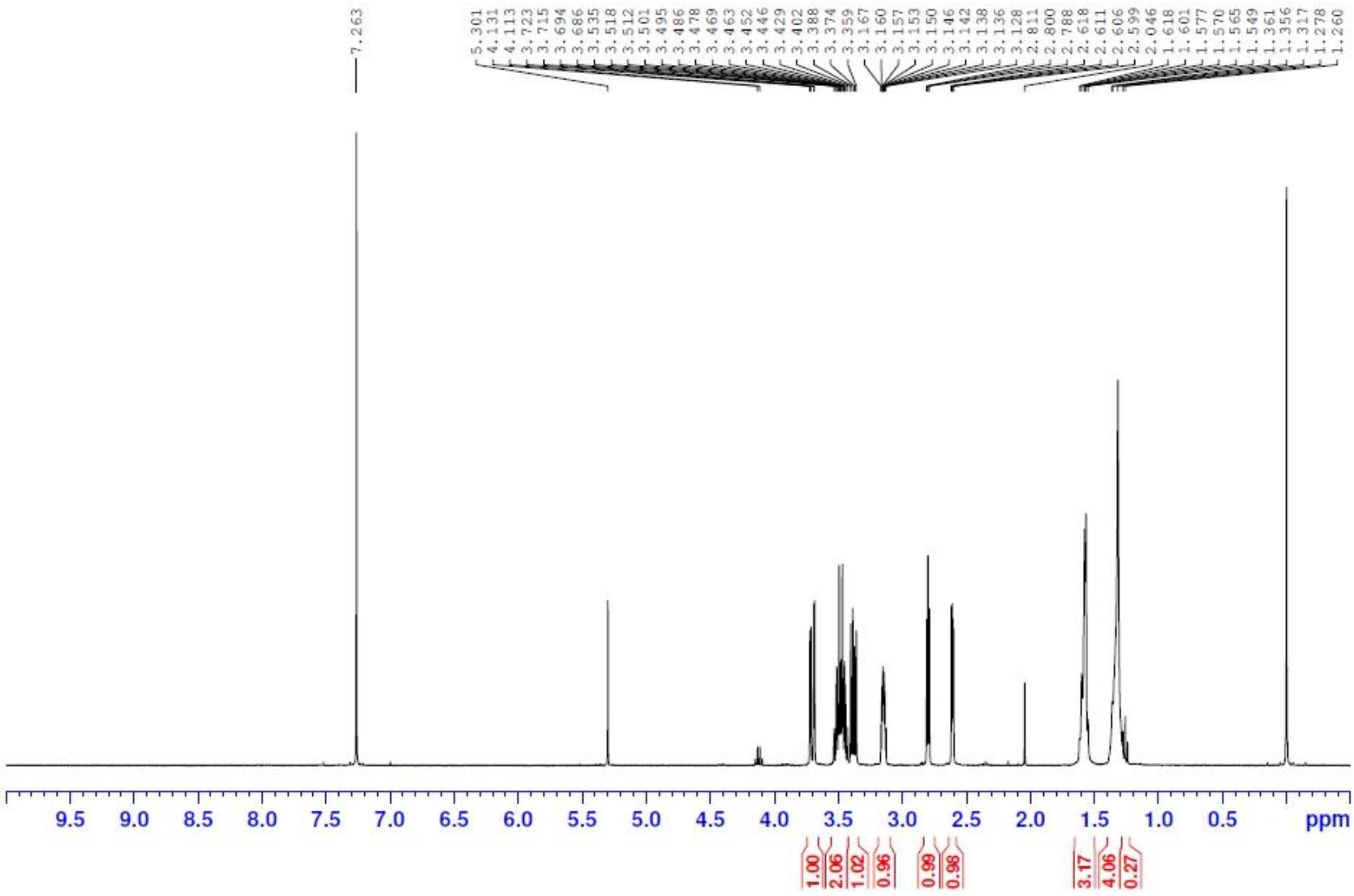

400 MHz ^{1}H NMR Spectrum ($CDCl_3$) of compound 10

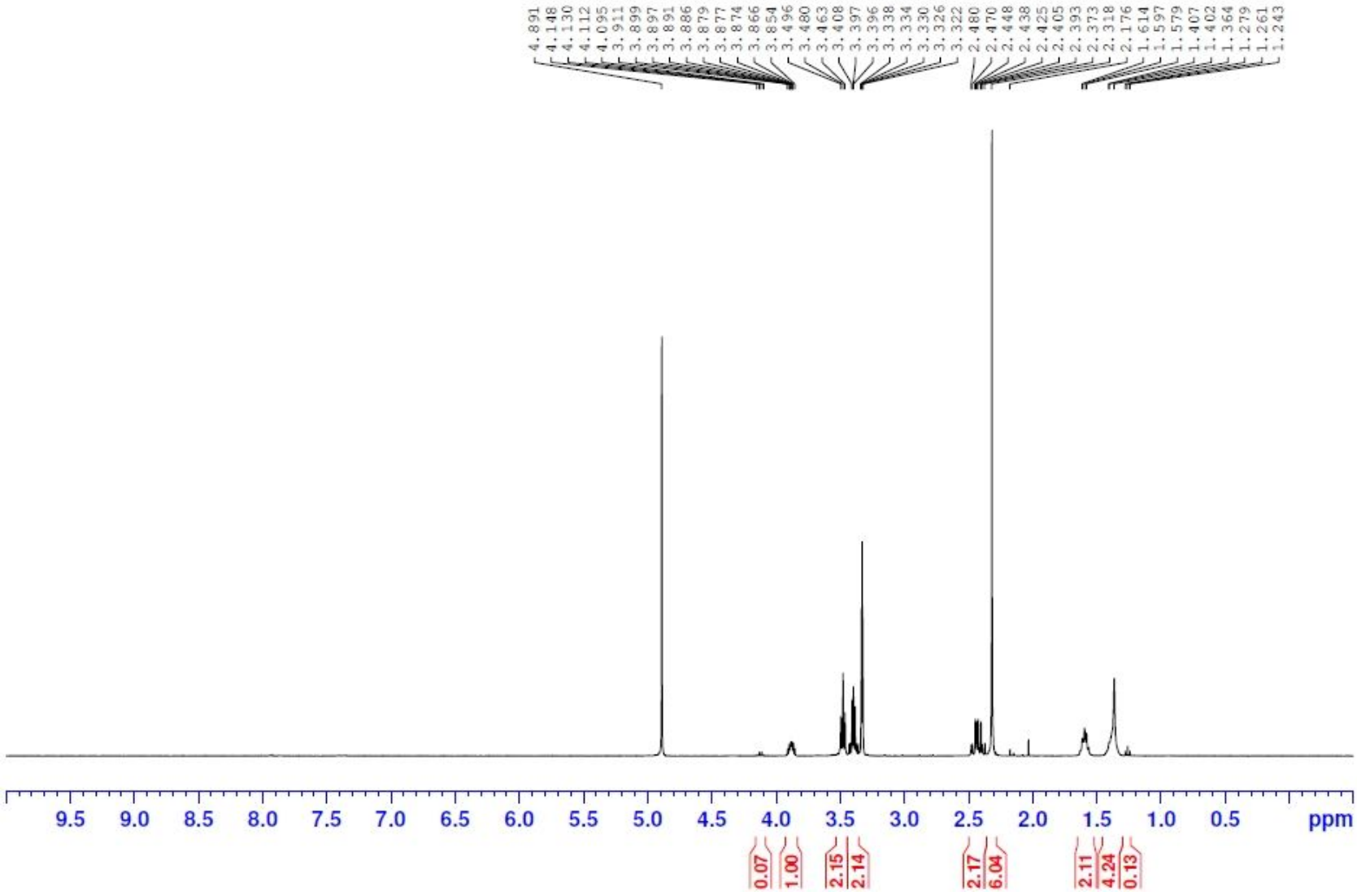

400 MHz ^{1}H NMR Spectrum ($CDCl_3$) of compound 11

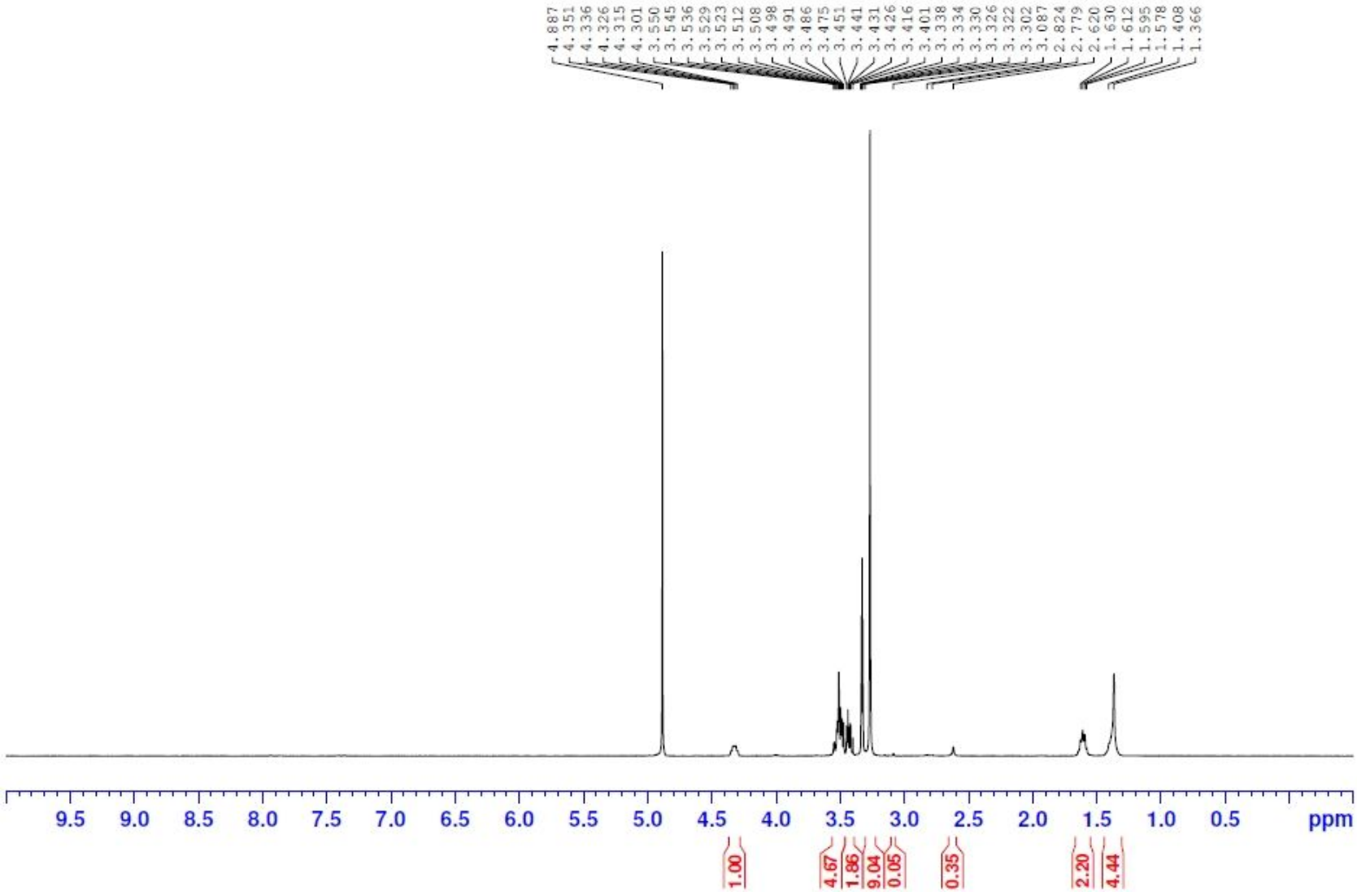

400 MHz ^{1}H NMR Spectrum ($CDCl_3$) of compound Lev (4)

List of ^{13}C NMR Spectra of Selected Compounds

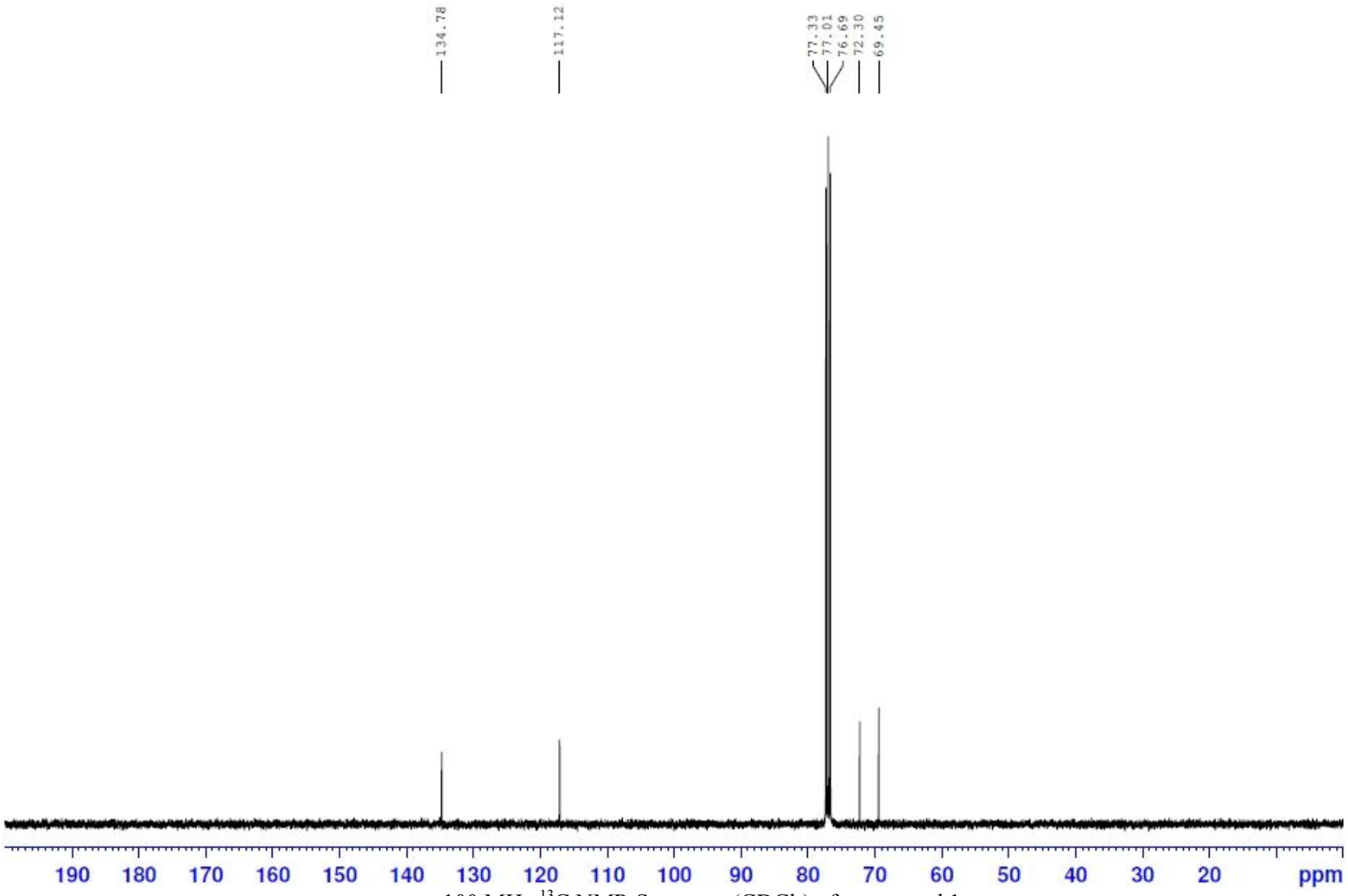

100 MHz ^{13}C NMR Spectrum ($CDCl_3$) of compound 1

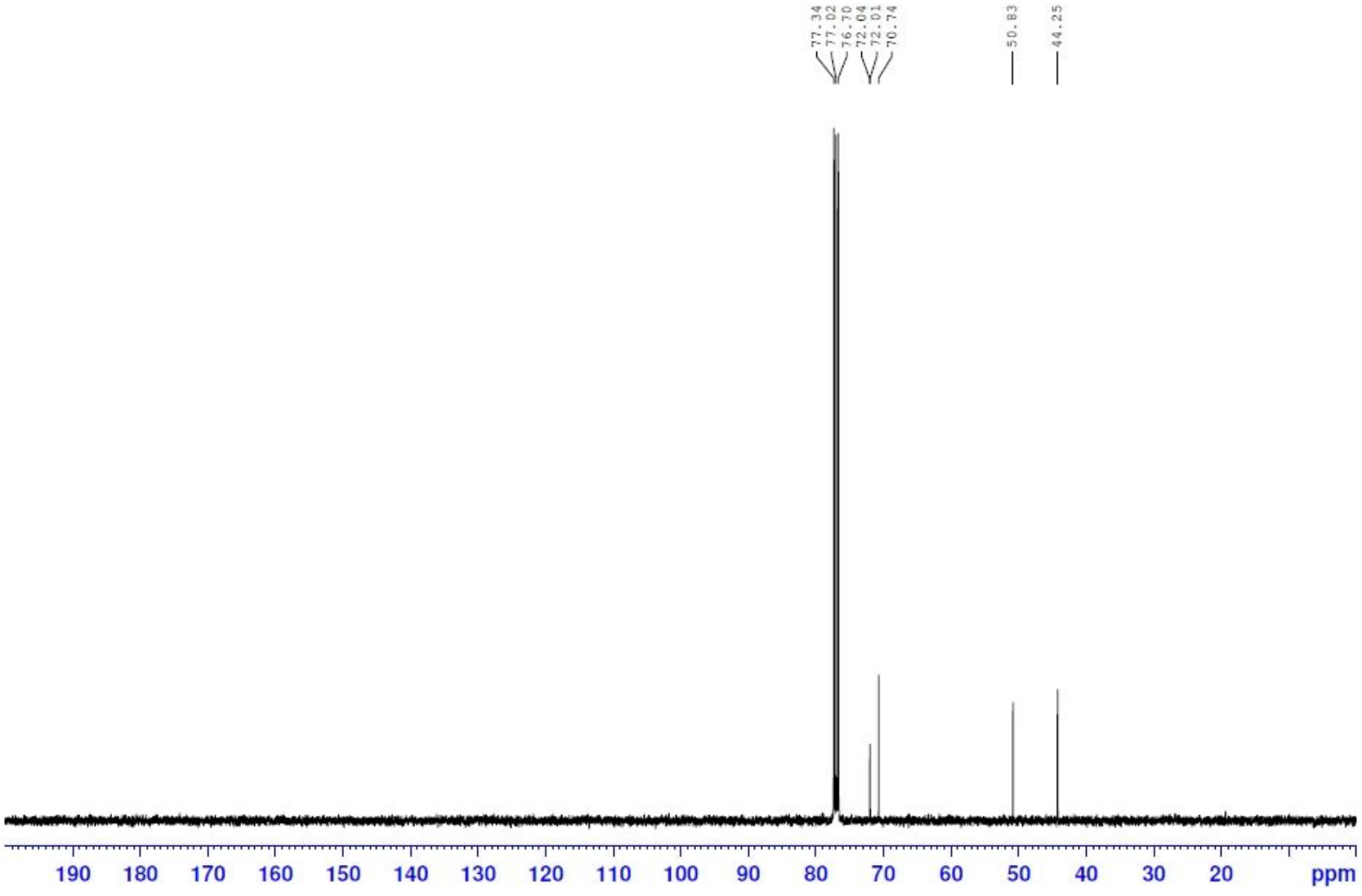

100 MHz ^{13}C NMR Spectrum ($CDCl_3$) of compound 2

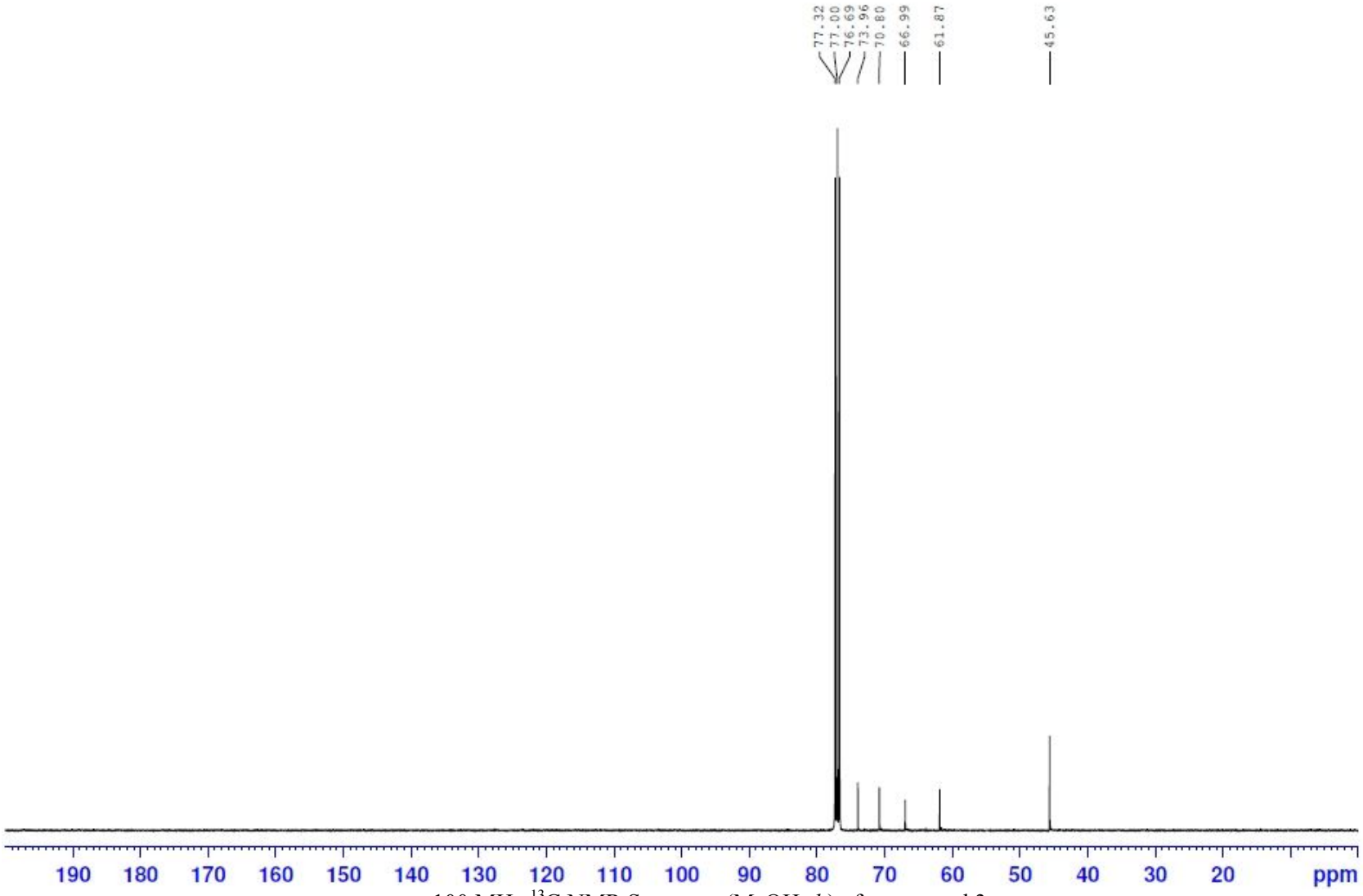

100 MHz ^{13}C NMR Spectrum (MeOH-d_6) of compound 3

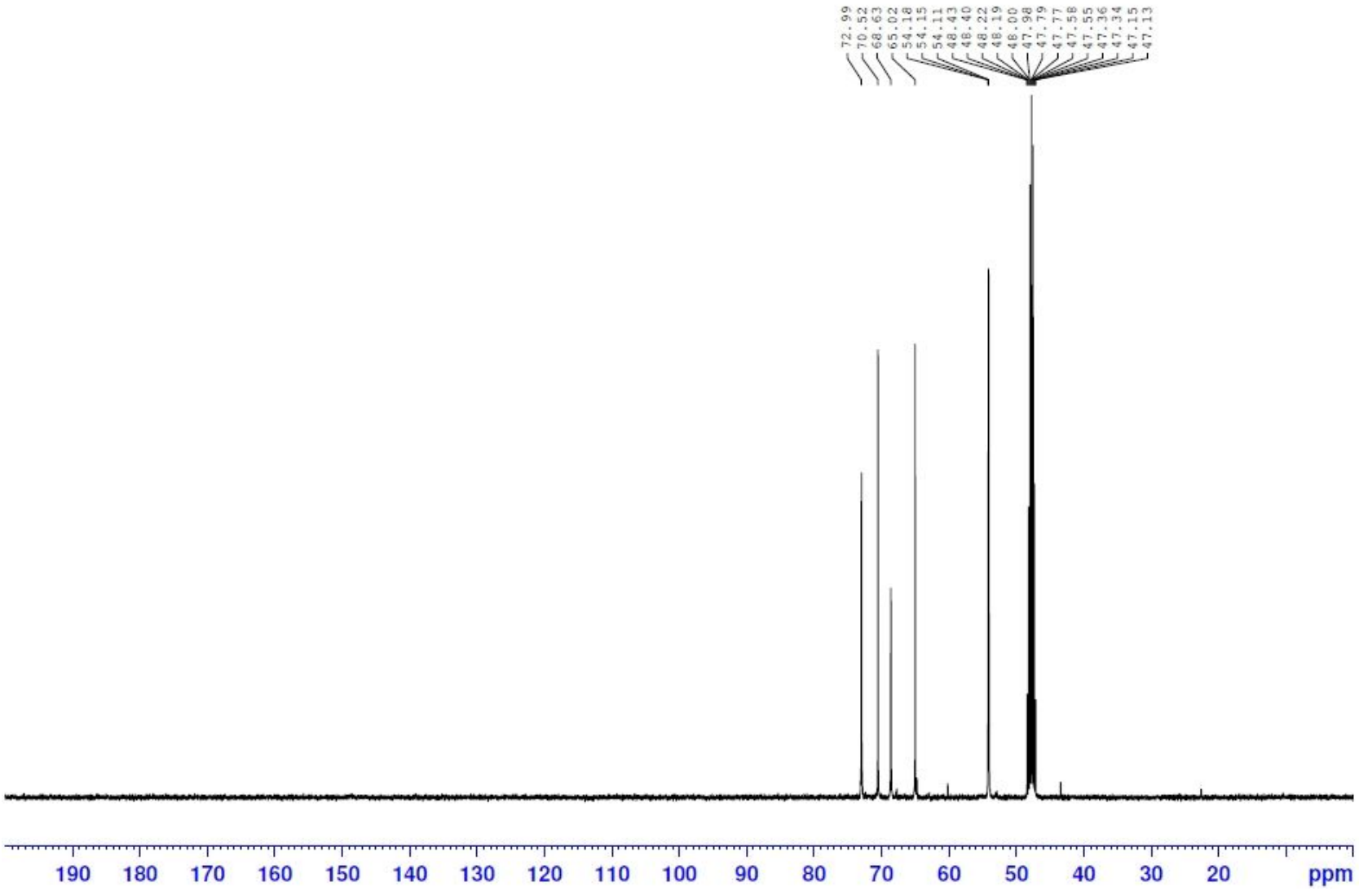

100 MHz ^{13}C NMR Spectrum (MeOH-d_6) of compound Lev (1)

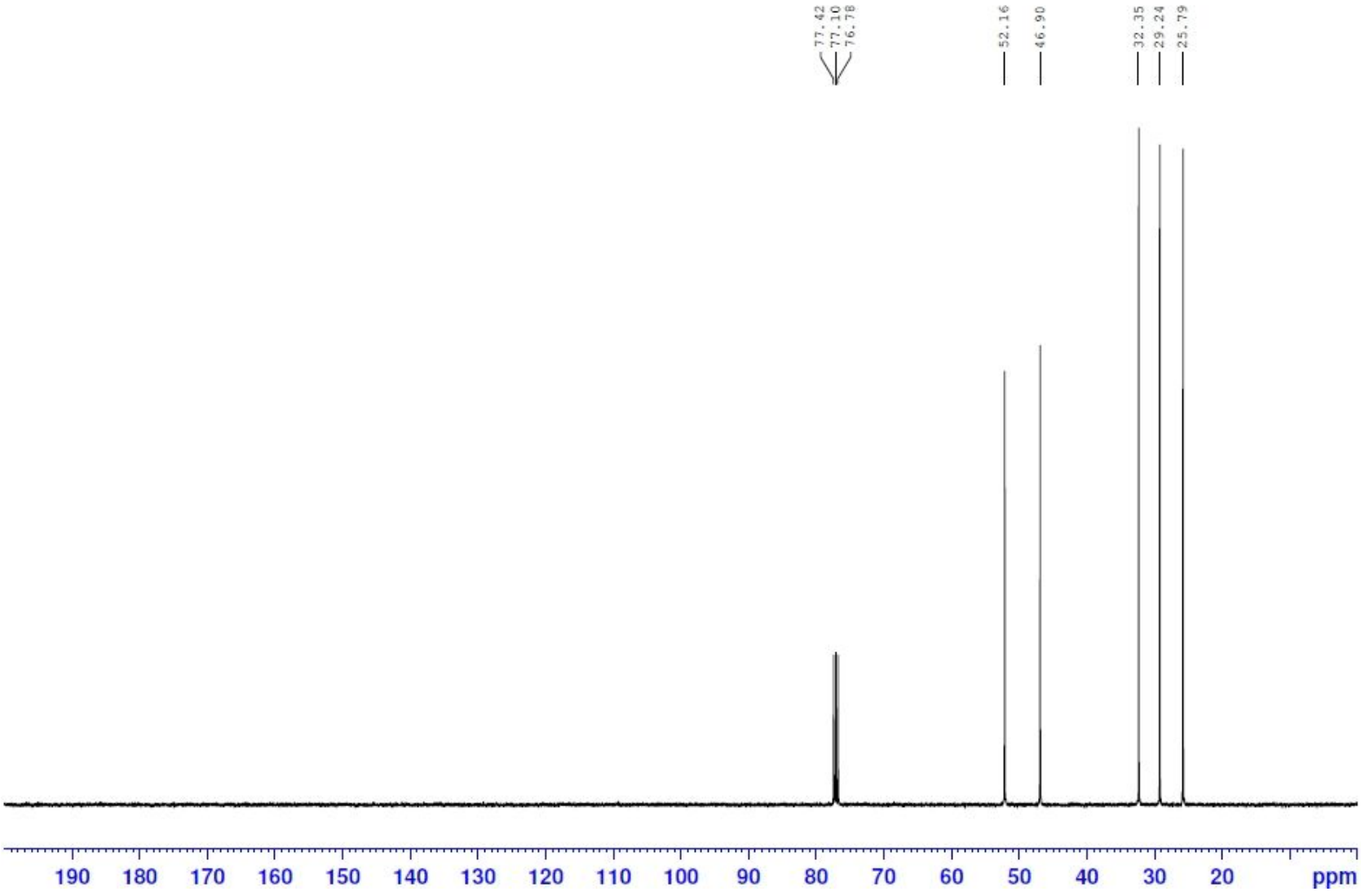

100 MHz ^{13}C NMR Spectrum (MeOH-d_6) of compound 4

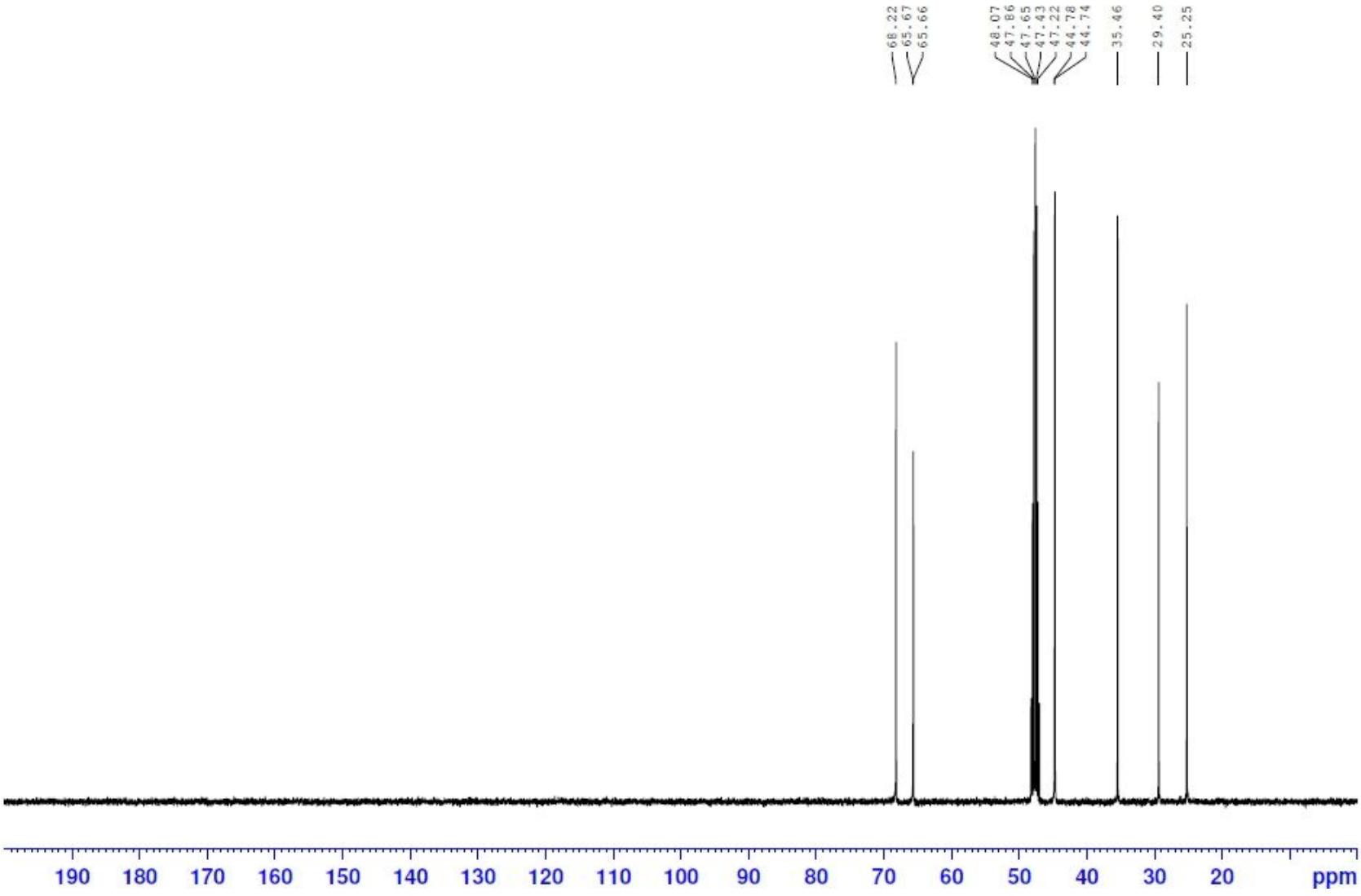

100 MHz ^{13}C NMR Spectrum (MeOH-d_6) of compound 5

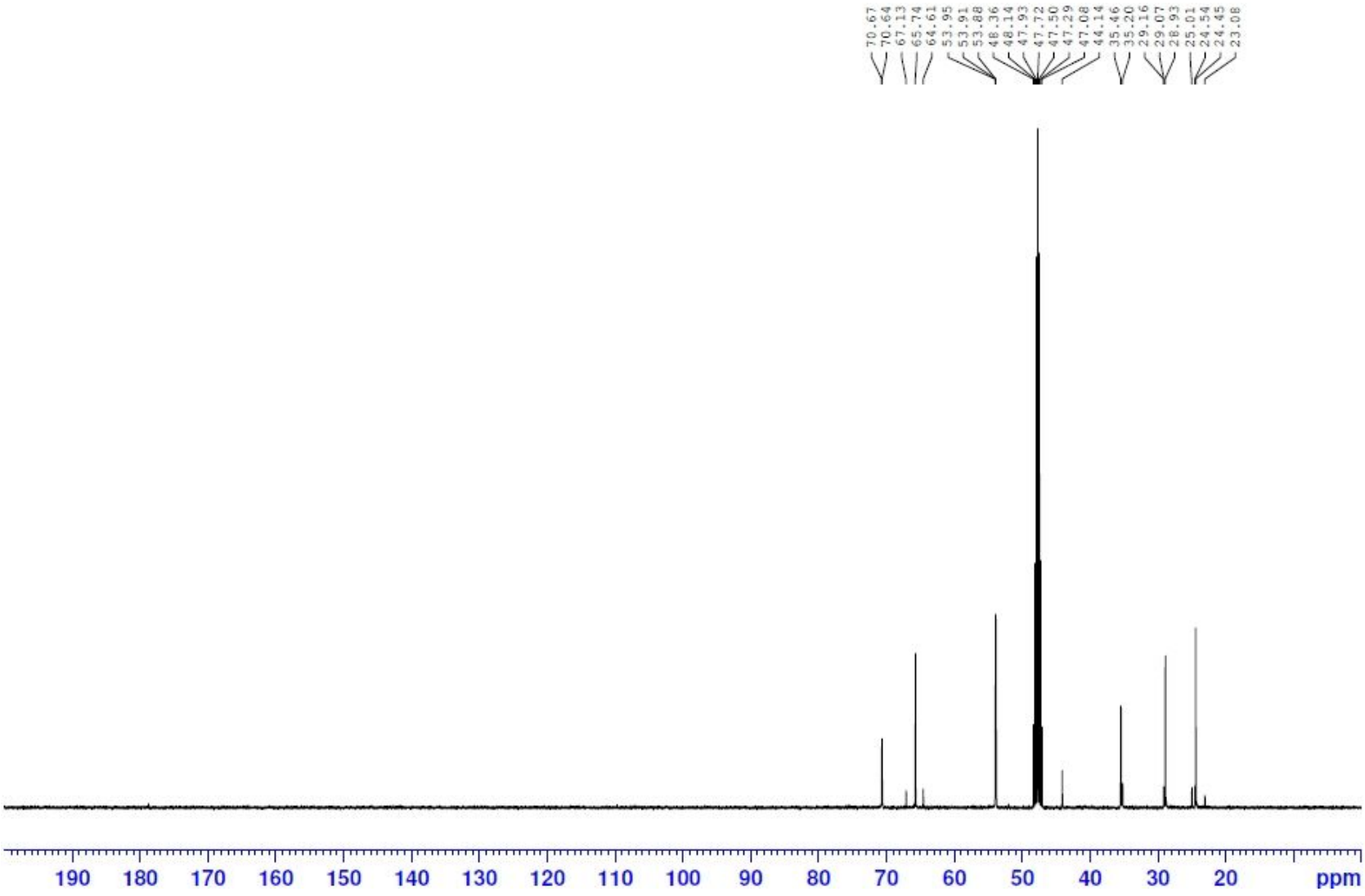

100 MHz ^{13}C NMR Spectrum (MeOH-d_6) of compound Lev (2)

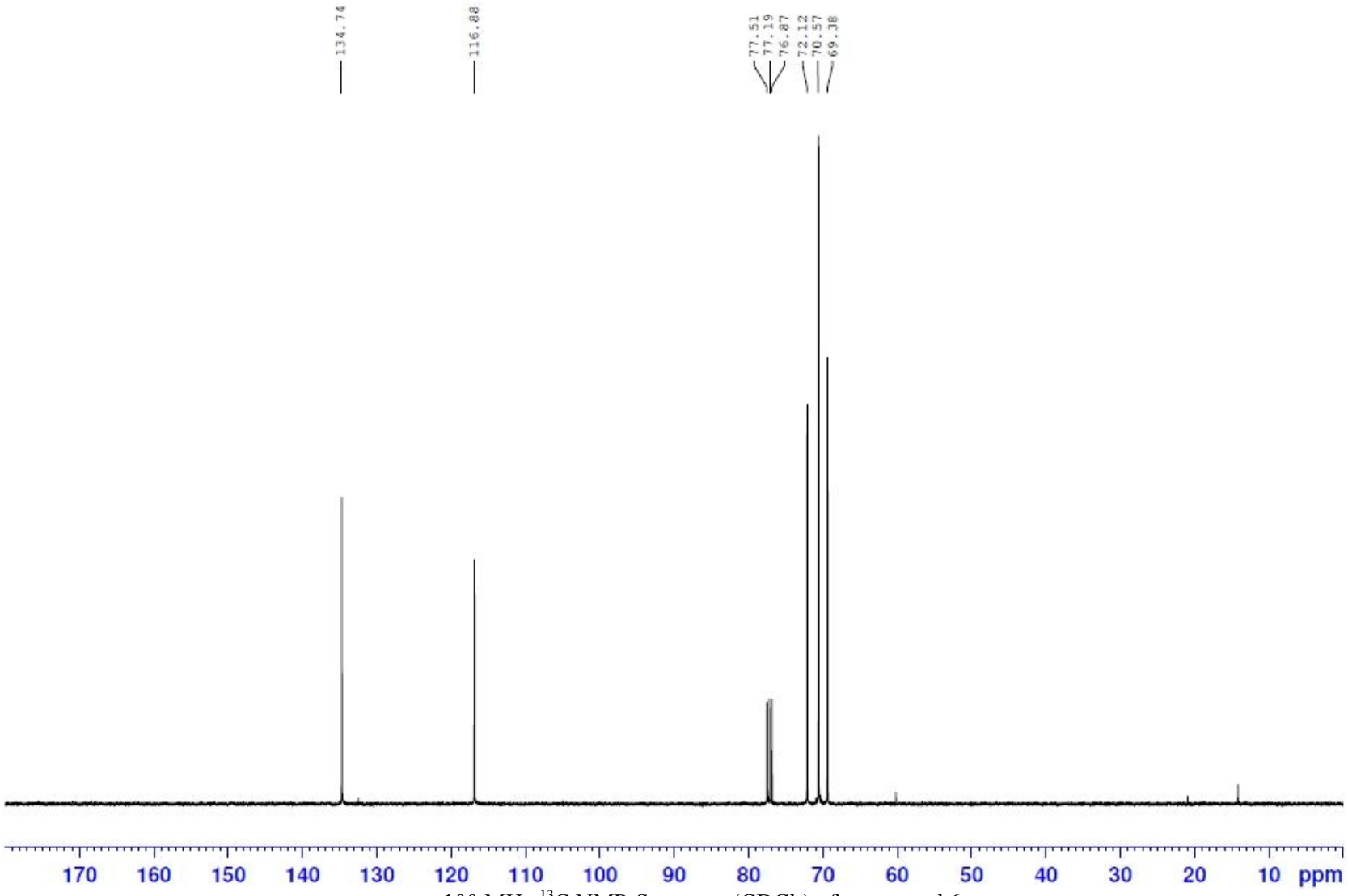

100 MHz ^{13}C NMR Spectrum ($CDCl_3$) of compound 6

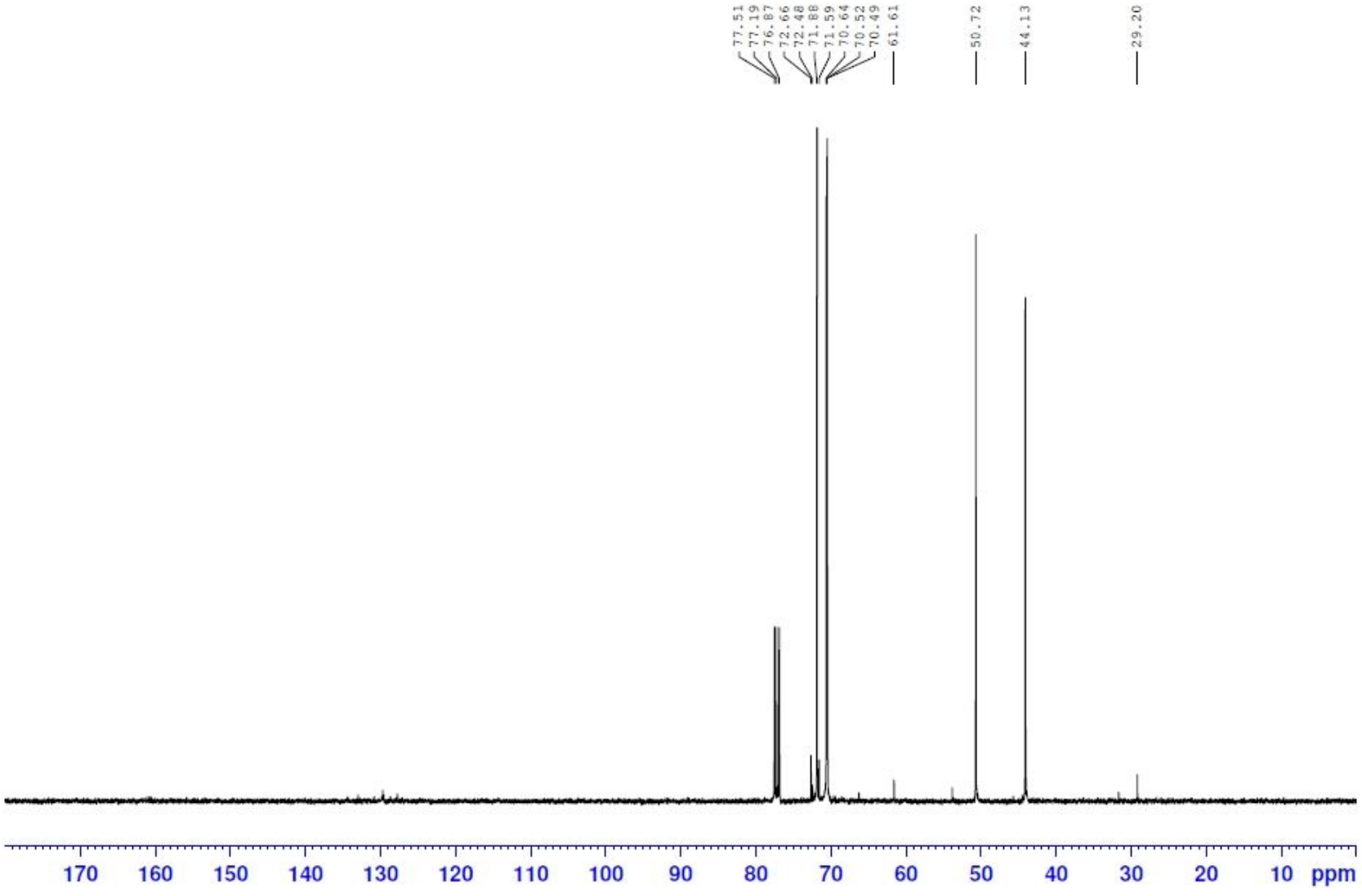

100 MHz ^{13}C NMR Spectrum ($CDCl_3$) of compound 7

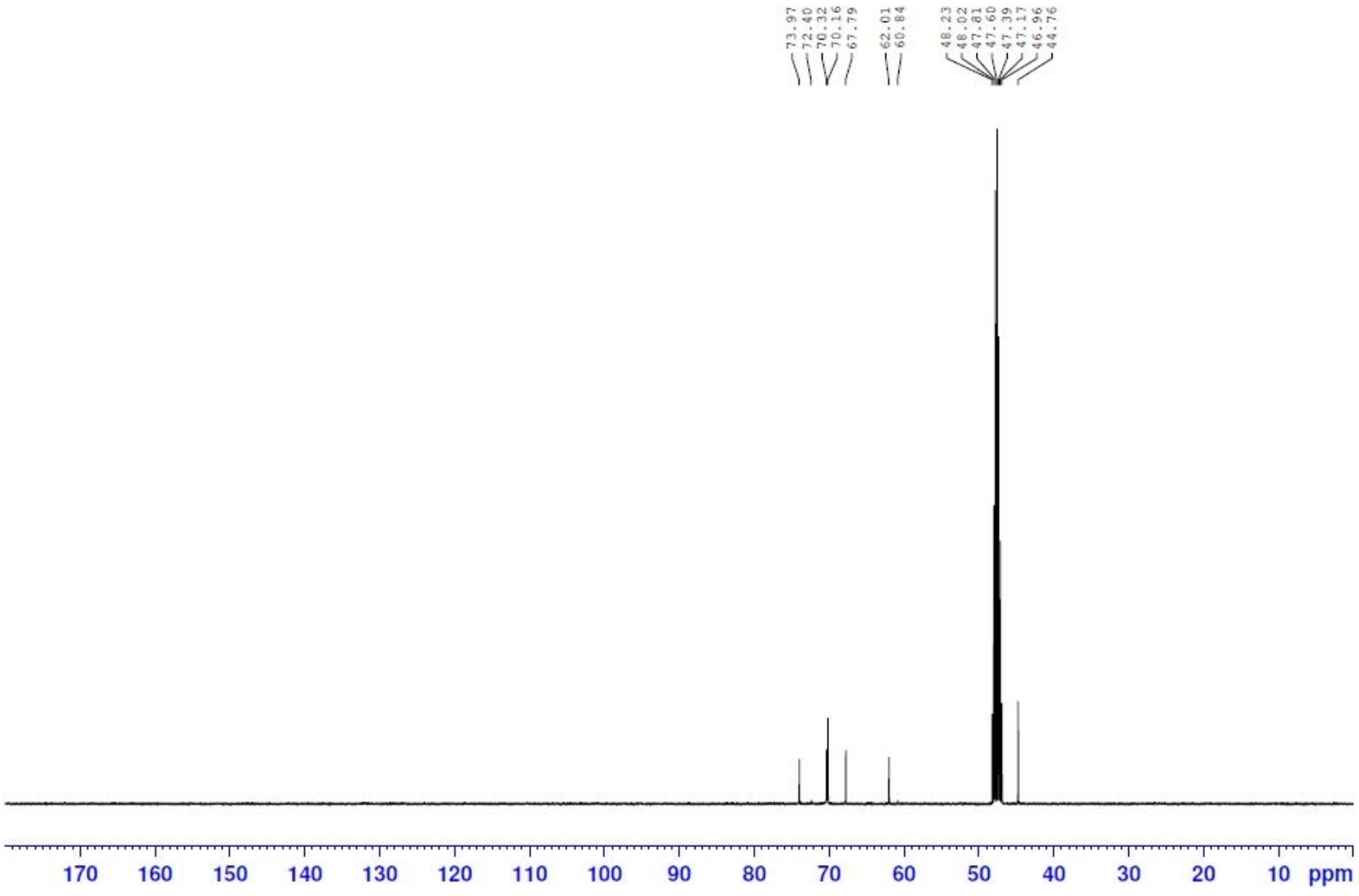

100 MHz ^{13}C NMR Spectrum (MeOH-d_6) of compound 8

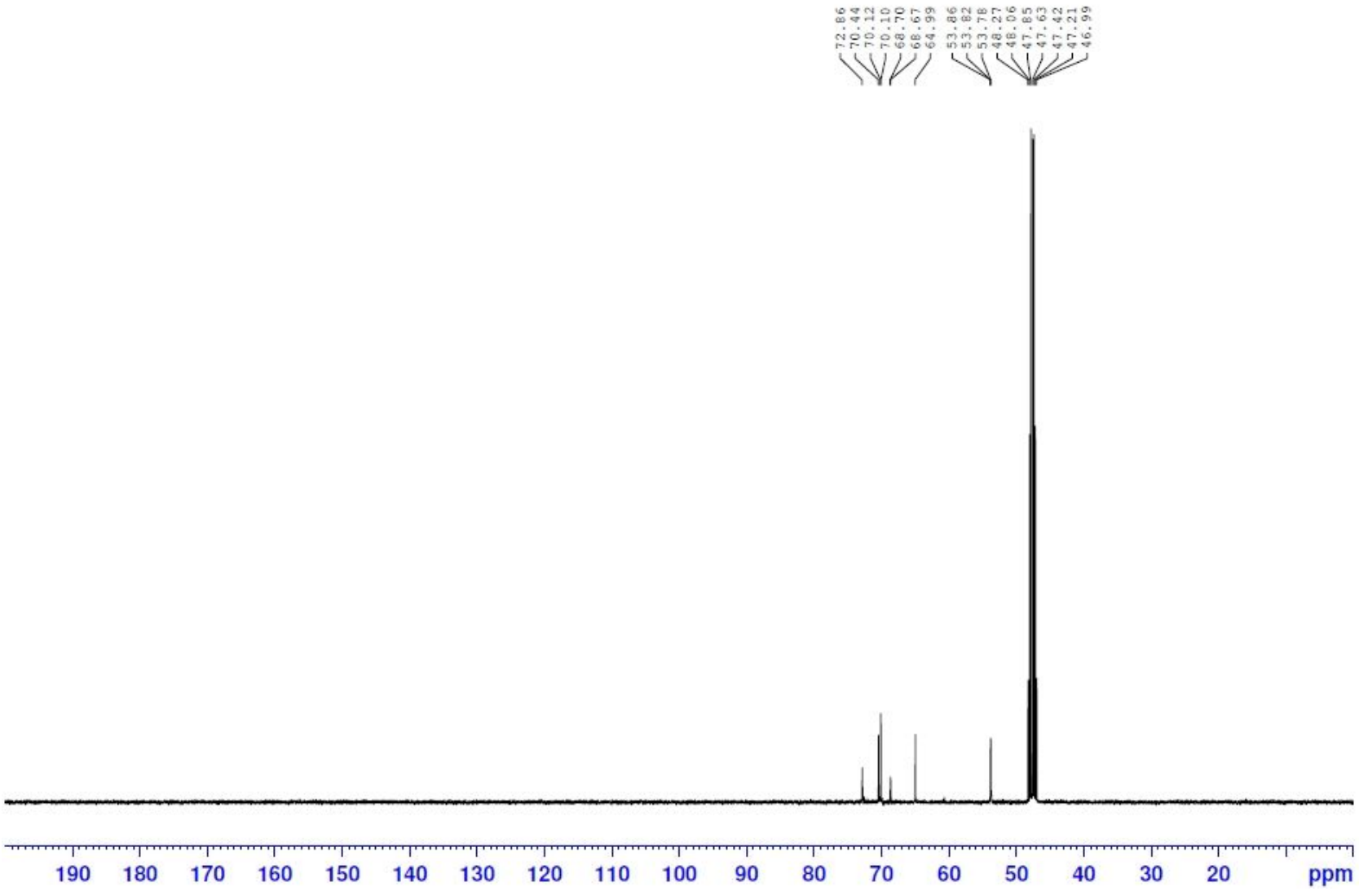

100 MHz ^{13}C NMR Spectrum (MeOH-d_6) of compound Lev (3)

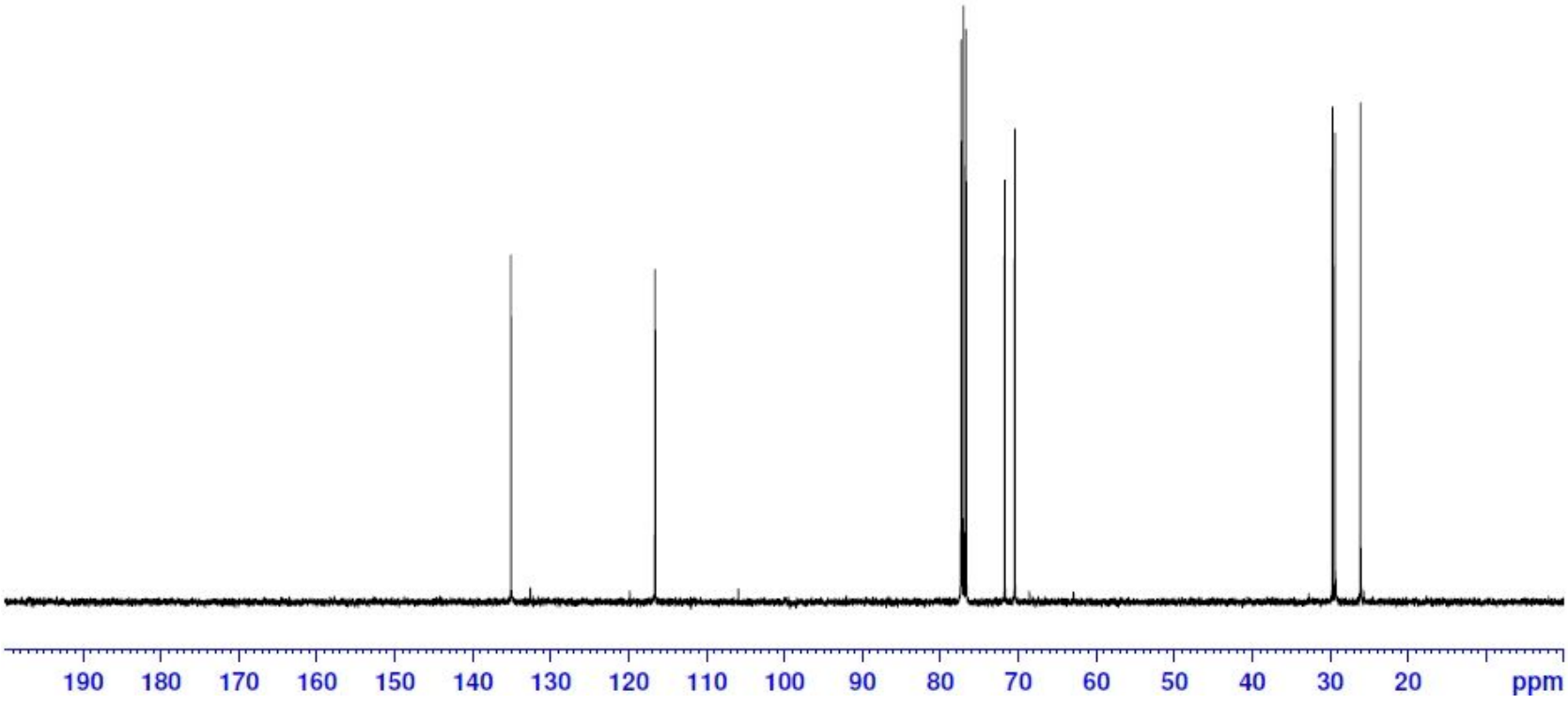

100 MHz ^{13}C NMR Spectrum (MeOH-d_6) of compound 9

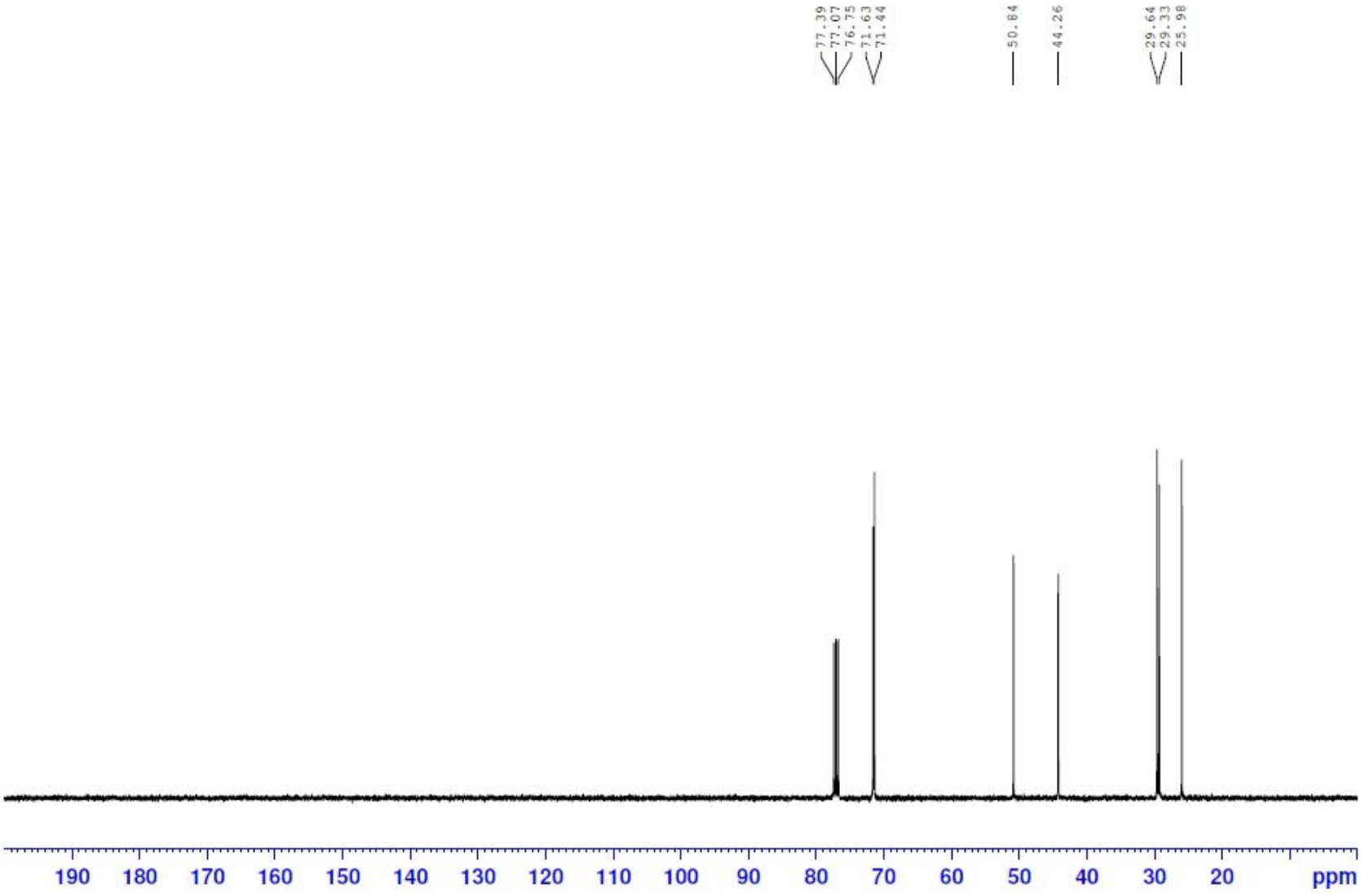

100 MHz ^{13}C NMR Spectrum (MeOH-d_6) of compound 10

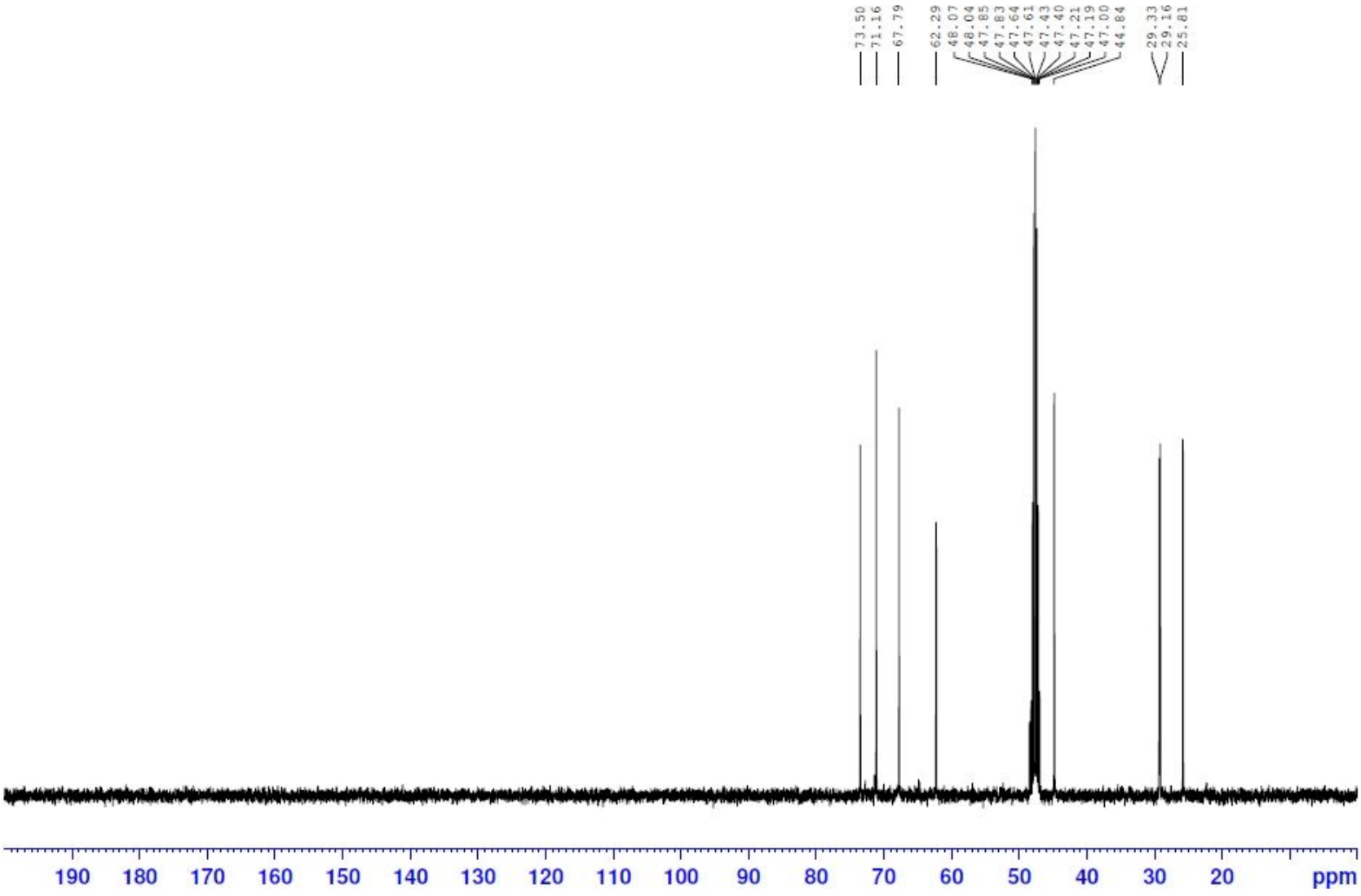

100 MHz ^{13}C NMR Spectrum (MeOH-d_6) of compound 11

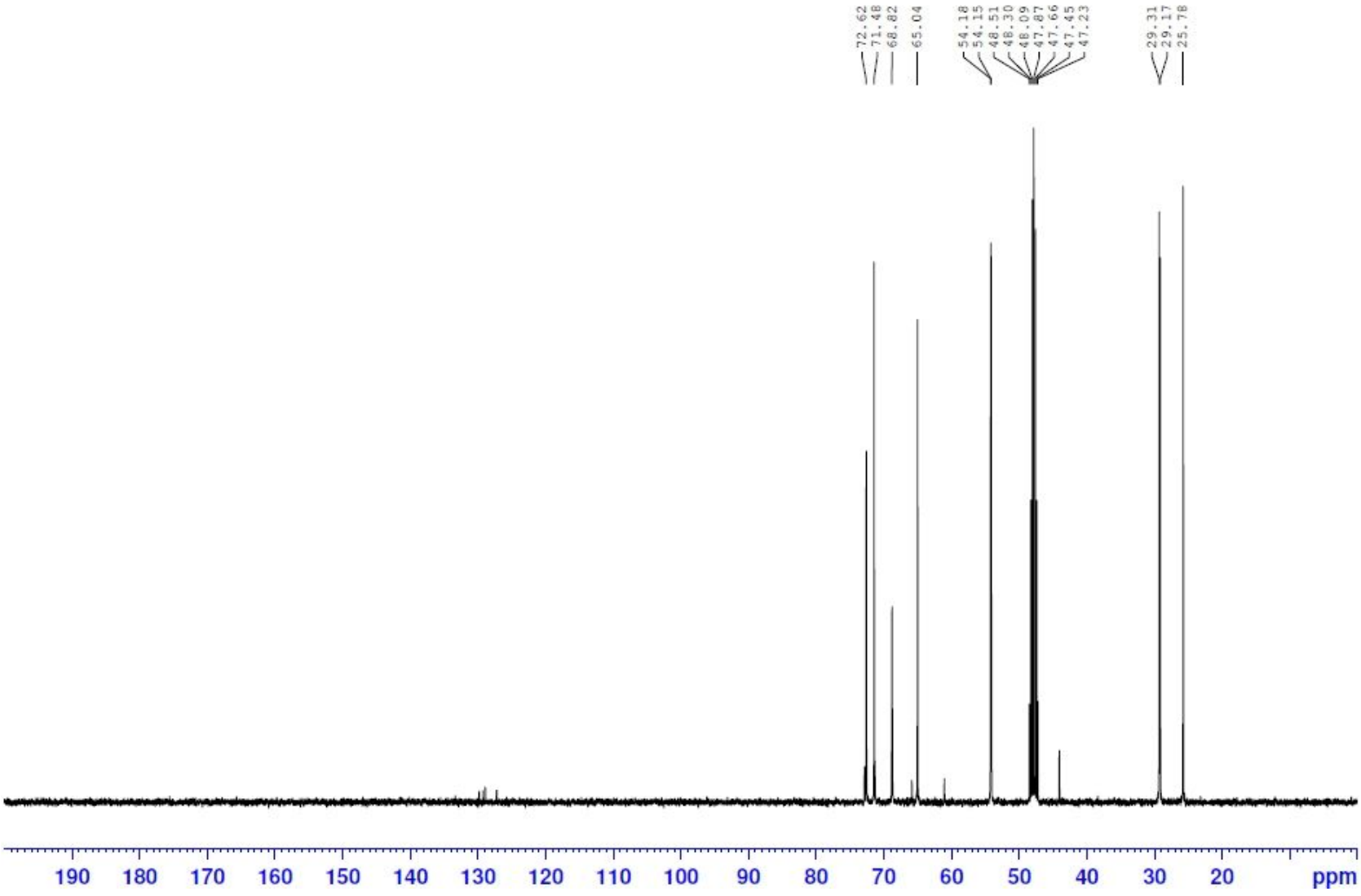

100 MHz ^{13}C NMR Spectrum (MeOH-d_6) of compound Lev (4)

국 문 초 록

실리콘 관통 전극 (TSV)은 실리콘 웨이퍼나 IC 칩들을 수직으로 연결시켜주는 기술이며, 여러 칩들 사이에 가장 짧은 연결 길이를 제공한다. TSV를 통해 초집적 고성능 반도체의 구현이 가능하지만 결함 없이 TSV를 도금하는 것이 아직 과제로 남아있다. 결함 없는 TSV의 도금을 위해서는 바닥부터 도금이 되어 차오르게 되는 Bottom-up filling이 필수적이다. 이를 위해 구리 전해도금 과정에서 유기 첨가제의 역할이 필수적이다. 이 첨가제들 사이에서 평탄제는 비아 (via)의 윗부분에만 선택적으로 흡착하여 구리 전해도금을 억제해주며 이를 대류 의존 흡착 특성이라고 한다.

본 연구에서는, 평탄제의 구조와 특성에 관한 연구를 진행하였고 이를 위해 새로운 구조를 가진 평탄제들이 합성되었다. 선형적인 구조를와 암모늄 구조를 양 말단에 가지고 있는 triethylene glycol 기반 평탄제인 Lev (1)를 설계하였고, 이의 특성을 분석해 보았다. Lev (1)은 ethylene glycol으로부터 총 46%의 수율로 합성되었다. 또한, 평탄제의 중심구조에 따른 영향을 확인하기 위해 Lev (1)의 구조를 수정한 Lev (2), (3), (4)가 총 25~ 50%의 수율로 합성되었다. Linear sweep volatammetry 분석을 통해 합성된 평탄제들이 모두 대류 의존 흡착 특성을 가지는 것을 확인하였고, 중심구조가 더 길고, 소수성의 특징을 가질수록 더 강한 흡착 특성을 보인다는 것을 확인하였다. 이렇게 합성된 평탄제들과 억제제, 첨가제를 이용해 TSV와 유사한 크기를 가지는 trench가 성공적으로 도금되었다.

주요어 : 평탄제, 구리전해도금, 실리콘 관통 전극, 유기 첨가제, 대류 의존 흡착.

학번 : 2014-20569